Structural Insufficiency Anomalies in Cardiac Valves

Edited by Kaan Kirali

STRUCTURAL INSUFFICIENCY ANOMALIES IN CARDIAC VALVES

Edited by **Kaan Kirali**

Structural Insufficiency Anomalies in Cardiac Valves
http://dx.doi.org/10.5772/intechopen.71281
Edited by Kaan Kirali

Contributors

Irina Ignatko, Leonid Strizhakov, Alexandra Rodionova, Ayse İnci Yıldırım, Aysu Türkmen Karaağaç, Edward Chen, Ziv Beckerman, Chukwuemeka Daniel Daniel Iroegbu, Zhou Zhongxin, Jindong Liu, Hao Zhang, Barbara Brzezińska, Krystyna Łoboz-Grudzień, Sotirios Korossis

Notice

Statements and opinions expressed in the chapters are these of the individual contributors and not necessarily those of the editors or publisher. No responsibility is accepted for the accuracy of information contained in the published chapters. The publisher assumes no responsibility for any damage or injury to persons or property arising out of the use of any materials, instructions, methods or ideas contained in the book.

We are IntechOpen,
the world's leading publisher of Open Access books
Built by scientists, for scientists

3,750+
Open access books available

116,000+
International authors and editors

120M+
Downloads

151
Countries delivered to

Our authors are among the

Top 1%
most cited scientists

12.2%
Contributors from top 500 universities

WEB OF SCIENCE™

Selection of our books indexed in the Book Citation Index
in Web of Science™ Core Collection (BKCI)

Interested in publishing with us?
Contact book.department@intechopen.com

Numbers displayed above are based on latest data collected.
For more information visit www.intechopen.com

Meet the editor

Professor Kırali, Director of Koşuyolu Heart and Research Hospital, is specialized in heart valve pathologies and focuses his scientific interests on surgical treatments requiring experience. With his expertise in coronary bypass surgery, congenital cardiac surgery, minimal invasive cardiac surgery, valve repair and aortic root surgery, he also has an interest in heart failure surgery. He has developed a new aortotomy incision for aortic valve surgery, a new measuring method for aortic valve sparing procedures, and a new approach for awake *coronary artery bypass* grafting surgery. He has published numerous SCI journal papers and book chapters and edited/reviewed many academic journals. He is a member of several international and national scientific societies.

Contents

Preface

Structural insufficiency of cardiac valves is the basic and featured cardiac pathology. Heart valves allow unidirectional and unobstructed passage of blood without regurgitation, trauma to blood elements, thromboembolism and excessive stress concentrations in the leaflet and supporting tissue. The ultrastructural histo-architecture of the valvular tissue is the basis of mechanical properties of heart valves. New technologies for diagnosis, new research for genetic structure, new definitions for the nature of malformations and malfunctions, new classifications for pathologic types and new surgical approaches to replace dysfunctional behavior will improve the survival of patients with these pathologies. This book tries to detail pathophysiology, general forms and also specific types of structural valvular insufficiencies.

Professor Dr Kaan Kırali
Director of Kartal Koşuyolu YIEA Hospital
Istanbul, Turkey

Structure-Function Relationship of Heart Valves in Health and Disease

Sotirios Korossis

Additional information is available at the end of the chapter

Abstract

The heart valves allow unidirectional and unobstructed passage of blood without regurgitation, trauma to blood elements, thromboembolism, and excessive stress concentrations in the leaflet and supporting tissue. In order to achieve this, the heart valves rely of their unique macroscale anatomy, histoarchitecture and ultrastructural features that allow them to accommodate repetitive changes in shape and dimension throughout the cardiac cycle. This chapter is focused on the structure-function relationship of the heart valves, with particular focus on the aortic and mitral valves, discussing how the biochemical, histoarchitectural and anatomical features influence valvular function during the cardiac cycle and how valvular function dictates valvular architecture and ECM constitution. The chapter examines the structure-function relationship of valvular tissue by correlating its microscale histoarchitecture and biochemical constitution to its mesoscale biomechanics and macroscale function during the cardiac cycle. Moreover, the chapter examines the influence of pathological alterations on the histoarchitectural and biochemical characteristics of the valves on their biomechanical behavior.

Keywords: heart valves, histoarchitecture, biochemistry, biomechanics, structure-function

1. Introduction

Connective tissues comprise a network of interweaving fibers with polysaccharide ground substance immersed in a pool of ionic fluid. Cells are attached to the fibers and are responsible for replenishing the extracellular matrix (ECM) macromolecules and the ground substance that carry out the physical function. The ECM contains three major classes of macromolecules, including structural proteins, such as collagen, elastin and fibrillin, specialized proteins, such

as fibronectin and laminin, and glycosaminoglycans (GAGs) and proteoglycans. The ECM is involved in many normal and pathologic processes, playing an important role in tissue development and pathology, and mechanotransduction of the cells [1]. The ground substance is a hydrophilic gel that fills the spaces between the cells and the ECM. Dense connective tissues contain a small amount of ground substance and the cells are mostly fibroblasts. Loose connective tissues contain significantly more ground substance. Ground substance in normal connective tissues is clear and colorless and its composition varies with the tissue. It has a dense consistency similar to that of maple syrup, due to the presence of GAGs and proteoglycans.

The structure and hence the properties of a tissue are dependent on the chemical and physical nature of its constituents and their relative amounts. For example, nervous tissue consists almost entirely of cells, whereas bone is composed of collagen fibers and calcium phosphate minerals with minute quantities of cells and ground substance. Depending on the functional requirements on a particular tissue, the organization of its ECM macromolecules, cells and ground substance, as well as its resulting mechanical properties, vary. The simplest structure from the point of view of the collagen fibers consists of parallel fibers, as in tendons and ligaments. The 2D and 3D networks of the skin are more complex, whereas the structure of blood vessels and heart valves are the most complex ones. This chapter describes the basic biochemistry and function of the major structural proteins, collagen and elastic fibers, as well as the major GAGs and proteoglycans, present in the ECM of the heart valves, and illustrates their physiological and pathological significance. In addition it examines the structural basis, organization and structure-function relationship of valvular tissue, with particular focus on the aortic and mitral valves, by correlating its microscale histoarchitecture and biochemical constitution to its mesoscale biomechanics. Finally, the chapter examines the influence of pathological alterations, as a result of major valvular disease, on the histoarchitectural, constitutional and biomechanical characteristics of the valves.

2. Structure-function of major ECM proteins of valvular tissue

Proteins are the most abundant organic components of the human body. There are roughly 100,000 different kinds of proteins and they account for about 20% of the total body weight [2]. All proteins contain carbon, hydrogen, oxygen, and nitrogen and in some cases small quantities of sulfur. Proteins are classified according to the function they perform into structural, contractile and transport proteins, buffers, enzymes, antibodies and hormones. From these types, structural proteins such as collagen, elastin and keratin create a 3D framework for the body, providing strength, organization, and support for cells, tissues, and organs. Proteins consist of chains of amino acids, with each amino acid comprising a central carbon atom to which four groups are attached, including a hydrogen atom, an amino group ($-NH_2$), a carboxylic acid group ($-COOH$) and a variable group, known as an R-group or side chain (**Figure 1a**). The amino and carboxylic acid groups are hydrophilic groups, and amino acids are relatively small, soluble molecules. Depending on the side chain the molecular structure changes drastically, giving each amino acid its individual chemical properties. The simplest R-group is hydrogen, which forms glycine (Gly). Within the physiological pH range, the carboxylic acid groups on many amino acids give up their hydrogen, going from $-COOH$ to $-COO^-$ and getting negatively charged. Two amino acids can be linked by dehydration, which creates a covalent bond between the carboxylic acid group of one amino acid and the amino group
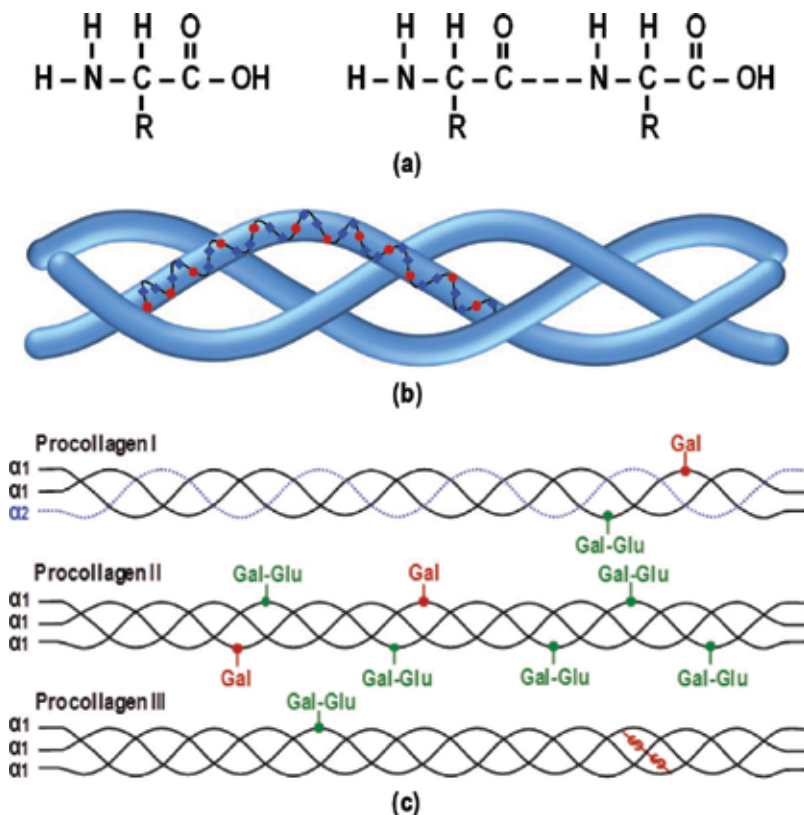
Figure 1. (a) Amino acid structure. (b) Peptide bond formation. (c) Schematic of the collagen triple helix (□ glycine; ♦ other amino acids). (d) Triple helices of procollagen I, II and III; Gal: galactose residue; Glu: glucose residue; redrawn from Nimni (1988) [5].

of the other (**Figure 1b**). Such a bond is known as a peptide bond, and the molecule created dipeptide. The chain can be lengthened by the addition of more amino acids forming polypeptides. Polypeptides containing more than 100 amino acids are usually called proteins. Proteins contain negatively charged amino acids and, therefore, have a net negative charge [2, 3].

Proteins are very versatile and have a variety of different functional properties, which are determined not only by the R-groups on their constituent amino acids, but also by their shape. The primary determinant of shape is the sequence of amino acids (primary structure). The 20 major amino acids present in the human body, can be linked in a high number of combinations, creating proteins that vary in shape and function. Changing the identity of a single amino acid out of 10,000 or more in a protein may significantly alter its functional properties. Further levels of structural complexity include the secondary, tertiary, and quaternary structures. The secondary structure appears as parts of the polypeptide chain, which are bonded together by hydrogen bonding. This usually creates a simple spiral, known as α-helix, or less often a flat pleated sheet, or both. The tertiary structure results primarily from interactions between the polypeptide chain and the surrounding water molecules, and partly from interactions between the R-groups of amino acids in different parts of the molecule. Structural proteins contain several polypeptide chains; each one with its own secondary and tertiary structure. Interactions between these chains determine the quaternary structure of these proteins. The

tertiary and quaternary structure of complex proteins depends not only on their amino acid sequence, but also on the local environmental characteristics, with small changes in the ionic composition, temperature, or pH affecting protein function [1–3].

2.1. Collagen fibers

Collagen is the major insoluble fibrous protein and the basic structural element for soft and hard tissues, supporting elements in the ECM. It is the main load-carrying element giving mechanical integrity and it is present in a variety of structural forms in different tissues. Collagen contains large domains of helical conformation, created by three α-helix polypeptide chains, each containing 1050 amino acids. The individual α-helix chains are left-handed helices with approximately three amino acid residues per turn. The chains are, in turn, coiled together to give a right-handed coiled triple helix (**Figure 1c**), which is the molecular basis of tropocollagen, the precursor of collagen. All collagens have been shown to contain three α-helix chains of similar structure, with each collagen type differentiating its individual properties mainly by incorporating segments that do not follow the triple helix conformation, and fold the collagen molecule into different kinds of three-dimensional structures [3]. The collagen molecule contains a high amount of three amino acids, including Gly, proline (Pro) and hydroxyproline (HYP), and since the latter is unique in collagen (elastin contains minute amount), the collagen content in a tissue can be easily determined by a HYP assay. The characteristic repeating amino acid sequence of the collagen molecule is Gly-X-Y, where X and Y can be any amino acid but are often proline and HYP and less often lysine (Lys) and hydroxylysine (Hyl) [4]. In the amino acid sequence of the collagen molecule every third residue is Gly (**Figure 1c**), whereas proline and HYP follow each other relatively frequently [3, 5, 6]. Hydrogen bonding between the peptide bond NH of Gly and the peptide carbonyl (C=O) group in an adjacent polypeptide (**Figure 1b**), holds the three α-helix peptide chains together in a three-stranded helix, which is formed due to the fixed angle of the C-N peptidyl-Pro or peptidyl-HYP bond [3]. In addition, the α-helixes are cross-linked via Lys, whereas collagen III also contains cysteine (Cys) that can be cross-linked within molecules through disulfide bonds [7]. The side chains of the amino acids of the collagen molecule are highly non-polar and, hence, hydrophobic, seeking the greatest number of contacts with the non-polar side chains of other amino acids. In cases that the hydrophobic contact is destroyed by a solution such as urea, ultrastructural changes are generated in the collagen fibers, such as shrinking [7, 8]. Collagen stability is also affected by the water content in its intra- and inter-chain structure. Specifically, when the water content is decreased the collagen structure gets destabilized, whereas lyophilized collagen also demonstrates decreased solubility [7, 8].

Depending on the source of tissues the collagen chains are different. A characteristic example is demonstrated in **Figure 1d**, which shows the triple helix conformation of three types of collagen, differing in α-helix composition and degree of glycosylation. The amino acid compositions of these chains are listed in **Table 1**. The collagen α-helix chains are synthesized by ribosomes attached to the rough endoplasmic reticulum (ER) as longer precursors called pro-α-helix chains. Subsequently, the pro-α-helix chains undergo a series of covalent modifications in the ER and fold into triple-helical procollagen molecules (**Figure 1d**) before they are released from the cells. Specifically, short non-triple-helical segments at either end (C– and N–terminus) of the pro-α-helix chains, called propeptides and containing Hyl, are covalently linked by disulfide bonds to form

trimers and align the three α-helix chains prior to the triple helix formation in the ER. In addition, specific Pro and Lys residues in the middle of the chains are hydroxylated by hydroxylases, and asparagine-linked oligosaccharides are added to the C-terminal propeptide, whereas galactose (Gal) or galactose-glucose (Gal-Glu) residues are attached to Hyl residues, in a process known as glycosylation [4]. Glycosylation is a common form of post-translational modification of proteins that occurs during processing in the ER and provides intrinsic stabilization of the protein structure and, thus, increases protein half-life and protects them against denaturation or proteolytic degradation [9–11]. The modifications of the α-helices in the ER facilitate their zipping from C- to N-terminus to form stable triple helices in the procollagen molecule. These modifications also allow the binding of the chaperone protein Hsp47 to the procollagen, which has been suggested to further stabilize the helices and/or prevent premature aggregation of the trimers [4]. The modification of the procollagen in the ER is crucial for the subsequent formation of mature collagen,

Amino acid	α1(I)*	α2(I)*	α1(II)*	α1(III)*	Elastin	Microfibril	Tropoelastin
Half-cysteine					4	48	0
Hydroxyproline	Content included in Others				26	151	39
Aspartic Acid	42	44	43	42	21	228	21
Glutamic Acid	73	68	89	71			
Proline	124	113	120	107	595	356	541
Alanine	115	102	103	96			
Valine	21	35	18	14			
Leucine	19	30	26	22			
Methionine	Content included in Others						
Tyrosine							
Phenylalanine							
Isoleucine							
Histidine							
Lysine	26	18	15	30	13	105	55
Arginine	50	50	50	46			
Glycine	333	338	333	350	324	110	334
4-Hydroxyproline	108	93	97	125			
Threonine	16	19	23	13			
Serine	34	30	25	39			
Others**	38	63	72	18			

*I, II and III indicate residues of collagen I, II and III α-helices, respectively.
**Others include 3-hydroxyproline, half-cysteine, methionine, isoleucine, tyrosine, phenylalanine, hydroxylysine, histidine, gal-hydroxylysine, and glc-gal–hydroxylysine.

Table 1. Amino acid residues per 1000 total residues in human collagen [6, 20] and elastin [7].

whereas defects in this process have been reported to have serious consequences. For example, hydroxylation requires the facilitation of vitamin C, and cells deprived of it cannot hydroxylate the procollagen chains sufficiently to form stable triple helices. As a result, non-hydroxylated procollagen chains are degraded within the cell and no collagen fibers can be formed [12]. As a result, in tissues where the turnover (degradation and replacement) of the collagen occurs relatively rapidly, such as in blood vessels and heart valves that experience significant collagen fiber damage due to the repetitive deformation during normal function, the gradual loss of preexisting ECM collagen, which is not supplemented by newly-formed collagen, leads to tissues that are extremely fragile and prone to disintegration [13]. However, in other tissues, such as bone, the turnover of collagen is very low, with collagen molecules reportedly remaining intact for about 10 years [13]. Following the post-translational modification in the ER, the procollagen molecules are transported to the Golgi apparatus, where they are associated laterally to form small bundles, before they are secreted in the extracellular space (exocytosis). Following exocytosis, procollagen peptidases cleave the N-terminal and C-terminal propeptides, transforming the procollagen to tropocollagen molecules, approximately 300 nm long and 1.5 nm in diameter [14]. This allows the tropocollagen molecules to assemble into collagen fibrils by covalent cross-linking between two Lys or Hyl residues at the C-terminus of one tropocollagen molecule with two similar residues at the N-terminus of an adjacent molecule. These cross-links stabilize the packing of the tropocollagen molecules in a quarter-staggered array architecture (**Figure 2a**), generating strong fibrils with a diameter of 50–200 nm and several micrometers long, depending of the species and tissue, with a cross-striated appearance under transmission electron microscopy (**Figure 2b**) [3–6]. The striation has a period (D) of approximately 67 nm, with the lighter part of the striation representing a gap of approximately 0.6D between successive molecules (**Figure 2b**) [6, 15]. The covalent cross-linking between Lys and Hyl residues of adjacent collagen molecules confers significant strength to the collagen fibrils. This type of covalent bonding is only found in collagen and elastin, and its inhibition results in a dramatic reduction of the tensile strength of the fibrils, making tissues fragile and prone to tearing. The extent and type of cross-linking vary from tissue to tissue; in tissues where tensile strength is crucial, collagen is highly cross-linked [13]. Although the alignment of the tropocollagen molecules in the collagen fibril has been idealized as perfectly straight and parallel in **Figure 2a**, in reality they are bent in various degrees, depending on the attachment of water molecules, and have varying spacing between neighboring molecules [6]. Bundles of collagen fibrils form collagen fibers, with diameters ranging between 0.2 and 12 μm, and increasing with age, whereas their length depends on the tissue [16, 17]. Moreover, collagen fibers appear to be crimped (**Figure 2c**), and when the tissue is stretched the amplitude of the crimp decreases [6, 18, 19]. It has been suggested that the crimping of the collagen fibers is generated by the shrinking of the non-collagenous components of the ground substance, which causes collagen fiber buckling [19], whereas enzymatic digestion of the non-collagenous components of the ground substance alters the mechanical properties of the tissue [6].

Collagens are differentiated in terms of their ability to form fibers and organize the fibers into networks. There are at least 20 types of collagen that have been identified and participate in the formation of the ECM of tissues [4]. Among these, types I, II, II, V and XI are fibrillar collagens, with types I, II, III comprising 80–90% of the total collagen in the body [3]. Collagen I is present in almost any tissue, but it predominantly present in bone, dermis, placental membranes, tendons, ligaments, blood vessels and heart valves. Collagen II is mainly located in
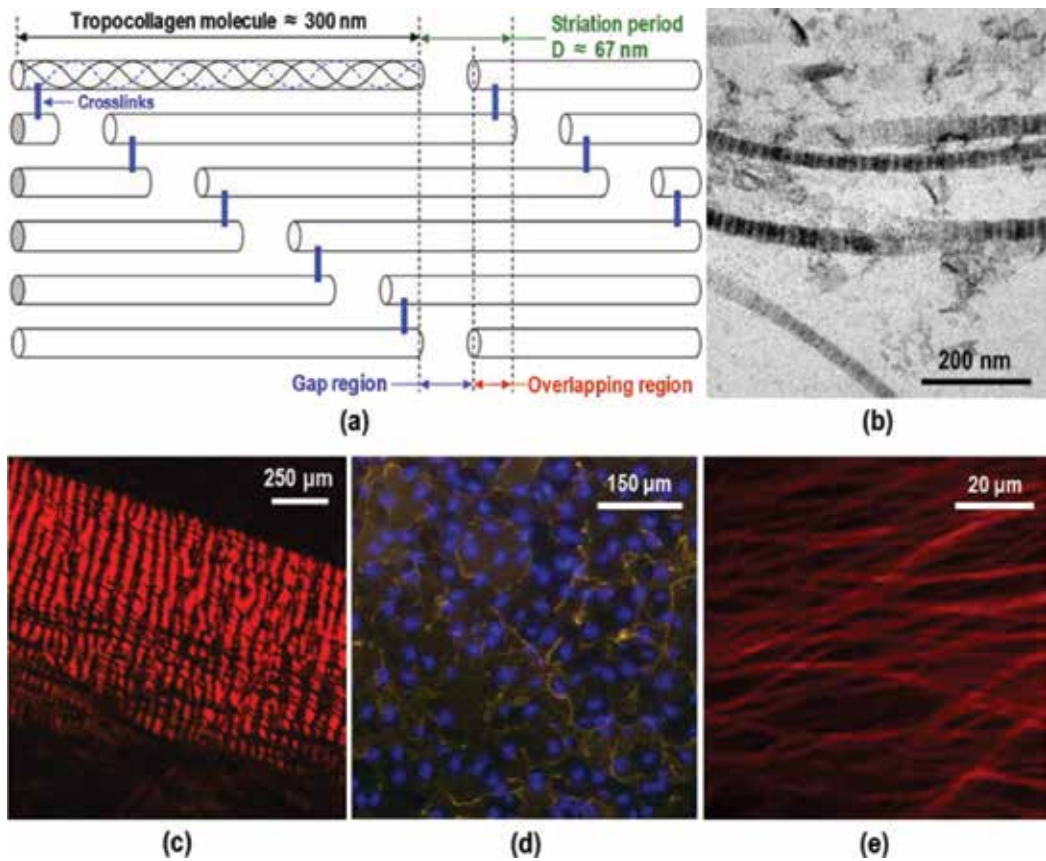
Figure 2. (a) Quarter-staggering of tropocollagen I molecules in collagen fibrils; redrawn from Lodish et al. (2003) [4]. (b) Transmission electron microscopy of the decellularised mitral valve leaflet showing the striations in the collagen I fibrils; adopted with permission from Granados et al. (2017) [68]. (c) Histological section of the anterior mitral valve leaflet stained with sirius red under polarized light, showing the crimping in the collagen I fibers; adopted with permission from Roberts et al. (2016) [18]. (d) Immunofluorescence staining for collagen IV produced by human endothelial cells seeded on culture plastic (yellow/orange: anti-collagen-IV; blue: Hoechst stain for nuclei); adopted with permission from Pflaum et al. (2017) [132]. (e) Two photon microscopy of the atrial surface of the native anterior mitral valve leaflet, showing the elastin in the elastic fiber network.

hyaline cartilage and cartilage-like tissues and the vitreous body of the eye [20]. Similarly to collagen I, collagen III is also quite common in most tissues and represents a major constituent of blood vessels and heart valves, as well as other more distensible connective tissue. Collagen V has a similar distribution to collagen I, but it is a minor constituent in the tissues, whereas collagen XI is found mainly in cartilage and is distributed similarly to collagen II [21]. Collagen VI and IX represent a separate class of collagens that are associated to fibrillar collagens, linking them to each other or to other ECM components. The collagen VI tropocollagen comprises short triple-helical regions of approximately 60 nm long, separated by globular regions of approximately 40 nm long [3]. Collagen VI is common in placental villi [6] and has also been found in many other connective tissues, where it is bound to collagen I fibrils and has been suggested to enable the formation of thicker collagen I fibers [3]. Collagen IX is a proteoglycan in that one of its polypeptide subunits serves as the core protein for a chondroitin

sulfate side chain [6]. The collagen IX molecule comprises two long triple helices connected by a flexible link, on the $\alpha2(IX)$ chain of which the chondroitin sulfate glycosaminoglycan (GAG) chain is covalently linked to [3, 6]. Collagen IX does not assemble into fibrils, due to its interrupted triple-helical conformation. Nevertheless, it is bound along collagen II fibrils at regular intervals, binding them to the GAG- and proteoglycan-rich ECM, and also reportedly contributing to their assembly in collagen II fibers [22]. In addition to collagen IX, collagens XVIII and XV also function as core proteins in proteoglycans.

Collagen IV is a sheet-forming collagen, which is of particular importance for endothelialized and epithelialized tissues, since, together with laminin, is the primary component of all basal laminae, forming their basic two-dimensional fibrous network. Collagen IV, as well as most of the other ECM components that form the basal laminae, is synthesized by the cells that reside on it (**Figure 2d**) [4]. The collagen IV molecule is formed by a 400-nm-long triple helix with large globular domains at the C-terminus and smaller non-collagen ones at the N-terminus, whereas Gly-X-Y sequences of its α-helices are interrupted with segments that do not form a triple helix, and introduce flexible links and flexibility into the molecule [3, 4]. Following exocytosis into the extracellular space, adjacent collagen IV molecules assemble either into groups of 4 molecules by association of their globular N-terminus domains, yielding tetrameric units, or into pairs by association of their globular C-terminus domains, yielding dimeric units [4]. Subsequently, triple-helical regions from several tetrameric and dimeric units associate laterally, similarly to the case of fibril formation in fibrillar collagens, to form branching two-dimensional mesh-like fibrous networks to which other ECM components and adhesion receptors can bind (**Figure 2d**). In addition to the aforementioned types of collagen, other minor classes of collagens include anchoring collagens, such as collagen VII, which connects the basal lamina to the underlying connective tissue, transmembrane collagens, which function as cell adhesion receptors, and host defense collagens, which help the body to recognize and eliminate pathogens [4].

Collagen is encoded by approximately 30 genes, whereas its biosynthetic pathway involves a number of post-translational phases. Owning to this, collagen-related disease most commonly arise from genetic mutations affecting collagen encoding or post-translational modifications, whereas nutritional deficiencies might also affect the post-translational modifications, assembly, or secretion of collagen [1, 13]. Moreover, autoimmune conditions have also been reported to affect collagen fibers, whereas a number of different bacteria and viruses can degrade collagen or interfere with its production pathway [1]. Goodpasture's autoimmune disease causes self-attacking antibodies to bind to the α-helices of collagen IV, setting off an immune response that causes cellular damage [4]. The Ehlers-Danlos syndrome comprises at least 10 types of congenital disorders whose principal features include tissue hyper-extensibility and abnormal fragility. Type IV disorder is the most serious one, especially for the cardiovascular system, which affects collagen III and is associated with spontaneous rupture of arteries or the bowel [1, 13]. Type VI disorder, together with the Bruck syndrome and Menkes disease, are associated with lysyl hydroxylase deficiency, leading to defective cross-linking of collagen and elastin [1, 4, 23], whereas type VIIC disorder causes formation of abnormally thin and irregular collagen fibrils [1]. Moreover, the Alport syndrome is another genetic disorder that alters the C-terminal domain of the tropocollagen IV α-helices and affects the structure of collagen IV fibers, causing structural abnormalities in basal laminae [1, 4].

2.2. Elastic fibers

Elastin is an another structural insoluble fibrous protein, forming a large proportion of the ECM of arteries and veins, especially near the heart, and in other deformable tissues such as ligaments, heart valves, skin, lungs and areolar connective tissue. Elastin is the dominant ECM protein in arteries, contributing about 28–50% of the dry weight of the aorta [13, 23, 24], whereas in elastic ligaments and tendons the elastin content attributes 50 and 4% of the dry weight, respectively [23]. Elastin is the main component of the elastic fibers, which are major insoluble assemblies of the ECM that generate resilience into the tissues by providing a mechanism that permits tissues to deform under load and passively recoil to their original configuration after the load is released, preventing dynamic tissue creep [13, 24–26]. These properties are critical to the function of heart valves, which undergo repeated dynamic cycles of large extension and recoil during opening and closing. In addition to contributing to ECM resilience, the elastic fibers are also an important load-bearing structure, complementing the function of the collagen fibers at the sites where mechanical energy needs to be stored [25]. In particular, the elastic fibers dictate tissue mechanics at low strains before the stiffer collagen fibers are engaged at higher strains [24]. Elastic fibers are the most linearly elastic biosolids known, and are at least five times more extensible than rubber. They are generally twisted or straight with a diameter ranging between about 0.2 and 1.5 μm forming coarse networks (**Figure 2e**) [27]. In dense elastic tissues, such as the arteries, the elastic fibers fuse during development to form flattened co-centric sheets, or elastic laminae, with numerous fenestrations [17, 28, 29].

The elastic fibers are complex structures that comprise several components, with elastin and microfibrils constituting their two major ones [30]. Ultrastructurally, elastic fibers are composed of a homogeneous inner core of laterally packed, thin cross-linked elastin filaments that make up more than 90% of fibers, and an outer fibrillar mantle that consists of microfibrils and surrounds the elastin, accounting for 5–10% of the elastic fibers [23, 25, 26]. The amino acid compositions of these components are given in **Table 1** [7]. The microfibrils are organized into 8–16 nm beaded fibrils and are predominantly made of five distinct proteins, including two fibrillin glycoproteins (fibrillin-1 and fibrillin-2) and two microfibril-associated glycoproteins (MAGP-1 and MAGP-2) [13, 23, 31]. Additional components of the elastic fibers include lysyl oxidase, elastin-binding protein (EBP), proteoglycans, osteopontin, emilin, fibulin-1, and various microfibril-associated proteins [23]. Early development of the elastic fibers involves the assembly of fibrillin molecules in the extracellular space, in enfoldings of the cell surface, into head-to-tail microfibrillar arrays of approximately 160 nm in length that are cross-linked by transglutaminase to form mature beaded microfibrils. Transglutaminase forms γ-glutamyl-e-Lys isopeptide bonds within or between peptide chains [25, 29]. The mature microfibrils, which have a length of approximately 100 nm, form loosely-packed parallel bundles with an one-third-staggered architecture, that have been hypothesized to be stabilized by inter-microfibrillar crosslinking [25]. Non-stretched microfibrils have been reported to have a beaded periodicity of approximately 56 nm, whereas models have predicted up to 8 fibrillin molecules in the microfibril cross-section [25, 27, 31, 32].

Following the formation of the microfibril bundles, intracellularly-produced tropoelastin [33] is gradually deposited among the preformed template of fibrillin-rich microfibrils, until the elastic fibers reach full maturation [7, 23, 25, 26]. Some tissues, even at their mature state, contain bundles of microfibrils devoid of tropoelastin (oxytalan fibers), as well as sites where bundles

of microfibrils are only partially intermixed with tropoelastin (elaunin fibers), and never developed into fully mature elastic fibers [26]. These microfibril states represent interruptions in successive phases of elastic fiber development, indicating that microfibrils can be both progenitors of fully mature elastic fibers in fetal tissues, and independent connective tissue components (oxytalan fibers) [26, 34]. Tropoelastin is the soluble precursor of elastin, which is synthesized by fibroblasts and smooth muscle cells (SMCs) and secreted as a soluble and highly hydrophobic monomer of about 750 amino acids long [13, 24, 35]. Similarly to tropocollagen, tropoelastin contains an abundance of Pro and Gly, but is not glycosylated and contains minute amounts of HYP and no Hyl [13]. Human tropoelastin contains more than 30% Gly, whereas about 75% of its amino acid sequence is made up of just four hydrophobic amino acids, including Gly, valine (Val), alanine (Ala) and Pro [23]. Structurally, tropoelastin comprises two types of alternating segments, including hydrophobic segments and Ala-/Lys-rich α-helical segments, which form cross-links between adjacent molecules [13]. During tropoelastin deposition among the microfibrils, the latter get displaced to the periphery of the growing fiber, allowing the formation of the elastin core by the accumulation of tropoelastin molecules [13, 31]. The accumulated tropoelastin molecules couple covalently to each other by lysyl oxidase-derived cross-links, to form the polymeric elastin, stabilizing the elastin core of the elastic fibers [25, 31]. Lysyl oxidase catalyzes the selective oxidative deamination of Lys residues in tropoelastin, leading to the formation of bi-functional (dehydrolysinonorleucine and allysine aldol), tri-functional (dehydromerodesmosine) and tetra-functional (desmosine and isodesmosine) crosslinks [25]. The resulting cross-linked mature elastin is a very stable and persistent structure that is extremely hydrophobic and insoluble due to the extensive cross-linking at Lys residues [23]. The high stability of elastin has been attributed to the low content of polar amino acid residues, including the anionic Lys, histidine (His) and arginine (Arg), as well as the cationic aspartic acid (Asp) and glutamic acid (Glu) [7].

The elastic recoil generated by the elastic fibers is a critical attribute for tissues that are required to undergo repetitive stretch/relaxation cycles. Tropoelastin is among the most elastic proteins, with a capacity to stretch eight times its resting molecular length ($\approx$20 nm) and recoil without damage, while showing no hysteresis after repeated stretch and relaxation cycles, demonstrating a near perfect spring behavior with minimal energy loss [36, 37]. Atomic force microscopy studies have estimated the Young's modulus of tropoelastin to approximately 3 kPa [37], which is two order of magnitudes smaller (more flexible) than mature cross-linked elastin, estimated between 0.6 and 1.1 MPa [6, 35], four orders of magnitude smaller than microfibrils, estimated between 78 and 96 MPa [38], and six orders of magnitude smaller than mature cross-linked collagen I, estimated between 1 and 1.2 GPa [6, 35]. Given the fact that elastin and elastic fibers are robust structures that effectively last for the lifetime of the organism, studies have suggested that the elastic recoil generated in the elastic fibers cannot be a result of the stressing of the chemical bonds, since this would lead to the fiber deterioration [32]. Several studies have proposed that elastic recoil could be potentially attributed to the change in the number of conformation states of the cross-linked polypeptide chains during stretching and relaxation [6, 7, 13, 39]. Elaborating, under relaxed conditions the cross-linked polypeptide chains adopt a loose random coil conformation, which results in an increased number of different intramolecular conformational states in the chains. Under stretching,

the chains adopt a relatively aligned conformation, limiting their conformational freedom and, thus, decreasing their entropy. Under relaxation, the chains resume their random conformation, increasing the number of different conformational states and, thus, their entropy. This change in the entropy of the cross-linked chains has been suggested to provide the free energy for the elastic recoil [6, 23, 32]. Along these lines, it has been suggested that intramolecular folding of fibrillin molecules at their termini and Pro-rich regions, and at flexible sites between 8-Cys motifs, provides the extension/recoil mechanism of microfibrils [25, 27]. Similarly, cross-linked mature elastin has been suggested to derive its high elasticity from the cross-linking of Lys residues into desmosine, isodesmosine, and lysinonorleucine [7].

In contrast to collagens that can be encoded by large gene families, there is only one gene (ELN) that is responsible for synthesizing tropoelastin [40, 41]. Tropoelastin is mainly synthesized *in utero* and early childhood, whereas by middle-age only a small amount of this molecule is produced [23, 42]. Owing to this, elastin is the longest lasting protein in the body, with a half-life of approximately 74 years [23, 43]. However, in the event of elastin damage due to acquired disease or aging, the low levels of tropoelastin produced mean that elastic fibers cannot be repaired sufficiently. Along these lines, loss of elasticity, due to degradative changes in elastic fibers, is a major contributing factor in connective tissue aging, and aortic aneurysm development [23, 25, 44, 45]. Elastic fiber degradation has also been reported to occur in atherosclerosis, with atherosclerotic vessels presenting increased stiffness, together with calcium and lipid accumulation in the elastic fibers [23, 46].

In the case of genetic disorders, mutations in the genes of the components of the elastic fibers have been associated with congenital disorders in elastic fiber-rich connective tissues. Specifically, Marfan syndrome and other overlapping disorders, such as MASS (mitral valve prolapse, aortic dilation, and skin/skeletal manifestations) syndrome, and autosomal TAAD (thoracic aortic aneurysms and dissections) [47], termed fibrillinopathies [48], have been associated with fibrillin-1 mutations, leading to increased fragmentation of the elastic fibers that, in turn, lead to life-threatening cardiovascular disease and severe skeletal and ocular defects [13, 25, 38]. Progressive aortic valve root dilation, aortic dissection and rupture, and aortic or mitral valve regurgitation are the most serious conditions associated with Marfan syndrome, with a 90% mortality rate in these patients. Neonatal patients with Marfan syndrome die perinatally from congestive heart failure and valvular deficiency [38].

Increased fragmentation of the elastic fibers has also been reported in cutis laxa and Menkes disease, the latter of which is associated with tortuous blood vessels and abnormalities in other tissues [23]. Moreover, the pseudoxanthoma elasticum and Buschke-Ollendorff syndromes have been associated with fragmentation, clumping and calcification of elastic fibers, leading to cardiovascular defects [23, 25]. Elastin mutations that cause elastin deficiency have been reported to cause reduced elastin content and disruption in the architecture of aorta and heart valves in Williams syndrome and supravalvular stenosis (SVAS) [23, 25, 29]. Elastin has been reported to induce actin stress fiber organization and inhibit SMC proliferation [24], indicating that apart from its structural role, elastin has a role in arterial morphogenesis [23]. Owing to this, reduction in the elastin content causes narrowing of the aorta and other arteries, and SVAS [23, 25], due to the excessive proliferation of SMCs [13, 24].

3. Glycosaminoglycans and proteoglycans

GAGs (also termed mucopolysaccharides) are the most abundant unbranched hetero-polysaccharides in the body, composed of repeating disaccharide units [1]. Disaccharides are formed by two simple sugars (monosaccharides; basic units of carbohydrates), which are joined by dehydration synthesis. Polysaccharide chains are large, stiff and complex molecules that exist in tissues as highly viscous materials that interact with proteins and readily bind both water and cations. The GAGs derive their name from the fact that one of the two sugars in their repeating disaccharide unit is always an amino sugar, either N-acetylglucosamine (N-acetyl-D-glucosamine; GlcNAc) or N-acetylgalactosamine (N-acetyl-D-galactosamine; GalNAc) [1, 7, 13]. The other of the two sugars is usually either an uronic acid (glucuronic acid or iduronic acid) or D-galactose [1, 4, 13], whereas one or both of the sugars contain at least one anionic group (carboxyl or sulfate) [4], rendering GAGs highly negatively charged [13]. Owing to the relatively high stiffness and hydrophilicity of the polysaccharide chains, GAGs form extended conformations with a large volume to mass ratio, forming hydrated gels even at very low concentrations, and imparting high viscosity and, thus, low compressibility, to the ECM. The gel-forming character of the GAGs is due to their high negative charge that attracts cations, especially Na^+, which causes large osmotic inflow of water into the ECM, creating a swelling pressure that enables the ECM to withstand compressive loads [1, 13]. The GAG gels can form with varying pore size and charge density, and it has been suggested that they act as selective sieves to regulate molecule and cell traffic according to their size and charge [13]. Although GAGs constitute less than 10% of the weight of the fibrous proteins in the ECM of connective tissues, their high volume to weight ratio and gel-forming ability enables them to fill most of the extracellular space, providing mechanical support to the tissue [7, 13], as well as lubrication between tissue (joints) and elastic and collagen fibers [2, 6].

Depending on the type of the repeating disaccharide unit, type of linkage between the sugars, and number and location of sulfate groups, GAGs are classified into four groups, including (i) hyaluronic acid, (ii) heparan sulfate and heparin, (iii) keratan sulfates (I and II), and (iv) chondroitin sulfates (chondroitin 4-sulfate and chondroitin 6-sulfate) and dermatan sulfate (**Table 2**) [1, 4, 13]. Hyaluronic acid is the simplest GAG and the only one that it does not contain any sulfate or attach covalently to proteins as a proteoglycan. However, it does form complexes with proteoglycans in the ECM, non-covalently [7]. All other GAGs contain sulfate groups, either as O-esters or as N-sulfate (in heparin and heparan sulfate) [1]. Heparin is a hyper-sulfated form of heparan sulfate that produced by mast cells and is an important anticoagulant that can activate the antithrombin III clotting inhibitor in plasma [1, 4]. It can also bind to the lipoprotein lipase, which is a membrane-associated enzyme present in capillary walls that hydrolyzes triglycerides to fatty acids, causing its release into the circulation [1, 4]. Hyaluronic acid is abundant in embryonic tissues and has been suggested to play an important role in facilitating cell migration during morphogenesis and wound repair, whereas high concentrations of hyaluronic acid, as well as chondroitin sulfates, in tissues contribute to their compressibility. Keratan sulfates and dermatan sulfate lie between collagen fibrils and play a critical role in their alignment. Heparan sulfate is associated with cell membranes and has been suggested to act as a receptor mediating in cell growth and cell-cell and cell-ECM communication [1]. In adult tissues, GAGs have a slow turnover, with half-lives between days and weeks [1].

With the exception of hyaluronic acid, all GAGs are found covalently linked to a polypeptide chain, or core protein, forming proteoglycans that are synthesized by most cell types [4]. Proteoglycans is a diverse group of highly glycosylated glycoproteins, which are distinguishable from other glycoproteins by the nature, quantity, and arrangement of their sugar side chains [13]. Proteoglycans feature at least one GAG side chain, whereas their carbohydrate content can reach up to 95% of their weight [1, 13]. On the other hand, the carbohydrate content of glycoproteins is between 1 and 60% of their weight, an is present in the form of numerous relatively short, branched oligosaccharide chains [2, 13]. Proteoglycans have the potential of almost limitless heterogeneity [13], differentiating in the type of core protein, number and types of GAG chains, and number of disaccharide modifications by sulfate groups [1, 4, 13]. Some of the most common proteoglycans that have been characterized are listed in **Table 2**. Similarly to other proteins, the core proteins of proteoglycans are synthesized by ribosomes attached to the ER, and translocated into the lumen of the ER. Subsequently, the core protein is transported to the Golgi apparatus where it is glycosylated [1, 2]. During glycosylation, the GAGs are linked to their core proteins in one of three different modes. The first two modes involve the formation of O-glycosidic bonds between the hydroxyl side chains of serine (Ser) residues in the core protein and a xylose (Xyl) residue, which is unique to proteoglycans, or between Ser residues in the core protein and GalNAc residues in the GAG chain (keratan sulfate II). In the first case, two Gal residues are subsequently added to the Xyl residue sequentially, forming a link trisaccharide (-Gal-Gal-Xyl-) that serves as a polysaccharide growth primer, followed by further linear growth of the GAG on the Gal terminal of the link trisaccharide (**Figure 3**). The third mode involves the formation of N-glycosylamine bonds, as found in N-linked glycoproteins, between the amide nitrogen of asparagine (Asn) residues in the core protein and the GlcNAc residues of the GAG chains [4, 13]. Subsequently, the polysaccharide chains are often modified in the Golgi apparatus by the covalent linkage of

GAG	Localization	Small Proteoglycans		Large Proteoglycans		
Hyaluronic acid	Synovial fluid, vitreous humor, loose connective tissue, heart valves, blood vessels	-		-		
Heparan sulfate	Basal laminae, cell surface, blood vessels, liver, skin	Bikunin	Decorin, Biglycan, Betaglycan	Testican, Syndecan-1	Neurocan, Aggrecan, Brevican	Versican	Perlecan
Chondroitin sulfate	Heart valves, blood vessels, basal laminae, cartilage, bone, cell surface					
Dermatan sulfate	Heart valves, blood vessels, skin					
Keratan sulfate	Cornea, bone, cartilage	Fibromodulin, Lumican		Aggrecan (with Chondroitin sulfate)		

Table 2. Prevalent localization of different GAG types and their associated proteoglycans.
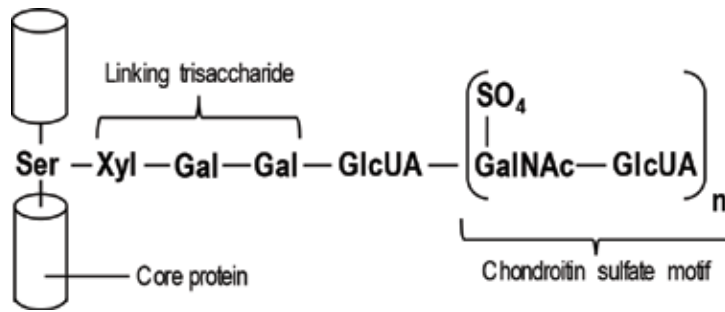
Figure 3. Biosynthesis of proteoglycans, showing the case of the linking of chondroitin sulfate chains to their core protein. Ser: serine residue; Gal: galactose residue; GlcUA: glucuronic acid residue; Xyl: xylose residue. Modified from Alberts et al. (2014) [13] and Lodish et al. (2003) [4].

small molecules, such as sulfate groups onto GalNAc and other moieties and the epimerization of GlcUA to IdUA residues. Following glycosylation, the completed proteoglycan is then exported in secretory vesicles to the ECM [1, 4, 13].

In the extracellular space, proteoglycans bind various secreted signal molecules, such as growth factors, enhancing or inhibiting their signaling activity [13]. They also bind to other types of secreted proteins, including proteases and protease inhibitors, regulating their activities [1, 4]. Moreover, GAGs and proteoglycans can associate to each other to form big aggregates. Such a case is the aggrecan proteoglycans, which comprise chondroitin sulfate and keratan sulfate, and assemble with hyaluronic acid. GAGs and proteoglycans also associate with fibrous proteins, such as collagen and basal laminae, creating extremely complex structures. Such a proteoglycan is decorin, which comprises chondroitin sulfate and dermatan sulfate, and binds to collagen fibrils, aiding in collagen fiber formation. Decorin deficiency has been reported to lead to reduced tensile strength in tissues [13, 49–52]. Another proteoglycan of this type is perlecan, which is major proteoglycan of basal laminae, consisting of heparan sulfate and chondroitin sulfate chains linked to a large multi-domain core protein. Perlecan is incorporated in the basal laminae by binding to both laminin and collagen IV, connecting the two networks, and defining the structure and function of basal laminae. Owing to its multi-domain components, perlecan can also cross-link cell surface molecules to ECM components [4]. In addition to proteoglycans that fully reside in the extracellular space, some proteoglycans form integral components of the cell membranes by having their core protein spanning or attached to the lipid bilayer of the cell membrane. Such proteoglycans are the syndecans, which comprise three chondroitin sulfate and heparan sulfate chains and are expressed by many cell types, including epithelial cells and fibroblasts [13, 53–55]. Syndecans bind to ECM collagens and other ECM proteins such as the fibronectins, anchoring cells to the ECM, while interacting with the intracellular actin cytoskeleton [4].

The importance of GAGs and proteoglycans is emphasized by the severe developmental defects that can occur when specific proteoglycans are inactivated by mutation. A number of congenital enzyme deficiencies have been linked to GAG metabolic disorders (mucopolysaccharidoses) [13]. Among mucopolysaccharidoses, the Hurler [56–59] and Hunter [60–62] syndromes are the most widely studied. Mucopolysaccharidoses are associated with mutations in the gene encoding lysosomal hydrolases, including endoglycosidases and exoglycosidases,

which are enzymes involved in GAG degradation [56, 57, 62]. Absence or malfunctioning of lysosomal hydrolases lead to GAG accumulation in various tissues, including liver, spleen, bone, skin, and central nervous system [1, 60, 61]. Moreover, severe congenital deficiency in dermatan sulfate synthesis leads to a short stature, prematurely aged appearance, and generalized defects in the skin, joints, muscles, and bones of individuals [13]. GAGs and proteoglycans have also been associated with major diseases, such as cancer and atherosclerosis, and aging. The intima of arterial walls contains, among others, dermatan sulfate proteoglycans, which are synthesized by arterial SMCs and bind plasma low-density lipoproteins that are involved in atherosclerotic plaque development. Since atherosclerotic lesions feature increased proliferation of SMCs, the dermatan sulfate content is increased in these sites, suggesting a potential role of this GAG in atherosclerotic plaque development [63]. Moreover, the amount of chondroitin sulfate diminishes with age, whereas the amounts of keratan sulfate and hyaluronic acid increase. These changes may contribute to conditions, such as osteoarthritis, and other degenerative diseases, as well as the characteristic changes in aged skin in the elderly [1, 2].

4. Structure and constituents of normal heart valves

Depending on the functional requirements for a particular tissue, the organization of fibers, cells and other ECM macromolecules in the tissue and, thus, the mechanical properties of the tissue vary. The simplest structure from the point of view of the collagen fibers consists of parallel fibers as in tendons and ligaments. The 2D and 3D networks of the skin are more complex, whereas the structures of aortic, pulmonary, mitral and tricuspid valves in the heart are the most complex ones. The structure of the heart valves is adapted to allow unidirectional and unobstructed passage of blood without regurgitation, trauma to blood elements, thromboembolism, and excessive stress concentrations in the valve leaflets and supporting tissue. The cellular and extracellular elements of normal valves accommodate repetitive changes in shape and dimension throughout the cardiac cycle. They provide effective stress transfer to the annulus and adjacent tissue, and mediate functional remodeling and repair of injury caused by the large repetitive deformations. The aortic and pulmonary valves comprise three similar-size leaflets, and are located between the left ventricle and aorta, and the right ventricle and pulmonary artery, respectively. Their leaflets resemble half-moons and, thus, they are referred to as semilunar (SL) valves. The mitral valve (MV) is located between the left ventricle and left atrium, and comprises two noticeably different leaflets that resemble a bishop's miter when they are closed. The tricuspid valve is located between the right ventricle and right atrium, and comprises three leaflets. Owing to their location between the atria and the ventricles, the mitral and tricuspid valves are referred to as the atrioventricular (AV) valves. In addition to their leaflets, the AV valves also comprise fan-shaped tendinous chord (chordae tendinae) that link the AV valve leaflets to protrusions on the ventricular wall, the papillary muscles, and act similarly to the parachute chords, preventing the AV valve leaflets to prolapse into the atria when they are fully closed.

The aortic and pulmonary valve leaflets open against the aorta and pulmonary artery, respectively, during ventricular systole, whereas the mitral and tricuspid valve leaflets open against the myocardial wall of the right and left ventricle, respectively, during ventricular diastole. The semilunar valves close during ventricular diastole and the atrioventricular valves

during systole. All four valves close rapidly and completely under minimal reverse pressure, stretching to maintain full competence during diastole. During these opening and closing movements, the valve leaflets withstand cyclic strains as high as 50%, whereas despite the pressure difference across the closed valves, which imposes large load on their leaflets, leaflet prolapse is prevented by large coaptation of the leaflets, reaching up to 40% of their surfaces [18, 64–68]. Even though each of the four heart valves has its own individual unique anatomical, structural and constitutional features that are adapted to their specific localization and function, they share common structural, constitutional and functional features. Moreover, the aortic and mitral valves are the ones most prone to disease, since they reside in the high pressure environment of the left ventricle. Owing to these, the discussion in the following paragraphs is focused on the aortic and mitral valves, as representatives of the SL and AV valves, respectively. Moreover, the discussion will focus on valve leaflets, since these are the most structurally complex and constitutionally diverse components of the heart valves.

The heart valve leaflets are layered with a highly specialized ECM, which provides the basis for normal valve function. Two types of cells are present, including a layer of endothelial cells (ECs) that covers the luminal surface of the leaflets and a deep layer of interstitial cells (VICs) that consists of SMCs and fibroblasts, which replenish and remodel the valvular ECM [69]. The EC layer is continuous with the luminal surface of the atrium and ventricle, in the case of the AV valves, and ventricle and adjacent artery (pulmonary artery or aorta) in the case of the SL valves. The aortic valve leaflets comprise three distinct layers, including the fibrosa, spongiosa and ventricularis, each enriched in a different ECM component (**Figure 4a–c**, **e**). The MV leaflets present a slightly different architecture, with four layers instead of three, including a ventricularis, a fibrosa, a spongiosa and an atrialis layer (**Figure 4c**, **e**). Within these layers, the structural elements are arranged in a methodical orientation, leading to leaflet properties that are highly anisotropic. Several structural features enable the semilunar and atrioventricular leaflets to be extremely soft and pliable when unloaded and inextensible when high transvalvular pressure is applied during the time the valves are fully closed [18, 65, 70, 71]. In the case of the aortic valve, the fibrosa layer faces the outflow (aorta side) of the valve, whereas in the case of the MV the fibrosa lies below a ventricularis layer, which faces the outflow (left ventricle side) of the valve. The fibrosa in both valve types is the primary structural layer and major load bearing layer that offers the mechanical integrity of the valve leaflets [72]. The predominant constituent of the fibrosa are large amounts of highly-aligned collagen I fibers (**Figure 4c**), which are organized into large bundles and are predominantly aligned along the circumferential direction of the leaflets. The collagen I fibers of the fibrosa are surrounded by glycosaminoglycans and proteoglycans, as well as a network of elastic fibers, which maintains the microstructure of the valve leaflet during unloading [73]. This directionality of the collagen fibers results in aortic and MV leaflet structures that are considerably stiffer along their circumferential direction than their radial [18, 67, 73]. Moreover, folds in the collagen layer of the fibrosa generate a macroscopically visible corrugations on the surface of the leaflets when they are un-stretched (**Figure 4a**).

The ventricularis layer of the aortic valve is equivalent to the atrialis of the MV in function and organization, with both facing the inflow of the valves. Although these layers are less organized than the fibrosa, they still contain significant amounts of collagen I (**Figure 4c**) and radially aligned elastic fibers (**Figure 4d**). However, because the collagen is not oriented in any
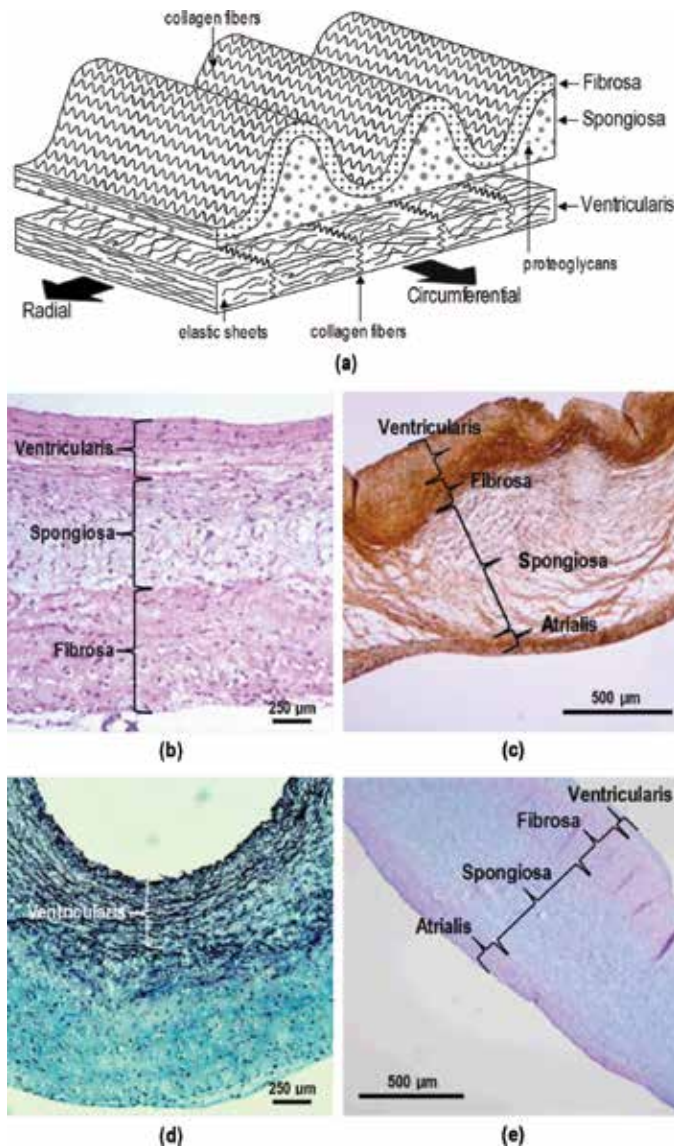
Figure 4. (a) Trilaminar leaflet structure of semilunar valves, showing the fibrosa, spongiosa and ventricularis layers, together with their major constituents. Note the macroscopically visible corrugations of the fibrosa layer. (b) H & E histological staining of the aortic valve leaflet (radial direction). ECM proteins were stained pink/light purple; cells were stained deep/purple. (c) Immunohistochemical staining against collagen I of the mitral valve posterior leaflet (radial direction). Collagen I was stained brown. (d) Miller's elastic histological staining of the aortic valve leaflet (radial direction). Elastic fibers were stained deep blue/black. (e) Alcian blue/PAS histological staining of the mitral valve anterior leaflet (radial direction), showing the ventricularis, fibrosa, spongiosa and atrialis layers; dark blue: cell nuclei; blue: acid mucosubstances (GAGs) and proteoglycans; magenta: Neutral polysaccharides.

specific direction, they tend to be more flexible than the fibrosa. The elastic fibers of the aortic valve ventricularis and MV atrialis extend when the leaflets stretch to enlarge the coaptation area, but recoil to make the leaflet smaller in the open valve phase. The ventricularis of the MV

is similar in structure and constituents to the MV atrialis and aortic valve ventricularis, with loosely arranged collagen fibers and radially-aligned elastic fibers (**Figure 5a**). The spongiosa layer is located between the fibrosa and ventricularis of the aortic valve, and between the fibrosa and atrialis in the MV. This layer is primarily composed of water, GAGs and proteoglycans (**Figure 4e**), but also contains loosely arranged collagens and elastin, which connect the fibrosa and ventricularis (or atrialis) together. Shear stresses caused by the differential movements of the leaflet layers and the shock of the valve closure are dissipated in the ground substance of the spongiosa, whose hydrophilic GAGs and proteoglycans absorb water and swell to form a deformable gel [69]. The thickness of the leaflet layers varies from the attachment site (basal area) at the valvular annulus to the free edge of the leaflets [72, 73]. At the basal area, the fibrosa comprises the thickest layer, becoming thinner and gradually overtaken by the spongiosa towards the free edge of the leaflets (**Figure 5b**). The spongiosa is the main component of both the SL and AV valve leaflets at their free edge, providing a natural shock-absorption mechanism along the coaptation region of the leaflets that dissipates the shocks of valve closure [67, 73]. The thickest regions of the leaflets, especially close to their basal regions, also feature venules and arterioles, which facilitate supplementary oxygen and nutrient transport in regions where simple diffusion is not sufficient for cell nourishment (**Figure 5a** and **b**) [18, 66, 72, 74].

During the cardiac cycle, the SL and AV valve leaflets undergo significant changes in their macroscale and microscale architectural configuration. When the valves are fully open, the gross corrugations of the fibrosa, which are caused by folds in the collagen fiber layer, produce a visible surface wrinkling (**Figure 5c**), which disappears when the leaflets are fully extended when the valve is fully closed and loaded under the peak transvalvular pressure (**Figure 5d**). During valve closing, the corrugations of the fibrosa expand along the radial direction, which is accompanied by radial stretching of the radially-aligned elastic fibers of the SL ventricularis (or MV atrialis) layer, permitting initial increase in dimension with minimal stress. Further stretching of the leaflets causes uncrimping of the collagen fibers along the circumferential direction. When the valve is fully closed, the collagen-layer folds are fully extended and the corrugations in the fibrosa are fully flattened along the radial direction, whereas collagen fibers are uncrimped along the circumferential direction. These changes produce stiffening of the leaflets, preventing their exaggerated sagging and ensuring optimal coaptation with the adjacent leaflets when the valve is fully closed [64, 69]. On the other hand, the stretching of the elastic fibers provides the energy that is necessary for the elastic recoil of the leaflets to their upstretched configuration when the valve is fully open. Moreover, the multilayered structure of the valve leaflets has been reported to contribute to the low flexural rigidity of the leaflets when the valves are fully open, possibly also due to interlayer slippage, that allows their passive interaction with the surrounding blood [75]. The multilayered leaflet structure also provides additional support during valve closure and coaptation, assisting the extended collagen fibers to generate a stiffened leaflet structure that prevents exaggerated sagging under the high transvalvular pressure [73].

In addition to collagen I, collagens III, IV, V and VI have also been identified in the heart valves [72, 76–78]. Even though these collagens are expressed in varying concentrations in the four valves, their localization and distribution has been shown to be similar in all valves. Apart from the fibrosa layer, were it is has a dominant presence, collagen I is expressed throughout the SL and AV valve leaflets (**Figure 4c**), whereas collagen III is most evident in
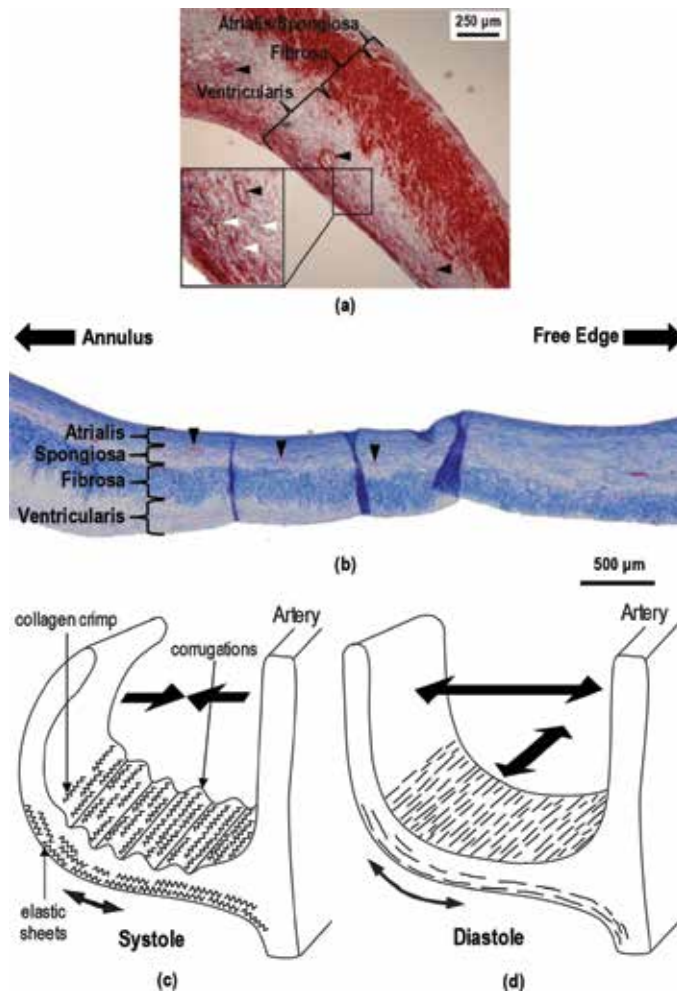
Figure 5. (a) Radial histological section of the basal region of the posterior MV leaflet stained with Miller's elastic and sirius red (red: collagen; blue/black: elastin). ▷ indicates elastic fibers; ▶ indicates blood vessels. Note the dominance of the fibrosa and ventricularis layers in the expense of the spongiosa layer in the basal region. (b) Radial histological section of the posterior MV leaflet stained with Masson's Trichrome stain (blue/black: cell nuclei; red: cytoplasm; blue: collagen). ▶ indicates blood vessels. Note the increase in the thickness of the spongiosa layer and the decrease in the thickness of the fibrosa layer towards the free edge of the leaflet. Adopted with permission from Roberts et al. (2016) [18]. (c, d) leaflet configuration and architecture of semilunar valves during peak systole (c; fully open) and peak diastole (d; fully closed). Redrawn and modified from Schoen (1999) [64].

the less-dense regions of the leaflets, such as the spongiosa [76]. Collagen IV has been shown to be localized in the basal lamina of the leaflets and collagen V to be predominantly distributed around interstitial cells. Collagen VI has been shown to form distinct structures within the fibrosa, surrounding the dense collagen I fibers of this layer [76]. The total collagen content in normal valve leaflets is approximately 50–63% (dry tissue weight ratio) [68, 71, 79, 80], and the elastin content is approximately 10–11% (dry tissue weight ratio), depending on the valve type (**Table 3**) [78, 80–83]. Previous studies have reported the relative percentages of

	Content			
Constituent	Aortic Leaflet	Pulmonary Leaflet	Mitral Leaflet	Mitral Chordae
Hydroxyproline (μm/mg dry tissue)	71.6±26.1 (H) [79]	70.7±6.2 (P) [71]	88.2±3.9 (P) [68]	88.6±7.1 (P) [68]
Total collagens (μm/mg dry tissue)	511.2±186.3(H) [79]	504.8±44.3 (P) [71]	629.7±17.8 (P) [68]	632.6±50.7 (P) [68]
Sulfated GAGs (μm/mg dry tissue)	11.4±0.4 (H) [79]	20.2±0.6 (P) [71]	26.8±3.5 (P) [68]	15.5±5.4(H)* [78]
Elastin (% of dry tissue weight)	11.2±1.0 (H)** [81]	N.A.	10.0±17.8 (H) * [78]	9.7±2.1 (H) * [78]

The results indicate mean ± 95% confidence intervals, or mean ± standard deviation (*), or means ± standard error (**). H: Human; P: porcine; N.A.: not available. Numbers in brackets indicate source document.

Table 3. Hydroxyproline, collagen, sulfated GAG and elastin content of normal heart valves.

collagen I, III, and V in normal human MV leaflets to be approximately 74, 24 and 2% of the total collagen content, respectively, whereas collagen IV and VI were below the detection limit of the technique used in those studies [72, 77]. A similar study by Lis et al. [78] reported a collagen I to collagen III ratio of 2.4 and 2.7 for human MV leaflets and chordae, respectively.

Three major GAGs have been identified in varying concentrations in heart valves, including chondroitin sulfate, dermatan sulfate and hyaluronic acid, together with decorin, biglycan and versican, which are chondroitin and dermatan sulfate proteoglycans [51, 84, 85]. The total content of sulfated GAGs (chondroitin and dermatan sulfate) in normal heart valves has been reported to range between 11 and 27% (dry tissue weight ratio), depending on valve type and site (**Table 3**) [68, 71, 78, 79]. Hyaluronic acid is the most abundant GAG in normal heart valves, accounting for up to half of the total leaflet GAG content, with chondroitin and dermatan sulfate accounting for about a quarter of the total GAG content of the leaflet each [86]. The relative percentages reported for normal human MV leaflets were 49, 25 and 23% of the total GAG content, for hyaluronic acid, chondroitin sulfate and dermatan sulfate, respectively, with the remaining 3% attributed to hyper-sulfated chondroitin/dermatan sulfate. In the case of the normal MV chordae, the corresponding percentages have been reported to be 24 (hyaluronic acid), 26 (chondroitin sulfate), 43 (dermatan sulfate) and 7% (hyper-sulfated chondroitin/dermatan sulfate) [84–86]. Moreover, differences in the absolute and relative GAG contents have been reported for different regions of the valves, subjected to different modes of loading during the cardiac cycle. Specifically, regions of the valves that are predominantly subjected to tensile loading, such as the leaflet belly and chordae (in the case of the AV valves), present a reduced overall GAG content compared to regions such as the free edge of the valve leaflets, which are predominantly subjected to compressive loading during coaptation with the other valve leaflets when the valve is fully closed. In addition, the regions that are predominantly subjected to tensile loading present significantly increased levels of chondroitin and dermatan sulfate compared to hyaluronic acid [85].

5. Physiological behavior of heart valves under loading

The ultrastructural histoarchitecture of the valvular tissue and the interaction of its collagen fibers with its non-collagenous components form the basis of the mechanical properties of heart valves. Similarly to other biological tissues that are subjected to high deformation and loading, collagen and elastic fibers act synergistically in heart valves to provide valvular tissue with strength and elasticity, respectively, which are required for their efficient function. The strength and stiffness of the collagen fibers prevent fracture of the valvular components when they are subjected to the peak transvalvular pressure during the time the valves are fully closed. The tensile strength of collagen is approximately 120 MPa, which is only one order of magnitude lower than high tensile steel (about 1110 MPa) and an elastic modulus of about 1.2 GPa, which confers substantial stiffness (**Table 4**) [35, 87]. However they stretch only minimally (about 13%) [35, 88]. On the other hand, elastic fibers are the most extensible biosolids known with very low modulus of approximately 0.3–1.1 MPa (**Table 4**) and capable of reaching failure strains in excess of 150%. However, elastic fibers demonstrate a low tensile strength of approximately 2 MPa, which limits their load-bearing capacity [35].

During the cardiac cycle, valvular tissue deforms to relative large strains, exhibiting non-linear stress-strain behavior. A typical stress-strain behavior for SL valve leaflet tissue within its physiological range is shown in **Figure 6a**. The graph describes the behavior of SL valve leaflets

Material	Young's modulus / Elastic phase modulus (MPa)	Collagen phase modulus (MPa)	Source
Tropoelastin	0.003	-	[37]
Microfibrils	78-96		[38]
Mature cross-linked elastin	0.3-1.1	-	[6, 35]
Collagen 1 fibrils		95.5	[75]
Mature cross-linked collagen 1	-	$1.0 - 1.2 \times 10^3$	[6, 35]
Aortic leaflet (C)	0.07	39.0	[65, 66]*
Aortic leaflet (R)	0.04	2.1	
Pulmonary leaflet (C)	0.76	15.3	[71]*
Pulmonary leaflet (R)	0.34	1.2	
Mitral leaflet (C)	0.02	10.2	[68]*
Mitral leaflet (R)	0.02	2.1	
Mitral chordae	0.10	113.7	

C: Circumferential direction, R: radial direction.
*Data obtained under uniaxial tensile testing.

Table 4. Indicative low-strain and high-strain modulus of valvular tissue and constituents.

from peak systole, when the SL valves are fully open, to peak diastole, when the SL valves are fully closed and loaded by the maximum transvalvular pressure. The graph also shows the contributions of the elastic and collagen fibers towards the overall behavior of the tissue and can be better comprehended in conjunction with **Figure 5c** and **d**. This type of stress-strain behavior has three distinct phases [65]. During the first phase (elastic phase), the leaflet offers little resistance to elongation since force transmission and load bearing is provided mainly by the elastic fibers. During this phase the collagen layer in the fibrosa unfolds and the collagen fibrils change their angular distribution [75]. Owing to these, the collagen fibers have minimal contribution to force transmission, resulting in a stress-strain response for this phase that is characterized by a low slope (low modulus). In the elastic phase the leaflet tissue behaves almost as an elastic solid with the stress increasing linearly with the strain. Under further loading, the leaflet enters the transition phase, during which the collagen fibers uncrimp and gradually align and uncoil, increasing their contribution to the force transmission. In the collagen phase, all the collagen fibers are uncoiled (recruited) and the load is entirely borne by them. Further extension in the collagen fibers occurs by extrafibrillar (between molecules) and interfibrillar shear in the fibers, as well as molecular distortion [35]. Interfibrillar shear has been reported to be dependent on the amount of proteoglycans associated with the surface of the fibrils, which influences the extent of GAG association and electrostatic interactions between the fibrils and the surrounding ECM [35]. The slope of the stress-strain curve for the collagen phase is steep (high modulus) and almost constant, reflecting the material properties of the collagen fibers, which allow limited elongation to fracture [89]. Although the collagen phase of the leaflet continues well beyond the physiological range before failure, corresponding to the reserve strength of the collagen fibers, after peak systole the valve starts opening again and the stress is relieved whilst the leaflets recoil back to their original shape/size at peak systole. A similar non-linear stress-strain profile can be observed for the case of the leaflets and chordae of the AV valve during their closing phase from peak diastole to peak systole. Moreover, experimental studies have indicated that the stress-strain response of valve leaflets were independent of strain rate [75]. The Young's modulus of different valvular tissue constituents, together with the elastic and collagen phase slopes of pulmonary and aortic valve leaflets, and MV leaflets and chordae, are listed in **Table 4**.

Similarly to other biological tissues, the stress-strain behavior of valvular tissue also demonstrates viscoelastic behavior. Generally, viscoelasticity is manifested by a number of different features, including hysteresis, preconditioning, stress relaxation and creep. Viscoelasticity is a fundamental characteristic of biological materials, which exhibit both viscous and elastic behavior, depending on their constitution, temperature and the time over which the tissue is observed. Under cyclic loading (**Figure 6b**), valvular tissue exhibits a hysteresis loop (a phase lag) between loading and successive unloading. The area under the loading curve represents the energy stored during the extension of the tissue, whereas the area under the unloading curve represents the energy recovered during the recoil of the tissue back to its unloaded state. The hysteresis is the area between the loading and unloading curves of the stress-strain response and it is proportional to the mechanical energy dissipated. The hysteresis provides a measure of the energy storage efficiency of the tissue, with the larger the hysteresis the less efficient is the energy storage capacity of the tissue during loading and the less energy is returned to the system on unloading [90, 91]. Both collagen and elastic fibers do not show significant hysteresis, which makes them efficient in energy storage and able to provide the

necessary energy for rapid retraction of the valve leaflets during opening [35, 75, 91]. The energy storage capacity of the elastic fibers has been linked the high entropy of the elastin molecules. In the case of collagen, the intrafibrillar and interfibrillar shear, and molecular distortion that occur during the collagen fiber stretching has been suggested to contribute to the elastic energy storage [35]. Overall, valve leaflets have been reported to demonstrate a relatively low hysteresis of approximately 12% (in the case of the MV), which is independent of the strain rate [75].
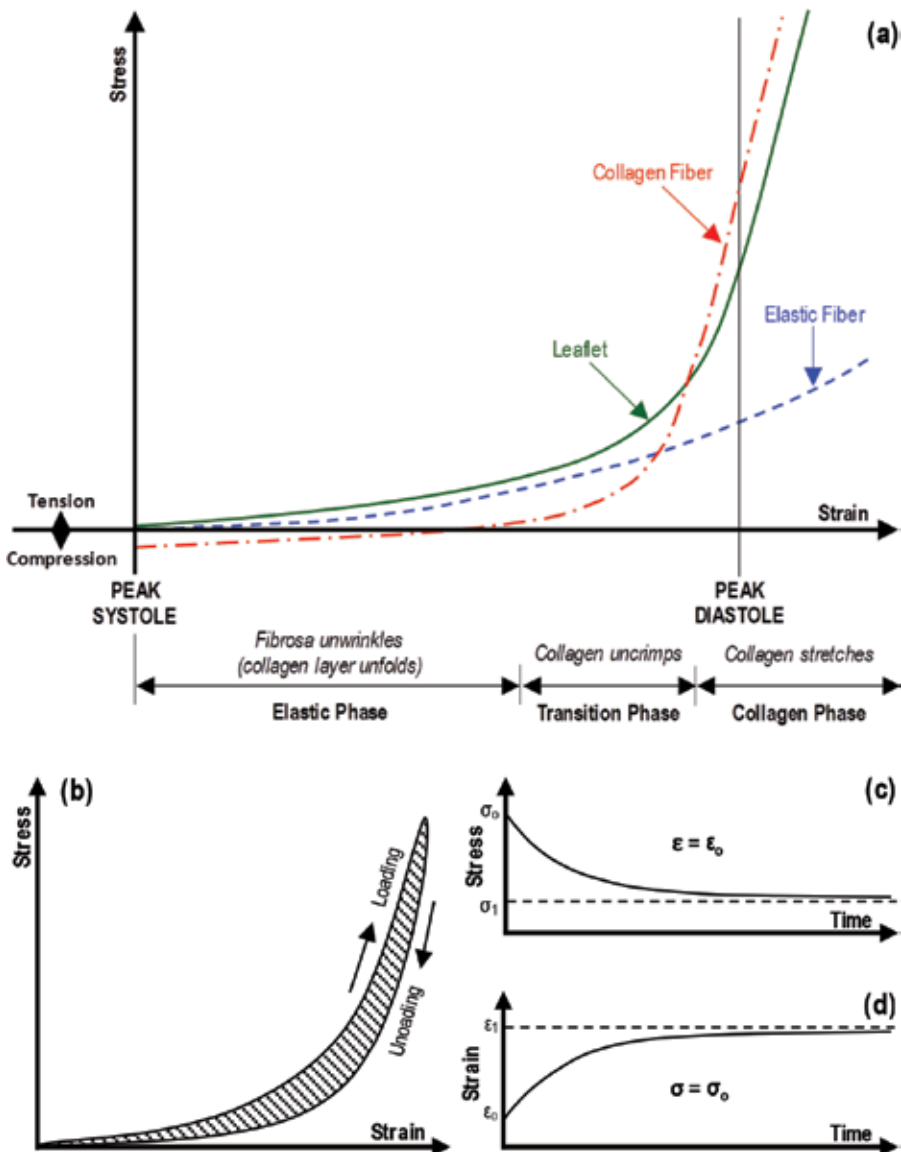

Figure 6. (a) Structure-property relation of SL valve leaflets within physiological ranges of stress and strain. Redrawn and modified from Schoen (1999) [64]. (b) Successive loading and unloading of biological tissue, showing the hysteresis loop (hashed area). (c) Stress relaxation under constant strain. (d) Creep under constant stress.

Following altered loading conditions, valvular tissue reorganizes itself to compensate for the altered mechanical stress, demonstrating an initial period of adjustment in its stress-strain behavior under cyclic loading [75]. This adjustment is manifested by an increased hysteresis loop, which subsequently decreases, tending to a steady state after a number of loading/ unloading cycles. Once this steady state is reached, no further change occurs in the stress-strain behavior, unless the loading routine is changed again. This period of adjustment after a large disturbance is called preconditioning and occurs due to internal changes in the structure of the tissue during cycling [6]. The viscoelastic feature of stress relaxation is manifested by the reduction of the stress generated in the tissue over time under constant strain (**Figure 6c**). Specifically, if the tissue is suddenly loaded to an initial stress σ_o and its length held constant, the stress relaxes asymptotically to a limiting value σ_1 following an exponential decay. Creep is the counterpart of stress relaxation in the sense that the tissue is loaded to a strain ε_o and the stress is held constant. Under these conditions the specimen continuous to deform asymptotically to a limiting value ε_1 (**Figure 6d**) [92]. Studies have reported that valve leaflets exhibit significant stress relaxation, but negligible creep over time, suggesting that they behave more like anisotropic quasi-elastic materials rather than viscoelastic materials. This behavior suggests that valve leaflets exhibit a load-locking behavior under maintained loading conditions that enables them to withstand high loading without any time-dependent deformation effects [75].

The degrees of non-linear stress-strain behavior, hysteresis, preconditioning, stress relaxation and creep are different for different tissues, depending on the type and amount of their individual constituents [6, 92]. Along these lines, the variability in the biomechanical properties between the different valves and valve components (**Table 4**) is predominantly due to the different fractions and organization of the major ECM constituents, including collagen fibers, elastic fibers, GAGs and proteoglycans, present in the different valves and valve components. These constitutional and organizational variations, which are dictated by the specific hemodynamic and biomechanical environment that the valves reside in, bequeath high directional and regional histoarchitectural and biomechanical anisotropy to the valvular tissue, assisting the heart valves to perform their specific function in the four different sites of the heart.

6. Structural, constitutional and biomechanical alterations in pathological heart valves

Heart valve surgery for repairing or replacing dysfunctional represents the second most common major heart operation in the western world [93]. In the US alone, approximately 5 million patients are diagnosed annually with heart valve disease [75, 94, 95]. Any one of the heart valves can potentially demonstrated valve disease; however, the aortic and mitral valves are most prone to disease, predominantly due to the higher stress that are subjected to and generated by the high pressure environment of the left heart [75]. Various conditions in isolation or in combination can cause valve dysfunction, including inflammation, degenerative valve disease, calcification, rheumatic or infective endocarditis, myocardial infarction and congenital defects, such as bicuspid aortic valve (BAV), MV prolapse (MVP), isolated anomalous lobar pulmonary veins and silent patent ductus arteriosus [96, 97]. Valve disease is manifested by

disruptions and alterations in the ECM histoarchitecture and constitution, disruptions in the distribution and organization of the EC and VIC populations, and malformation of the heart valves, which can render them stenotic and/or regurgitant [74, 75]. Moreover, several ECM gene mutations have been linked to valve disease, including fibrillin 1 gene mutations, which have been associated with BAVs and MVP, and elastic fiber component gene mutations also associated with MVP (Williams and Marfan syndromes) [98–100]. MVP and pulmonary valve stenosis have also been linked to collagen III and tenascin X gene mutations [98], whereas Notch1 gene mutations have been associated with BAV development and early calcification [101, 102]. Several studies have suggested that the abnormal organization of the ECM induced by these mutations may lead to abnormal VIC signaling and subsequent dysregulation of ECM synthesis [98, 103–105].

BAVs in the most common form of congenital valve disease, affecting 1–2% of the general population and eventually leading to aortic valve stenosis or regurgitation, infective endocarditis, and aortic dilation and/or dissection later in life [80, 97, 98, 106, 107]. Stenotic BAVs explanted from pediatric patients have been reported to exhibit excessive ECM production and disorganization, and VIC disarray without calcification. [98]. Specifically, the valve leaflets demonstrated loss of the typical trilaminar structure of the normal aortic valve leaflets, with disorganized, fragmented and abnormally oriented collagen and elastic fibers, increased proteoglycan presence throughout the leaflets, leaflet thickening, and large areas relatively void of cells. Moreover, elastin content was decreased, whereas collagen and proteoglycan content were substantially increased [75, 98]. The abnormalities in BAV histoarchitecture, constitution and anatomy, have been show to affect leaflet kinematics and stress distribution in computational studies, suggesting that early occurrence of regurgitation or stenosis might strictly depend on those abnormalities [107]. Alterations in the mechanical loading of the heart valves, due to abnormalities in histoarchitecture, constitution and anatomy, induce tissue remodeling though abnormal VIC mechanotransduction, which can lead to further valvular disease and dysfunction. Several studies have characterized VIC response against alterations in the biomechanical environment, and demonstrated a clear link between abnormal VIC stimulation, valvular tissue deformations and disease development and progression, highlighting the fundamental role of the mechanical environment on the mechanobiology of VICs [108–111]. As a result, BAVs are highly susceptible to calcification in later life, due to an induced osteoblastic VIC phenotype and subsequent matrix mineralization [80, 112]. Calcification causes valvular tissue to become thicker and stiffer (representative of a higher modulus), which eventually leads to valve stenosis and inevitable valve replacement [75].

Calcified aortic valve disease (CAVD) is not restricted to BAVs alone. CAVD is a slow, progressive, multifactorial disorder that is frequently driven by aging and the obesity-associated metabolic syndrome, and affects 25–30% of the population aged over 65 years old [75, 84, 100, 105, 113, 114]. Initially, the disease in manifested by mild leaflet thickening of the leaflets alongside with increase in the proteoglycan and hyaluronic acid content, which progressively become more severe and lead to impaired leaflet motion, valvular tissue adaptation and stenosis, [75, 84]. In spite of the leaflet thickening, studies have indicated that there is little change in the mechanical properties of the valve at the early stages of the disease [75]. Although this makes the condition asymptomatic at its initial phases, 10% of the patients develop severe symptoms within 10 years

of the initial diagnosis, and require immediate AV replacement [115]. Accumulating evidence suggests that apart from the upregulation of certain cellular pathways that can activate VIC trans-differentiation into osteogenic phenotype and promote osteogenic ECM remodeling, several non-cellular mechanisms, such as epitaxial calcification, can also induce calcium deposition in heart valves [116]. Calcific deposits in CAVD typically occur in regions of high stress concentration [117], highlighting the importance of mechanical factors in valve calcification, and initiate on the outflow surface of the leaflets [80, 106, 118]. It has been hypothesized that valvular ECs may regulate VIC function, and that the initiation of calcific deposits on the outflow, rather than the inflow, surface of the leaflets is due to differences in the hemodynamic microenvironment on the two sides of the leaflet. Elaborating, the different hemodynamic environments generate different mechanical forces that induce different phenotypic modulations on the ECs on the opposing sides. This, in turn, causes variations in the regulation of VIC function [80, 119]. Moreover, accumulating evidence suggests that CAVD shares common features with atherosclerosis, particularly the early accumulation of low-density lipoproteins (LDL), possibly by proteoglycan retention, and the attraction of inflammatory cells by hyaluronic acid, in the early stages of both pathologies [84]. These commonalities have led to the suggestion that there might be an regulatory mechanism of CAVD, similar to that in arterial atherosclerosis [84, 106, 120]. It has been suggested that a potential mediator of the hemodynamics-induced differential EC modulation might be Kruppel-like factor 2 (KLF2) [80]. KLF2 is a shear-stress-regulated transcription factor that is selectively induced in ECs localized in arterial regions that are protected from atherosclerosis [121]. Along these lines, ECs exposed to the same shear stress as the inflow surface of the aortic valve leaflets, demonstrated upregulation of KLF2 relatively to ECs exposed to shear stress levels equivalent to the outflow surface the aortic leaflets [80]. Moreover, it has also been suggested that the initiation of calcific deposits on the outflow surface of the leaflets might be due to the presence of nucleation sites, which provide the starting point for calcium nodule formation [75].

MVP is another common form of congenital valve disease that affects more than 2% of the general population, and it is the most common indication for surgical MV repair or replacement. MVP refers to the displacement of one (unileaflet MVP) or both (bileaflet MVP) MV leaflets into the left atrium during systole [80]. MVP is not apparent at birth and it usually remains asymptomatic till late adulthood [75, 80]. The condition is characterized by gross changes in the MV components, including thickening, enlargement and hooding of the leaflets, annular dilation, and elongated and/or ruptured chordae [86, 122]. The underlying pathology of MVP is myxomatous degeneration, which is defined by the abnormal accumulation of mucopolysaccharides. The pathology engulfs a number of processes, including diminishing of the fibrosa and thickening of the spongiosa layer of the leaflets, increased cellularity in the spongiosa, deposition of randomly oriented collagens, accumulation of GAG- and proteoglycan-rich myxomatous material in the leaflets and chordae, fragmentation of collagen and elastic fibers, and production of abundant matrix metalloproteases [80, 86, 123, 124]. These changes in the histoarchitecture and constitution lead to the biomechanical weakening of the MV components, which ultimately leads to mitral regurgitation, thromboembolism, heart failure and atrial fibrillation [75, 80]. Myxomatous MVs have been reported to demonstrate a lower strength, increased extensibility and decreased modulus compared to normal MVs in both the leaflets and chordae [86, 125, 126]. Myxomatous degeneration has also been reported to affect the biomechanical integrity of the chordae more that it does in the case of the leaflets [125, 126]. This finding is in accord with clinical reports that have indicated that most cases of myxomatous mitral regurgitation

involve chordal elongation and/or rupture rather than isolated leaflet prolapse due to annular dilation [86, 122]. In terms of constitution, human myxomatous MV leaflets and chordae have been reported to contain 3–9% more water and 2.4–7% more collagen compared to the normal tissues. In addition, the myxomatous leaflets and chordae contained 30–150% more GAGs compared to the normal tissues, with chordae from unileaflet prolapsing valves demonstrating 62% more GAGs than chordae from bileaflet ones [86]. The alteration in the histoarchitecture and biochemical constitution is an attribute of the altered biosynthetic response of the VICs [80]. This leads to the pathological remodeling of the myxomatous valves, which coupled with their normal wear induced during the cyclic loading, leads to the deterioration of their mechanical integrity. As discussed above, abnormalities in histoarchitecture and constitution cause alterations in the mechanical loading generated in the heart valves and, thus, abnormal VIC mechanotransduction. Indeed, VICs have been shown to respond to mechanical strain *in vitro* and modulate their biosynthetic and ECM-degradation activity. Under cyclic straining, VICs, isolated from porcine MV leaflets and chordae, produced upregulation of GAGs, with chordal VICs responding more rapidly to the cyclic strain than leaflet VICs [127, 128]. Moreover, studies with human MV explants have reported that during MVP development, healthy quiescent VICs undergo a phenotypic activation though the upregulation of the BMP4-mediated pathway [75, 129, 130]. BMP4 is an osteogenic morphogen that, together with BMP2, have been shown to be present in ossified valves [131]. BMP4 is also a potent inducer of collagen and proteoglycan synthesis, and matrix mineralization [75].

Acknowledgements

Conflict of interest

The author has no conflict of interest to report.

Author details

Sotirios Korossis

Address all correspondence to: korossis.sotirios@mh-hannover.de

Hannover Medical School, Hannover, Germany

References

[1] Murray RK, Keeley FW. The extracellular matrix. In: Murray RK, Granner DK, Mayes PA, Rodwell VW, editors. Harper's Illustrated Biochemistry. 26th ed. New York, NY: McGraw Hill; 2003. pp. 535-555

[2] Martini FH, Nath JL, Bartholomew EF. Fundamentals of Anatomy & Physiology. 9th ed. Harlow, UK: Pearson (Verlag); 2011. pp. 1-1264

[3] Lodish H, Berk A, Zipursky L, Matsudaira P, Baltimore D. Molecular Cell Biology. 4th ed. Proto-Oncogenes and Tumor-Suppressor; 2000; Section 24.2

[4] Lodish H, Arnold B, Matsudaira P, Kaiser CA, Krieger M. Molecular cell biology. 5th ed. New York, NY: W. H. Freeman; 2003. 973p

[5] Nimni ME. The cross-linking and structure modification of the collagen matrix in the design of cardiovascular prosthesis. Journal of Cardiac Surgery. 1988;**3**(4):523-533

[6] Fung Y-C. Biomechanics. New York, NY: Springer New York; 1993

[7] Park J, Lakes RS. Biomaterials: An introduction. In: Biomaterials: An Introduction. 3rd ed. New York, NY: Springer-Verlag; 2007. pp. 1-561

[8] Lee JH, Khang G, Lee HB. Blood leak-proof porous vascular grafts. In: Wise DL, Trantolo DJ, Lewandrowski K-U, Gresser JD, Cattaneo MV, editors. Biomaterials Engineering and Devices: Human Applications: Volume 1: Fundamentals and Vascular and Carrier Applications Basis. Totowa, NJ: Humana Press; 2000. pp. 161-179

[9] Shental-Bechor D, Levy Y. Folding of glycoproteins: Toward understanding the biophysics of the glycosylation code. Current Opinion in Structural Biology. 2009;**19**(5):524-533

[10] Sarkar A, Wintrode PL. Effects of glycosylation on the stability and flexibility of a metastable protein: The human serpin α1-antitrypsin. International Journal of Mass Spectrometry. 2011;**302**(1-3):69-75

[11] Varki A. Biological roles of oligosaccharides: All of the theories are correct. Glycobiology. 1993;**3**(2):97-130

[12] Gelse K, Pöschl E, Aigner T. Collagens—structure, function, and biosynthesis. Advanced Drug Delivery Reviews. 2003;**55**:1531-1546

[13] Alberts B, Johnson A, Lewis J, Morgan D, Raff M, Roberts K, et al. Molecular Biology of the Cell. 6th ed. Vol. 6. New York, NY: Garland Science; 2014. p. 1465

[14] Canelón SP, Wallace JM. β-Aminopropionitrile-induced reduction in enzymatic cross-linking causes in vitro changes in collagen morphology and molecular composition. PLoS One. 2016;**11**(11)

[15] Viidik A. Thermal contraction-relaxation and dissolution of rat tail tendon collagen in different ages. Aktuelle Gerontologie. 1977;**7**(9):493-498

[16] de Souza RR. Aging of myocardial collagen. Biogerontology 2002;**3**(3):325-335

[17] Ushiki T. Collagen fibers, reticular fibers and elastic fibers. A comprehensive understanding from a morphological viewpoint. Archives of Histology and Cytology. 2002;**65**(2): 109-126

[18] Roberts N, Morticelli L, Jin Z, Ingham E, Korossis S. Regional biomechanical and histological characterization of the mitral valve apparatus: Implications for mitral repair strategies. Journal of Biomechanics. 2016;**49**(12):2491-2501

[19] Dale WC, Baer E, Keller A, Kohn RR. On the ultrastructure of mammalian tendon. Experientia. 1972;**28**(11):1293-1295

[20] Kühn K. The classical collagens: Types I, II, and III. In: Mayne R, Burgeson RE, editors. Structure and Function of Collagen Types. Orlando: Academic Press; 1987. pp. 1-42

[21] van der Rest M, Garrone R. Collagen family of proteins. The FASEB Journal. 1991;**5**(13): 2814-2823

[22] Olsen OH, Samuelsen MR, Petersen SB, Norskov L. Excitations in three-dimensional models of alpha-helix structures in proteins. Physical Review A. 1988;**38**(11):5856-5866

[23] Vrhovski B, Weiss AS. Biochemistry of tropoelastin. European Journal of Biochemistry. 1998;**258**(1):1-18

[24] Patel A, Fine B, Sandig M, Mequanint K. Elastin biosynthesis: The missing link in tissue-engineered blood vessels. Cardiovascular Research. 2006;**71**(1):40-49

[25] Kielty CM, Sherratt MJ, Shuttleworth CA. Elastic fibres. Journal of Cell Science. 2002; **115**(Pt 14):2817-2828

[26] Montes GS. Structural biology of the fibres of the collagenous and elastic systems. Cell Biology International. 1996;**20**(1):15-27

[27] Baldock C, Koster AJ, Ziese U, Rock MJ, Sherratt MJ, Kadler KE, et al. The supramolecular organization of fibrillin-rich microfibrils. The Journal of Cell Biology. 2001;**152** (5, 5):1045-1056

[28] Chapman SL, Sicot F-X, Davis EC, Huang J, Sasaki T, Chu M-L, et al. Fibulin-2 and fibulin-5 cooperatively function to form the internal elastic lamina and protect from vascular injury. Arteriosclerosis, Thrombosis, and Vascular Biology. 2010;**30**(1):68-74

[29] Albert EN. Developing elastic tissue. An electron microscopic study. The American Journal of Pathology. 1972;**69**(1):89-102

[30] Wise SG, Weiss AS. Tropoelastin. The International Journal of Biochemistry & Cell Biology. 2009;**41**(3):494-497

[31] Mecham RP. Elastin synthesis and fiber assembly. Annals of the New York Academy of Sciences. 1991;**624**(1):137-146

[32] Rosenbloom J, Abrams WR, Mecham R. Extracellular matrix 4: The elastic fiber. The FASEB Journal. 1993;**7**(13):1208-1218

[33] Mecham RP, Heuser J. Three-dimensional organization of extracellular matrix in elastic cartilage as viewed by quick freeze, deep etch electron microscopy. Connective Tissue Research. 1990;**24**(2):83-93

[34] Cotta-Pereira G, Guerra Rodrigo F, Bittencourt-Sampaio S. Oxytalan, elaunin, and elastic fibers in the human skin. The Journal of Investigative Dermatology. 1976;**66**(3):143-148

[35] Muiznieks LD, Keeley FW. Molecular assembly and mechanical properties of the extracellular matrix: A fibrous protein perspective. Biochimica et Biophysica Acta. 2013;**1832**(7):866-875

[36] Holst J, Watson S, Lord MS, Eamegdool SS, Bax DV, Nivison-Smith LB, et al. Substrate elasticity provides mechanical signals for the expansion of hemopoietic stem and progenitor cells. Nature Biotechnology. 2010;**28**(10):1123-1128

[37] Baldock C, Oberhauser AF, Ma L, Lammie D, Siegler V, Mithieux SM, et al. Shape of tropoelastin, the highly extensible protein that controls human tissue elasticity. Proceedings of the National Academy of Sciences of the United States of America. 2011;**108**(11):4322-4327

[38] Kielty CM, Sherratt MJ, Marson A, Baldock C. Fibrillin microfibrils. In: Anfinsen CB, Edsall JT, Richards FM, Eisenberg DS, editors. Advances in Protein Chemistry. New York: Academic Press; 2005. pp. 405-436

[39] Flory PJ. Crystallinity and dimensional changes in fibrous proteins. Journal of Cellular Physiology. Supplement. 1957;**49**(Suppl 1):175-183

[40] Indik Z, Yeh H, Ornstein-Goldstein N, Kucich U, Abrams W, Rosenbloom JC, et al. Structure of the elastin gene and alternative splicing of elastin mRNA: Implications for human disease. American Journal of Medical Genetics. 1989;**34**(1):81-90

[41] Bashir MM, Indik Z, Yeh H, Ornstein-Goldstein N, Rosenbloom JC, Abrams W, et al. Characterization of the complete human elastin gene. Delineation of unusual features in the 5′-flanking region. The Journal of Biological Chemistry. 1989;**264**(15):8887-8891

[42] Cleary EG, Sandberg LB, Jackson DS. The changes in chemical composition during development of the bovine nuchal ligament. The Journal of Cell Biology. 1967;**33**(3):469-479

[43] Shapiro SD, Endicott SK, Province MA, Pierce JA, Campbell EJ. Marked longevity of human lung parenchymal elastic fibers deduced from prevalence of D-aspartate and nuclear weapons-related radiocarbon. The Journal of Clinical Investigation. 1991;**87**(5): 1828-1834

[44] Watson RE, Griffiths CE, Craven NM, Shuttleworth CA, Kielty CM. Fibrillin-rich microfibrils are reduced in photoaged skin. Distribution at the dermal-epidermal junction. The Journal of Investigative Dermatology. 1999;**112**(5):782-787

[45] Riches K, Angelini TG, Mudhar GS, Kaye J, Clark E, Bailey MA, et al. Exploring smooth muscle phenotype and function in a bioreactor model of abdominal aortic aneurysm. Journal of Translational Medicine. 2013;**11**(1):1-13

[46] Sandberg LB, Soskel NT, Leslie JG. Elastin structure, biosynthesis, and relation to disease states. The New England Journal of Medicine. 1981;**304**(10):566-579

[47] Hasham SN, Willing MC, Guo D, Muilenburg A, He R, Tran VT, et al. Mapping a locus for familial thoracic aortic aneurysms and dissections (TAAD2) to 3p24-25. Circulation. 2003;**107**(25):3184-3190

[48] Robinson PN, Arteaga-Solis E, Baldock C, Collod-Béroud G, Booms P, De Paepe A, et al. The molecular genetics of Marfan syndrome and related disorders. Journal of Medical Genetics. 2006;**43**(10):769-787

[49] Danielson KG, Baribault H, Holmes DF, Graham H, Kadler KE, Iozzo RV. Targeted disruption of decorin leads to abnormal collagen fibril morphology and skin fragility. The Journal of Cell Biology. 1997;**136**(3):729-743

[50] Nikolovska K, Renke JK, Jungmann O, Grobe K, Iozzo RV, Zamfir AD, et al. A decorin-deficient matrix affects skin chondroitin/dermatan sulfate levels and keratinocyte function. Matrix Biology. 2014;**35**:91-102

[51] Stephens EH, Saltarrelli JG, Baggett LS, Nandi I, Kuo JJ, Davis AR, et al. Differential proteoglycan and hyaluronan distribution in calcified aortic valves. Cardiovascular Pathology. 2011;**20**(6):334-342

[52] Tan HT, Lim TK, Richards AM, Kofidis T, Teoh KL-K, Ling LH, et al. Unravelling the proteome of degenerative human mitral valves. Proteomics. 2015;**15**(17):2934-2944

[53] Park PW. Isolation and functional analysis of syndecans. Methods in Cell Biology. 2018;**143**:317-333

[54] Latif N, Sarathchandra P, Taylor PM, Antoniw J, Yacoub MH. Molecules mediating cell-ECM and cell-cell communication in human heart valves. Cell Biochemistry and Biophysics. 2005;**43**(2):275-287

[55] Balaoing LR, Post AD, Lin AY, Tseng H, Moake JL, Grande-Allen KJ. Laminin peptide-immobilized hydrogels modulate valve endothelial cell hemostatic regulation. PLoS One. 2015;**10**(6):e0130749

[56] Robinson CR, Roberts WC. Outcome of combined mitral and aortic valve replacement in adults with mucopolysaccharidosis (the Hurler syndrome). The American Journal of Cardiology. 2017;**120**(11):2113-2118

[57] Pierce OM, McNair GR, He X, Kajiura H, Fujiyama K, Kermode AR. N-glycan structures and downstream mannose-phosphorylation of plant recombinant human alpha-L-iduronidase: Toward development of enzyme replacement therapy for mucopolysaccharidosis I. Plant Molecular Biology. 2017;**95**(6):593-606

[58] Braunlin E, Steinberger J, DeFor T, Orchard P, Kelly AS. Metabolic syndrome and cardiovascular risk factors after hematopoietic cell transplantation in severe mucopolysaccharidosis type I (Hurler syndrome). Biology of Blood and Marrow Transplantation. 2018. pii: S1083-8791(18)30044-2. DOI: 10.1016/j.bbmt.2018.01.028. [Epub ahead of print]

[59] Eisengart JB, Rudser KD, Xue Y, Orchard P, Miller W, Lund T, et al. Long-term outcomes of systemic therapies for Hurler syndrome: An international multicenter comparison. Genetics in Medicine. 2018. DOI: 10.1038/gim.2018.29. [Epub ahead of print]

[60] Sestito S, Falvo F, Scozzafava C, Apa R, Pensabene L, Bonapace G, Moricca MT, Concolino D. Genetics and Gene Therapy in Hunter Disease. Current Gene Therapy. 2018;**18**(2):90-95

[61] Chlebowski MM, Heese BA, Malloy-Walton LE. Early childhood onset of high-grade atrioventricular block in hunter syndrome. Cardiology in the Young. 2018;**28**(5):786-787

[62] Stapleton M, Kubaski F, Mason RW, Yabe H, Suzuki Y, Orii KE, et al. Presentation and treatments for mucopolysaccharidosis type II (MPS II; Hunter syndrome). Expert Opinion on Orphan Drugs. 2017;**5**(4):295-307

[63] Tovar AMF, de Mattos DA, Stelling MP, Sarcinelli-Luz BSL, Nazareth RA, Mourão PAS. Dermatan sulfate is the predominant antithrombotic glycosaminoglycan in vessel walls: Implications for a possible physiological function of heparin cofactor II. Biochimica et Biophysica Acta. 2005;**1740**(1):45-53

[64] Schoen FJ. Future directions in tissue heart valves: Impact of recent insights from biology and pathology. The Journal of Heart Valve Disease. 1999;**8**(4):350-358

[65] Korossis SA, Booth C, Wilcox HE, Watterson KG, Kearney JN, Fisher J, et al. Tissue engineering of cardiac valve prostheses II: Biomechanical characterization of decellularized porcine aortic heart valves. The Journal of Heart Valve Disease. 2002;**11**(4):463-471

[66] Booth C, Korossis SA, Wilcox HE, Watterson KG, Kearney JN, Fisher J, et al. Tissue engineering of cardiac valve protheses I: Development and histological characterization of an acellular porcine scaffold. The Journal of Heart Valve Disease. 2002;**11**(4):457-462

[67] Korossis SA, Wilcox HE, Watterson KG, Kearney JN, Ingham E, Fisher J. In-vitro assessment of the functional performance of the decellularized intact porcine aortic root. The Journal of Heart Valve Disease. 2005;**14**(3):408-421. discussion 422

[68] Granados M, Morticelli L, Andriopoulou S, Kalozoumis P, Pflaum M, Iablonskii P, et al. Development and characterization of a porcine mitral valve scaffold for tissue engineering. Journal of Cardiovascular Translational Research. 2017;**10**(4):374-390

[69] Schoen FJ. Aortic valve structure-function correlations: Role of elastic fibers no longer a stretch of the imagination. The Journal of Heart Valve Disease. 1997;**6**(1):1-6

[70] Morticelli L, Thomas D, Roberts N, Ingham E, Korossis S. Investigation of the suitability of decellularized porcine pericardium in mitral valve reconstruction. The Journal of Heart Valve Disease. 2013;**22**(3):340-353

[71] Luo J, Korossis SA, Wilshaw S-P, Jennings LM, Fisher J, Ingham E. Development and characterization of acellular porcine pulmonary valve scaffolds for tissue engineering. Tissue Engineering Parts A. 2014;**20**:21-22

[72] McCarthy KP, Ring L, Rana BS. Anatomy of the mitral valve: Understanding the mitral valve complex in mitral regurgitation. European Journal of Echocardiography. 2010;**11**(10):i3-i9

[73] Stella JA, Sacks MS. On the biaxial mechanical properties of the layers of the aortic valve leaflet. Journal of Biomechanical Engineering. 2007;**129**(5):757-766

[74] Wang L, Korossis S, Ingham E, Fisher J, JZ. Computational simulation of oxygen diffusion in aortic valve leaflet for tissue engineering applications. The Journal of Heart Valve Disease. 2008;**17**(6):700-709

[75] Ayoub S, Ferrari G, Gorman RC, Gorman JH, Schoen FJ, Sacks MS. Heart valve biomechanics and underlying Mechanobiology. Comprehensive Physiology. 2016;**6**(4):1743-1780

[76] White JF, Werkmeister JA, Hilbert SL, Ramshaw JAM. Heart valve collagens: Cross-species comparison using immunohistological methods. The Journal of Heart Valve Disease. 2010;**19**(6):766-771

[77] Cole WG, Chan D, Hickey AJ, Wilcken DE. Collagen composition of normal and myxomatous human mitral heart valves. Biochemical Journal. 1984;**219**(2):451-460

[78] Lis Y, Burleigh MC, Parker DJ, Child AH, Hogg J, Davies MJ. Biochemical characterization of individual normal, floppy and rheumatic human mitral valves. Biochemical Journal. 1987;**244**(3):597-603

[79] Vafaee T, Thomas D, Desai A, Jennings LM, Berry H, Rooney P, et al. Decellularization of human donor aortic and pulmonary valved conduits using low concentration sodium dodecyl sulfate. Journal of Tissue Engineering and Regenerative Medicine. 2018;**12**(2):e841-e853

[80] Schoen FJ. Evolving concepts of cardiac valve dynamics: The continuum of development, functional structure, pathobiology, and tissue engineering. Circulation. 2008;**118**(18):1864-1880

[81] Bashey RI, Torii S, Angrist A. Age-related collagen and elastin content of human heart valves. Journal of Gerontology. 1967;**22**(2):203-208

[82] Vesely I. The role of elastin in aortic valve mechanics. Journal of Biomechanics. 1997;**31**(2):115-123

[83] Bashey RI, Bashey HM, Jimenez SA. Characterization of pepsin-solubilized bovine heart-valve collagen. Biochemical Journal. 1978;**173**(3):885-894

[84] Grande-Allen KJ, Osman N, Ballinger ML, Dadlani H, Marasco S, Little PJ. Glycosaminoglycan synthesis and structure as targets for the prevention of calcific aortic valve disease. Cardiovascular Research. 2007;**76**(1):19-28

[85] Grande-Allen KJ, Calabro A, Gupta V, Wight TN, Hascall VC, Vesely I. Glycosaminoglycans and proteoglycans in normal mitral valve leaflets and chordae: Association with regions of tensile and compressive loading. Glycobiology. 2004;**14**(7):621-633

[86] Grande-Allen KJ, Griffin BP, Ratliff NB, Cosgrove DM, Vesely I. Glycosaminoglycan profiles of myxomatous mitral leaflets and chordae parallel the severity of mechanical alterations. Journal of the American College of Cardiology. 2003;**42**(2):271-277

[87] Pollock CM, Shadwick RE. Relationship between body mass and biomechanical properties of limb tendons in adult mammals. The American Journal of Physiology. 1994;**266** (3 Pt 2):R1016-R1021

[88] Gosline J, Lillie M, Carrington E, Guerette P, Ortlepp C, Savage K. Elastic proteins: Biological roles and mechanical properties. Philosophical Transactions of the Royal Society of London. Series B, Biological Sciences. 2002;**357**(1418):121-132

[89] Broom ND. The stress/strain and fatigue behaviour of glutaraldehyde preserved heart-valve tissue. Journal of Biomechanics. 1977;**10**(11/12):707-724

[90] Liu J, Qi H. Dissipated energy function, hysteresis and precondition of a viscoelastic solid model. Nonlinear Analysis: Real World Applications. 2010;**11**(2):907-912

[91] Green EM, Mansfield JC, Bell JS, Winlove CP. The structure and micromechanics of elastic tissue. Interface Focus. 2014;**4**(2):20130058

[92] Flügge W. Viscoelasticity. Berlin, Heidelberg: Springer; 1975

[93] Korossis SA, Fisher J, Ingham E. Cardiac valve replacement: A bioengineering approach. Bio-medical Materials and Engineering. 2000;**10**(2):83-124

[94] Nkomo VT, Gardin JM, Skelton TN, Gottdiener JS, Scott CG, Enriquez-Sarano M. Burden of valvular heart diseases: A population-based study. Lancet (London, England). 2006;**368**(9540):1005-1011

[95] Lloyd-Jones D, Adams RJ, Brown TM, Carnethon M, Dai S, De Simone G, et al. Heart disease and stroke statistics—2010 update: A report from the American Heart Association. Circulation. 2010;**121**(7):e46-e215

[96] Chehab G, Saliba Z, El-Rassi I. The silent patent ductus arteriosus. Le Journal Médical Libanais; **56**(1):7-10

[97] Hoffman JI. The global burden of congenital heart disease. Cardiovascular Journal of Africa. 2013;**24**(4):141-145

[98] Hinton RB, Lincoln J, Deutsch GH, Osinska H, Manning PB, Benson DW, et al. Extracellular matrix remodeling and organization in developing and diseased aortic valves. Circulation Research. 2006;**98**(11):1431-1438

[99] Milewicz DM, Dietz HC, Miller DC. Treatment of aortic disease in patients with Marfan syndrome. Circulation. 2005;**111**(11):e150-e157

[100] Pasipoularides A. Calcific aortic valve disease: Part 1—Molecular pathogenetic aspects, hemodynamics, and adaptive feedbacks. Journal of Cardiovascular Translational Research. 2016;**9**(2):102-118

[101] Garg V, Muth AN, Ransom JF, Schluterman MK, Barnes R, King IN, et al. Mutations in NOTCH1 cause aortic valve disease. Nature. 2005;**437**(7056):270-274

[102] Miller JD, Weiss RM, Heistad DD. Calcific aortic valve stenosis: Methods, models, and mechanisms. Circulation Research. 2011;**108**(11):1392-1412

[103] Walker GA, Masters KS, Shah DN, Anseth KS, Leinwand LA. Valvular myofibroblast activation by transforming growth factor-beta: Implications for pathological extracellular matrix remodeling in heart valve disease. Circulation Research. 2004;**95**(3):253-260

[104] Brooke BS, Karnik SK, Li DY. Extracellular matrix in vascular morphogenesis and disease: Structure versus signal. Trends in Cell Biology. 2003;**13**(1):51-56

[105] Pasipoularides A. Calcific aortic valve disease: Part 2—Morphomechanical abnormalities, gene reexpression, and gender effects on ventricular hypertrophy and its reversibility. Journal of Cardiovascular Translational Research. 2016;**9**(4):374-399

[106] Weiss RM, Miller JD, Heistad DD. Fibrocalcific aortic valve disease: Opportunity to understand disease mechanisms using mouse models. Circulation Research. 2013;**113**(2):209-222

[107] Conti CA, Della Corte A, Votta E, Del Viscovo L, Bancone C, De Santo LS, et al. Biomechanical implications of the congenital bicuspid aortic valve: A finite element study of aortic root function from in vivo data. The Journal of Thoracic and Cardiovascular Surgery. 2010;**140**(4):890-896

[108] Konduri S, Xing Y, Warnock JN, He Z, Yoganathan AP. Normal physiological conditions maintain the biological characteristics of porcine aortic heart valves: An ex vivo organ culture study. Annals of Biomedical Engineering. 2005;**33**(9):1158-1166

[109] Balachandran K, Konduri S, Sucosky P, Jo H, Yoganathan AP. An ex vivo study of the biological properties of porcine aortic valves in response to circumferential cyclic stretch. Annals of Biomedical Engineering. 2006;**34**(11):1655-1665

[110] Quick DW, Kunzelman KS, Kneebone JM, Cochran RP. Collagen synthesis is upregulated in mitral valves subjected to altered stress. ASAIO Journal; **43**(3):181-186

[111] Balachandran K, Alford PW, Wylie-Sears J, Goss JA, Grosberg A, Bischoff J, et al. Cyclic strain induces dual-mode endothelial-mesenchymal transformation of the cardiac valve. Proceedings of the National Academy of Sciences of the United States of America. 2011;**108**(50):19943-19948

[112] Rajamannan NM, Subramaniam M, Rickard D, Stock SR, Donovan J, Springett M, et al. Human aortic valve calcification is associated with an osteoblast phenotype. Circulation. 2003;**107**(17):2181-2184

[113] Leopold JA. Cellular mechanisms of aortic valve calcification. Circulation. Cardiovascular Interventions. 2012;**5**(4):605-614

[114] Zhiduleva EV, Irtyuga OB, Shishkova AA, Ignat'eva EV, Kostina AS, Levchuk KA, et al. Cellular mechanisms of aortic valve calcification. Bulletin of Experimental Biology and Medicine. 2018;**164**(3):371-375

[115] Gharacholou SM, Karon BL, Shub C, Pellikka PA. Aortic valve sclerosis and clinical outcomes: Moving toward a definition. The American Journal of Medicine. 2011;**124**(2):103-110

[116] Owens DS, Otto CM. Is it time for a new paradigm in calcific aortic valve disease? JACC. Cardiovascular Imaging. 2009 Aug;**2**(8):928-930

[117] Thubrikar MJ, Aouad J, Nolan SP. Patterns of calcific deposits in operatively excised stenotic or purely regurgitant aortic valves and their relation to mechanical stress. The American Journal of Cardiology. 1986;**58**(3):304-308

[118] Lindman BR, Clavel M-A, Mathieu P, Iung B, Lancellotti P, Otto CM, et al. Calcific aortic stenosis. Nature Reviews Disease Primers. 2016;**2**:16006

[119] Dai G, Kaazempur-Mofrad MR, Natarajan S, Zhang Y, Vaughn S, Blackman BR, et al. Distinct endothelial phenotypes evoked by arterial waveforms derived from athero-sclerosis-susceptible and -resistant regions of human vasculature. Proceedings of the National Academy of Sciences of the United States of America. 2004;**101**(41):14871-14876

[120] Otto CM. Calcific aortic stenosis--time to look more closely at the valve. The New England Journal of Medicine. 2008;**359**(13):1395-1398

[121] Parmar KM, Larman HB, Dai G, Zhang Y, Wang ET, Moorthy SN, et al. Integration of flow-dependent endothelial phenotypes by Kruppel-like factor 2. The Journal of Clinical Investigation. 2006;**116**(1):49-58

[122] Cosgrove DM, Stewart WJ. Mitral valvuloplasty. Current Problems in Cardiology. 1989;**14**(7):359-415

[123] Whittaker P, Boughner DR, Perkins DG, Canham PB. Quantitative structural analysis of collagen in chordae tendineae and its relation to floppy mitral valves and proteoglycan infiltration. British Heart Journal. 1987;**57**(3):264-269

[124] Rabkin E, Aikawa M, Stone JR, Fukumoto Y, Libby P, Schoen FJ. Activated interstitial myofibroblasts express catabolic enzymes and mediate matrix remodeling in myxoma-tous heart valves. Circulation. 2001;**104**(21):2525-2532

[125] Barber JE, Kasper FK, Ratliff NB, Cosgrove DM, Griffin BP, Vesely I. Mechanical proper-ties of myxomatous mitral valves. The Journal of Thoracic and Cardiovascular Surgery. 2001;**122**(5):955-962

[126] Barber JE, Ratliff NB, Cosgrove DM, Griffin BP, Vesely I. Myxomatous mitral valve chor-dae. I: Mechanical properties. The Journal of Heart Valve Disease. 2001;**10**(3):320-324

[127] Gupta V, Werdenberg JA, Blevins TL, Grande-Allen KJ. Synthesis of glycosaminogly-cans in differently loaded regions of collagen gels seeded with valvular interstitial cells. Tissue Engineering. 2007;**13**(1):41-49

[128] Gupta V, Werdenberg JA, Lawrence BD, Mendez JS, Stephens EH, Grande-Allen KJ. Reversible secretion of glycosaminoglycans and proteoglycans by cyclically stretched valvular cells in 3D culture. Annals of Biomedical Engineering. 2008;**36**(7):1092-1103

[129] Combs MD, Yutzey KE. Heart valve development: Regulatory networks in develop-ment and disease. Circulation Research. 2009;**105**(5):408-421

[130] Sainger R, Grau JB, Branchetti E, Poggio P, Seefried WF, Field BC, et al. Human myxomatous mitral valve prolapse: Role of bone morphogenetic protein 4 in valvular interstitial cell activation. Journal of Cellular Physiology. 2012;**227**(6):2595-2604

[131] Mohler ER, Gannon F, Reynolds C, Zimmerman R, Keane MG, Kaplan FS. Bone formation and inflammation in cardiac valves. Circulation. 2001;**103**(11):1522-1528

[132] Pflaum M, Kühn-Kauffeldt M, Schmeckebier S, Dipresa D, Chauhan K, Wiegmann B, et al. Endothelialization and characterization of titanium dioxide-coated gas-exchange membranes for application in the bioartificial lung. Acta Biomater. 2017;**50**:510-21

Mitral Valve Insufficiency, a Constituent of Left Atrial Myxoma: Pathobiology, Physiopathology, and Pathophysiology of Left Atrial Myxoma; Are Long-Term Results Still Feasible?

Iroegbu Chukwuemeka Daniel, Zhongxin Zhou, Zhang Hao and Jindong Liu

Additional information is available at the end of the chapter

Abstract

Mitral valve is a complex cardiac structure whose function depends on a proper synchronization between each mitral valve apparatus. Considerable headway over the years has been made toward unraveling the theoretical aspects which unifies the dynamic function, structural properties, and pathobiological, pathophysiological performance of the cardiac valves. However, the aspect of mitral valve regurgitation caused by left atrial myxoma still remains a gray area in the field as the mechanism(s) behind the masked and/or the resultant mitral valve regurgitation in relation to left atrial myxoma remains elusive. Although the regurgitations in most scenarios are masked due to the presence of the myxoma itself, however, both invasive and noninvasive techniques employed cannot ascertain if the regurgitation seen is a resultant or concomitant factor as the underlying pathological processes causing mitral valve regurgitation play key roles in the disease pathology as it could be a series of activated measures caused by the myxoma itself. Elucidating the role left atrial myxoma plays in mitral valve regurgitation is critical to improving our understanding as the aim of this chapter is to discuss the current knowledge of mitral valve regurgitation caused by left atrial myxoma in succinct with the elusive underlying pathological sequential cascade activated due to the presence of this neoplasm.

Keywords: myocardial infarction, myxoma, cardiac imaging techniques, echocardiography, embolism, mitral valve insufficiency, ischemic heart disease, degenerative heart disease, rheumatic heart disease, endocarditis

1. Introduction

Atrial myxomas are primary cardiac tumors which are more than usually found accidentally on routine clinical investigations toward other medical ailments commonly growing on the interatrial septum with the fossa ovalis been the most common site. However, it might also arise from the posterior, anterior and left atrial appendage. Cardiac myxomas are generally a rear occurrence with benign left atrial myxomas (LAM) being the most predominant type after pathological examinations. They are however two known basic types of cardiac myxoma; firm smooth and gelatinous irregular fond-like surface type with LAM mainly exhibiting symptoms of left-sided heart failure such as dyspnea when lying flat or on either the left or right side, arrhythmias, pulmonary edema, and even paroxysmal nocturnal dyspnea as a result of obstruction of the mitral valve orifice. Other associating symptoms such as malaise, Reynaud phenomenon, clubbing localized swelling, weight loss without trying and joint pain present themselves as the myxoma increases in size. LAM could also be sessile or pedunculated with pedunculated myxomas being the more frequent of the two. LAM is a multifactorial entity as at its diagnosis could spell the presence of diverse underlying cardiac alignments apart from the classic Goodwin's triad while been silent and/or masked as some could be asymptomatic or vague presenting with just fever and fatigue. Apart from the required prompt clinical investigative and the timely surgical interventions long-term morbidity and the permanent damage done by the constant pendulum-like movement to the mitral valve and its associated apparatus only but leads to possible irreversible progressive permanent cardiac damage and eventually sudden death. The resultant life-threatening complications encountered with LAM such as stroke, acute heart failure, arrhythmias and sudden death produces a thromboembolic-ischemic effect, valvular obstructions and other constitutional symptoms due to the silent masking nature of all LAM with vague symptoms which eventually lead to evident mitral valve insufficiencies [1].

Normal heart valve ensures a one-way blood flow all through the entire cardiac cycle with little interference and without any form of regurgitation. The semilunar valve [i.e., the aortic valve and the pulmonary valve] prevents backflow of blood into the ventricles during the diastolic phase, and the atrioventricular valves [mitral valve and tricuspid valve] prohibit reverse flow from the ventricle to the atrium during systole. The ability for the mitral valve to allow unrestricted forward flow largely depends on the structure, pliability, integrity, and mobility of the entire mitral valve apparatus. The longtime continuous left atrial pendulum-like movement made by the LAM leads to disturbances in the function of the mitral valve which affects the entire cardiac function due to the failure of the valve to shut properly allowing blood leak into the left atrium [regurgitation]. Significant changes done to the structure of the mitral valve such as annular dilatation results to an increase in mechanical stress over the entire valve structure sufficient enough to eventually produce Mitral valve regurgitation coupled with poor leaflet appositions or leaflet tears caused by the size of the myxoma as it constantly rebounds against the leaflets protruding into the left ventricle during systole as far as rupturing the tendinaes and over extending both the papillary muscle base initiating a vicious circle leading to mitral regurgitation. The resultant thromboembolic-ischemic effect of the papillary muscle caused by the multi-level blockage of the coronary artery plays a major role to the degree of mitral regurgitation seen [mild, moderate and sever] as the posterior aspect of the muscle receives blood supply from branches of the posterior descending artery,

taking its course from either the right or the circumflex coronary artery, depending on which is the dominant system as its much inclined to ischemia and necrosis produced by the occlusion as compared to the anterior muscle which invariably secures its supply from either the branches of the circumflex artery and the septal left anterior descending artery which is less predisposed to ischemia and rupture caused by occlusion [1–3].

However, achieving a favorable better long-term results with any effective medical interventions used in the management or treatment of mitral valve regurgitation produced by the resultant LAM is dependent on tackling the known types of processes responsible for mitral valve insufficiencies namely; rheumatic, ischemic, degenerative, infectious type [endocarditis] and other related etiological factors such as calcific degeneration and collagen vascular disorders [2, 3]. Being the most common type of heart valve disorders with vast non-surgical and technical surgical methods used in treating mitral valve regurgitation, in-depth knowledge to the known underlined process involved with mitral valve insufficiencies as a result of the consequent presence of the LAM is pivotal to achieving favorable long-term results as masked mitral valve regurgitation are always almost evident at diagnosis. It is therefore imperative for practicing cardiologist, pulmonologist, echo-cardiologist, cardiac surgeons and any other therapist and/or interventionist involved at the diagnostic work up to bear in mind the high possibility of a resultant mitral valve regurgitation produced by the atrial myxoma not also forgetting the associative know processes of mitral valve insufficiencies as all this could be masked by the presence of the myxoma itself limiting the chance for a proper intervention both therapeutically or surgically [1].

Be it as it may, this only adds to the existing questions in the field by practitioners regarding the pathology and physiology of LAM, the accompanied masked regurgitations, mitral valve prolapse and the underlying process involved with mitral valve insufficiencies along with the long-term prognosis. This scientific chapter aims to discuss the clinical implications of mitral valve regurgitation produced by LAM and the underlying processes involved with mitral valve insufficiencies.

2. Anatomy and physiology of mitral valve

The mitral valve is a complex anatomical structure made of an annulus, two leaflets, chordae tendineae, and the anterior and posterior papillary muscle. A synchronized movement of all the mitral valve apparatus is essential for the valve to function normally and their structural architecture enables them to cause a very low level of mechanical stress during the ventricular systole. Mitral valve insufficiencies occur due to structural defects or change affecting the normal architecture of the mitral valve apparatus as an effective function of the mitral valve solely depends on an efficient interaction of the whole mitral valve components including the left ventricle itself. The annulus is generally saddled in shape taking a kidney-like shape in systole and a round shape at diastole. However, it is anatomically divided into two distinct parts; an anterior and posterior portion with the former considered to be non-distensible found between two fibrous bodies while the latter accounts for about 2/3 of the mitral valve orifice and is considered to be easily prone to distention and dilatation with LAM and other

diseases affecting the mitral valve and the left heart [4, 5] (**Figure 1**). The two leaflets are also described as anterior and posterior with the anterior leaflet being wider with a shorter base while the posterior leaflet is narrower but with a much broader attachment. Three distinctive scallops can be related to the posterior leaflet which is clinically distinctive and vital for proper mitral valve function in addition to the lateral and medial small commissural scallops namely; medial, middle and a lateral scallop with the middle scallop being the largest among the three (**Figure 2**) [6–8]. The rough zone of each leaflet comes in contact with that of its other counterpart as the total surface area of the leaflets is twice the total surface area of the mitral orifice itself giving a border surface area for leaflet coaptation during systole which in turn decreases the mechanical stress during a single cardiac circle. A decrease in mechanical stress is achieved with a synchronous contractive action produced by the papillary muscles during left ventricular systole which further leads to an adequate tethering of the mitral valve thereby ensuring that the rough zones of both leaflets are in a properly oriented vertical direction [9–11]. Any destructive or nondestructive change to the normal structure and architecture of the mitral valve apparatus caused by the resultant long-standing pendulum-like effect of the LAM such as annular dilatation [anterior and posterior], leaflet prolapse and/or retraction
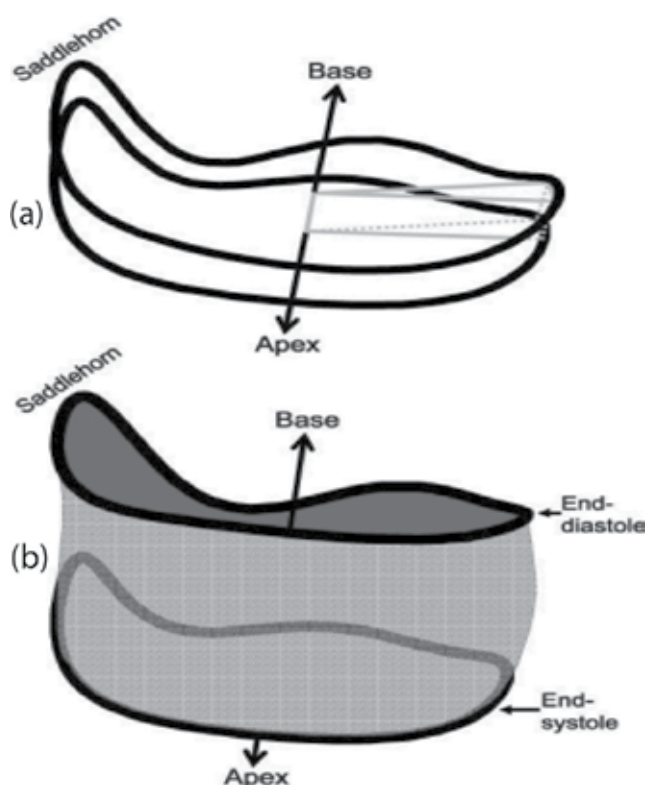

Figure 1. Schematic of the mitral annulus (black lines) (A): Time frames during the cardiac cycle and the volume change (gray lines) between both time frames (B): End systole and diastole (shaded gray). Saddle horn, the annular region closest to the aortic annulus.
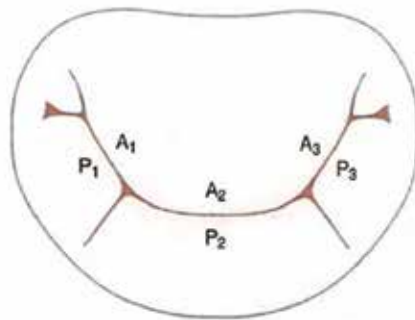
Figure 2. Carpentier classification of a well-structured mitral valve leaflet. A: anterior; P: posterior.

[anterior and posterior], chordae tendineae rupture or elongation and left ventricular abnormalities produced during the course of forward and backwards movement into the left ventricle and back to the left atrium during systole and diastole results in mitral valve regurgitation [1, 4, 7, 11] .

3. Left atrial myxoma

Myxomas are the most prevalent primary cardiac tumors, with 80–85% found in the left atrium and an annual incidence of 0.5 per million commonly arising from the interatrial septum at the fossa ovalis to be precise but can, however, be found in any chamber of the heart and structures with timely surgical resection playing a vital role in its treatment and recovery. The "tumor plop" sound heard during auscultation is a pathognomonic sign as a result of the penetrating myxoma in and out of the left ventricle. Symptoms caused by LAM are intermittent due to the occasional prolapse of the tumor through the atrioventricular valve and is also highly dependent on body position [1]. Cardiac myxomas usually occur between the third and sixth decades of an adult life taking a preference for the female sex with varying growth rate ranging from an absolute nonexistent growth to several millimeters per month. Familial inheritance, multicentricity, metastasis and inadequate excision increases the chance of cardiac myxomas recurrences, increased morbidity and mortality rates leading to poor prognosis and further possibly irreversible cardiac conditions either by medicamentous therapy alone and/or in combination with other various surgical therapies. Planned scheduled follow-up is of great importance in ruling out the possibility of a tumor reoccurrence even after proper surgical therapy employed. Cardiac computed tomography, magnetic resonance imaging, Doppler assessment and a combination of both outpatient transthoracic echocardiography with intra and postoperative Transesophageal echocardiography are essential for identifying and grading the regurgitation which is essential for an adequate left atrial myxoma therapy as they help in making precise judgment and assessment of anatomical valvular structures, which are destroyed by the tumor and are easily missed as most regurgitation are masked by the sole presence of LAM, different loading conditions, body structure and position [1, 12–24].

4. Pathology and physiopathology

The tendency of mitral valve regurgitation and the adjunct mitral valve prolapse development is inevitably high with the presence of left atrial myxoma either before or after any interventions been made. The development of mitral valve prolapse is due to the persistent rebound pendulum-like motion of the left atrial myxoma on the valve apparatus during each cardiac circle. Echocardiographically, mitral valve prolapse is defined as the upward displacement of the mitral leaflets above 2 mm in diastole [silent] which is usually the case in patients presenting with LAM and above 3 mm [massive] which increases the regurgitant jets seen during the echocardiographic studies. However, mid-systolic click to late systolic murmur is pathognomonic auscultatory findings with mitral valve prolapse and underling regurgitation as it varies from being benign to a gradual or sudden advance stage depending on the prolapse and regurgitation grade either before or after therapeutic interventions with a significant morbidity and mortality rate. Fortunately, apart from the massive prolapse, bacterial endocarditis, thromboembolism, atrial fibrillations, myxomatous degenerations [Barlow's disease] and rheumatic heart diseases play key roles in the resultant regurgitations caused by the left atrial myxoma. Histological features of mitral valve prolapse and regurgitation are marked spongiosa proliferation, mucopolysaccharide acid replacement of the leaflet collagen causing thickening and leaflet redundancy. As a result of the changes made such as fibrotic leaflets, thinning and/or elongation of the chordae tendineae, proper valve coaptation during systole is rendered impossible due to the redundant and elongated leaflets coupled with overshooting into the left atrium and the disrupted tendineae which eventually ruptures leading to regurgitation.

5. Mitral regurgitation

Mitral valve regurgitation is a complex entity that could be caused by either one of the following etiological factors such as; Marfan syndrome, acute rheumatic valve disease, degenerative [myxomatous], bacterial endocarditis, acute ischemia, papillary muscle rupture. However, mitral regurgitations are further categorized into two broad groups; acute and chronic [primary and secondary] mitral regurgitation and into two generally accepted classifications namely; Carpentier and Duran's classification. Although identifying patients at risk, symptomatic, asymptomatic and progressive stage of mitral valve regurgitation encountered in clinical settings have been made easier as compared to previous years with the most recent American Heart Association (AHA) and the American College of Cardiology (ACC) guidelines for patient management (see appendix A and B) [25].

Common clinical presentations encountered with LAM are either stenosis due to tumor prolapse into mitral orifice or regurgitation due to tumor induced valve trauma. Furthermore, Mitral valve regurgitation associated with LAM is caused by ventricular and annular dilatation, failure of leaflet coaptation and the direct damage of the leaflets and/or subvalvular apparatus due to the presence of the myxoma body itself as it transverses through the mitral

valve during each systolic and diastolic phase coupled with the myxoma body adherence to nearby structures of the mitral valve. The myxoma prolapse from the left atrium toward the left ventricle during the entire cardiac cycle eventually leads to mitral valve regurgitations of varying degrees, cause volume overload propagating both left atrial and left ventricular dilatation, annular dilatation due to the continuous mechanical stretch of the prolapsing tumor on the mitral annulus during each systolic and diastolic phase. However, the extent of valvular obstruction varies with body position as the presence of the myxoma body itself affects transmitral blood flow and also tends to mask mild and moderate to severe mitral regurgitations due to the huge and floating myxoma body where large myxomas with long stalk produces a temporally complete obstruction of the mitral valve orifice resulting in syncope. The continuous pendulum like or "wrecking ball" effect of the myxoma during each cardiac circle against the entirety of the mitral valve apparatus gives raise to regurgitations and its severity is highly dependent on the resultant effect of the myxoma body itself on the mitral valve [26–35]. The grade and severity of the regurgitation is highly dependent on the myxomas body size, stalk length [small, large, prolapsing and non- prolapsing] and to some varying degree body position and the resultant changes of blood flow through the left heart [36].

5.1. Carpentier classification

As widely used and proposed by Carpentier, the anterior leaflet is indicated as A1, A2, and A3 but lacks a clear distinction between A1 and A2 and also between A2 and A3 because of its smooth surface. However, the analogous segments of the posterior leaflets are also indicated as P1 [anterolateral], P2 [middle], and P3 [posteromedial] and highly distinctive from each other [37]. Regurgitations occur when there is an annular dilatation and/or the free edge of one or both leaflets overrides the entire valve orifice during systole, chordae tendineae destruction or rupture, a papillary muscle tear or detachment, architectural left ventricular destruction and acute ischemia as a result of embolization due to the myxoma friability (**Table 1**). Regurgitations caused by LAM express themselves differently according to grades, degree, and size of the myxoma, different loading conditions, body structure, position and other masked underlying pathology so therefore, for a successfully understanding of mitral regurgitation caused by LAM, a clear knowledge of the components and anatomy of the mitral valve apparatus, possible functional alterations, analysis of the leaflet motion, and a proper grading system is essential for a better prognosis after management or repair [1] (**Figure 2**).

Type A	The manifestation or appearance of mitral regurgitations is as a result of annular dilatation
Type B	The manifestation or appearance of mitral regurgitations is as a result of .one of either leaflets overriding the annular plane during systole
Type C	The manifestation or appearance of mitral regurgitations is as a result of restricted leaflet motion during both systole and diastole
Type D	The manifestation or appearance of mitral regurgitations is as a result of restricted leaflet motion during systole only

Table 1. Carpentier's classification of regurgitation of the mitral valve.

- Type A is evident when there is annular dilatation only or in combination with leaflet perforation, as in endocarditis.

- Type B is caused by elongated chordae tendineae, as constantly seen in degenerative disease, or thinning of the papillary muscle, found in ischemic heart disease.

- Type C occurs when there is leaflet perforation or chordal rupture, as found in rheumatic diseases.

- Type D there is chordal rupture [rheumatic] or in combination with papillary muscle detachment or displacement [ischemic].

5.2. Duran classification

Kumar et al. proposed their classifications based on the chordae tendineae insertion gotten from the two papillary muscle groups. Thus, the posterior leaflet scallops were designated as P1 [anterolateral] and P2 [posteromedial] and the larger middle scallop as posterior middle which was subdivided as PM1 and PM2 based on chordal origins while the anterior leaflets were divided into A1 with chordae crossing from the anterolateral papillary muscle and A2 with chordae from the posteromedial papillary muscle [38] (**Figure 3**).

5.3. Acute mitral regurgitation

Acute mitral regurgitation occurs due to annular prolapse and the disruption of other different structures of the mitral valve. The papillary muscle rupture or the detachment of the chordae tendineae from the papillary muscles caused by the resultant myxoma pendulum-like movement during each cardiac circle causing disrupted valve motion and a rise in volume overload in combination with the high friable tendencies of LAM leading to embolization of the coronary arteries which eventually ends in myocardial infarction. The acute volume overload on the left ventricle combined with the regurgitant flow of blood into the left atrium during systole results in acute pulmonary congestion, dyspnea, and poor cardiac output [39].

5.4. *Chronic mitral regurgitation*

When categorizing chronic mitral regurgitation caused by left atrial myxoma, it is important that the physician gives a proper distinction between chronic primary [degenerative] and chronic secondary [functional] mitral regurgitation as it clearly helps in identifying the underlying pathology in relation to the resultant effect caused by the myxoma itself.

- *Chronic primary mitral regurgitation:* This regurgitation is as a result of the myxomas destruction of a single valve component either in its function or architecture such as annular dilatation with regurgitant jets from the left ventricle to the left atrium. However, the prolonged and severe volume overload produced eventually causes irreversible myocardial damage, episodic periods of heart failure and finally sudden death

- *Chronic secondary mitral regurgitation:* In this type of regurgitation, the entire valve apparatus is somewhat normal but the regurgitant jets are caused by embolization of the coronary arteries on different levels from the fragments of the myxoma giving rise to myocardial

infarction precipitating severe left ventricular dysfunction and adverse remodeling which eventually causes papillary muscle detachment, tethering leaflets with associated annular dilatation preventing proper coaptation [40].

5.5. Ischemic heart disease

Ischemic mitral regurgitation is defined as a moderate to severe mitral leak precipitated by acute myocardial infarction caused by partial or total complete obstruction of one or more coronary arteries on a different level due to the myxoma friability which gives rise to various degree of mitral regurgitation by changing the geometry of the ventricle [spherical shape], distorted wall motion, lateral and apical deracinated papillary muscles or its deformation due to ischemia [41].

5.6. Degenerative heart disease

This type of regurgitation is perpetuated as little pieces of embolus from the myxoma gets stocked at the edges of the leaflets forming small nodules which prevents complete valve closure
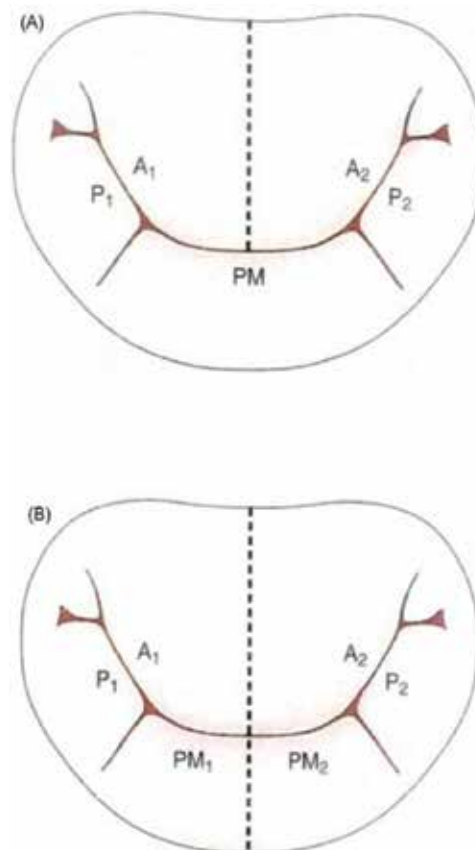

Figure 3. (A) Duran classification of a well-structured mitral valve leaflet, A: anterior; PM: posterior middle; P1: posterior lateral; P2: posterior medial. (B) Modified type A: anterior. P: posterior. PM: posterior middle [1: lateral. 2: Medial].

leading to regurgitant backflow of blood into the left atrium during the course of each cardiac circle which over time leads to an enlarged left atrium and ventricle causing heart failure.

5.7. Rheumatic heart disease

Myxoma [Latin Greek word "muxa" for mucus] means a myxoid tumor of primitive connective tissue, a primary tumor affecting adult hearts commonly in the left atrium but can, however, be found in other locations. LAM inflammatory process gives rise to a rapid sequence of chordal thickening and retraction, commissural fusion and finally thickened leaflets [incomplete opening and closure of the leaflets] with an enlarged annulus which eventually leads to regurgitation. Though an uncommon relation to the underlying processes involved with LAM throughout its development until therapy, pathologist has confirmed postoperatively the pathological component of LAM to be a spindle tumor with mucus production histologically made up of fusiform, stellate, and or polygonal cells [42–45] and histologically associated with interleukin-6 [46].

5.8. Endocarditis

This type of regurgitation caused by LAM is rear as compared to other underlying resultant pathological cause and may even be described by some physicians, surgeons, and interventionist as idiopathic due to its ambiguity. The vegetations formed involves series of the pathological process which is activated as a result of incomplete resection of the LAM in combination with natural human oral streptococcal inhabitants [Streptococcus sanguinis and/or dysgalactiae] which gets into the bloodstream when opportunities present themselves such as during surgeries and colonize the heart valves especially the mitral valve. The result at first is noninfective, but as the collection of platelets, fibrin, microcolonies of microorganisms, and the scant inflammatory cells increases, it shifts to a subacute stage and finally to full-blown endocarditis due to bacterial accumulations as they lodge and aggregate at the site of the incomplete LAM resection [1, 47].

6. Conclusion and future directions

Being the most common primary cardiac neoplasm in adults, the present state of research on its set cause, Pathobiology, physiopathology, and pathophysiology are still elusive as clinical and research efforts are being channeled toward its morbidity, mortality and its possible reoccurrence after surgery. If resultant mitral regurgitations and long-term survival for patients is to be achieved as it's the main goal in all neoplastic diseases, a proper understanding of myxomas pathology and the probable underlying process that could occur before and after therapeutic and/or surgical interventions employed is highly essential to tackle the un resolving issue in the field. Management of this condition requires adequate therapeutical background knowledge of the various possible outcomes to allow for an early identification of masked regurgitations caused by the LAM as a result of the probably altered valve motion or damaged valve apparatus in combination with the activated underlying processes

involved with a well-planned follow-up regimen as regurgitations in some cases might not be detected immediately after the intraoperative Transesophageal echocardiography is used to check if the myxoma was totally resected and the surgery satisfactory as it could be termed by the physician as a physiological residual regurgitation seen after such kind of surgery which could be detrimental in the long term. However, current clinical features and echocardiographic criteria's are not sufficient enough to detect mitral regurgitations and probable underlying pathological conditions early to achieve an effective medical management and/or surgical therapy.

The most challenging problem both surgeons and interventionist face is the doubtful nature surrounding possible resultant masked regurgitations with LAM as this could be residual following myxomas resection coupled with the underlying pathological factors aligned with this neoplasm as it propagates the destruction, perforation, elongation, thinning, tethering, thickening, retraction, displacement and ischemic changes seen in mitral valve regurgitation and/or prolapse. Bearing this in mind, at the slightest suspicion of hemodynamic and architectural change in mitral valve apparatus and ventricular geometry [remodeling] during medical management or surgical intervention, a thorough assessment of the mitral valve apparatus should be made using Transthoracic echocardiography [outpatient settings] and Transesophageal echocardiography [inpatient settings] in combination with the surgeons direct vision assessment if surgery was the treatment of choice irrespective of the known diagnosis [myxoma] in order to rule out any possible concomitant pathology such as coronary embolization to achieve favorable long-term prognosis. Finally, future directions and approaches made by the various scientific communities should be directed toward identifying the key dynamic concepts behind LAM biological, physiological and pathological components, clinical features and the echocardiographic criteria's to be used in an early detection of mitral valve regurgitation and the possible underlying pathological processes and/or complications that could precipitate silent mitral valve insufficiencies after medical management or surgical interventions as this will be an important achievement and a novel contribution to the field.

Conflict of interest

The authors declare no conflict of interest.

Author's contributions

We the authors appreciate the contributions Iroegbu Phoebe Chioma and Adeghe Peace Eseose made to the manuscript.

ICD: Concept and design, a major contributor to the interpretation and writing of the manuscript.

ZZ, ZH & JL: Critically revised and analyzed the manuscript for scientific logic and reasoning.

Funding

List of abbreviated words

LAM   left atrial myxoma

AHA   American Heart Association

ACC   American College of Cardiology

AppendixA. American Heart Association (AHA) and the American College of Cardiology (ACC) guidelines for the clinical management of patients with primary mitral regurgitations.

Class	Class interpretation	Anatomy	Valvular hemodynamics	Resultant consequence	Symptoms
I	At potential risk of mitral valve regurgitation development	*Valve prolapse [mild] but with adequate coaptation *Valvular thickening accompanied with restriction of both leaflet	Absence of any visible regurgitant jets with Doppler and little vena contracta of 0.3 cm	Nonexistent and uneventful	None
II	Gradual progressive mitral regurgitation	*Valve prolapse [severe] but with an adequate leaflet coaptation *Loss of leaflet coaptation probably cause by [rheumatic valve] *previous infective endocarditis	*Evident regurgitant jets <50%, vena contracta of <0.7 cm, with an effective regurgitant orifice of <0.40 cm^2 and an angiographic grade between 1 and 2[+]	Adequate pulmonary pressure with a mild left atrial enlargement and normal left ventricle geometry.	None
III	Tolerant asymptomatic mitral regurgitation [Severe]	Same as the above with an addition of leaflets thickening with radiation heart disease	Same as the above but with an increase in: angiographic grade 3–4[+]	Possible pulmonary hypertension, with a moderate to severe left atrial and ventricular enlargement	None
IV	Symptomatic Severe mitral regurgitation	Same as the above	Same as the above	Pulmonary hypertension is evidently present with a moderate to severe left atrial and ventricular enlargement	Decreased exercise tolerance, Exertional dyspnea

AppendixB. American Heart Association (AHA) and the American College of Cardiology (ACC) guidelines for the clinical management of patients with secondary mitral regurgitations.

Class	Class interpretation	Anatomy	Valvular hemodynamics	Resultant consequence	Symptoms
I	At potential risk of mitral valve regurgitation development	Normal valve architecture in patients with cardiomyopathy or coronary diseases	Absence of any visible regurgitant jets with Doppler and little vena contracta of <0.30 cm	*Motion abnormalities with probably dilated left vertical with geometric change *Myocardial disease	Evident symptoms are those of coronary ischemia which could be reversed with adequate therapy
II	Gradual progressive mitral regurgitation	Loss of leaflets coaptation centrally combined with annular dilatation and motion abnormalities which are regional	ERO <30 cm² and a regurgitant volume and fraction of <30–40 ml and <50% respectively	*Motion abnormalities with probably dilated left vertical with geometric change *Myocardial disease	Evident symptoms are those of coronary ischemia which could be reversed with adequate therapy
III	Tolerant asymptomatic mitral regurgitation [Severe]	Loss of leaflets coaptation centrally combined with annular dilatation and motion abnormalities which are regional	ERO ≥30 cm² and a regurgitant volume and fraction of ≥30–40 ml and ≥50% respectively	*Motion abnormalities with probably dilated left vertical with geometric change *Myocardial disease	Evident symptoms are those of coronary ischemia which could be reversed with adequate therapy
IV	Symptomatic Severe mitral regurgitation	Loss of leaflets coaptation centrally combined with annular dilatation and motion abnormalities which are regional	*ERO 0.20 cm² *Regurgitant volume 30 mL *Regurgitant fraction 50%	*Motion abnormalities with probably dilated left vertical with geometric change *Myocardial disease	* Evident symptoms are those of coronary ischemia which could be reversed with adequate therapy *Exertional dyspnea *Decreased exercises tolerance level

Author details

Iroegbu Chukwuemeka Daniel[1], Zhongxin Zhou[1]*, Zhang Hao[1] and Jindong Liu[1,2]

*Address all correspondence to: 100000105023@xzhmu.edu.cn

1 Department of Thoracic Cardiovascular Surgery, The Affiliated Hospital of Xuzhou Medical University, Xuzhou, Jiangsu, PR China

2 Department of Anesthesiology, The Affiliated Hospital of Xuzhou Medical University, Xuzhou, Jiangsu, PR China

References

[1] Iroegbu DC, Zhou Z. Huge pedunculated left atrial myxoma with mitral valve replacement due to annular dilatation and concomitant coronary artery disease: A literature review. Italian Journal of Vascular and Endovascular Surgery. 2017;**24**:70-75. DOI: 10.23736/S1824-4777.17.01289-X

[2] Carabello BA. The current therapy for mitral regurgitation. Journal of the American College of Cardiology. 2008;**52**(52):319-326

[3] Donnelly KB. Cardiac valvular pathology: Comparative pathology and animal models of acquired cardiac valvular diseases. Toxicologic Pathology. 2008;**36**(36):204-217

[4] Hueb AC, Jatene FB, Moreira LF, et al. Ventricular remodeling and mitral valve modifications in dilated cardiomyopathy: New insights from anatomic study. The Journal of Thoracic and Cardiovascular Surgery. 2002;**124**:1216-1224

[5] Tibayan FA, Rodriguez F, Langer F, et al. Annular remodeling in chronic ischemic mitral regurgitation: Ring selection implications. The Annals of Thoracic Surgery. 2003;**76**: 1549-1554

[6] Berne RM, Levy MN. Cardiovascular Physiology. St. Louis: Mosby; 1986

[7] Hashim SR, Fontaine A, He S, Levine RA, Yoganathan AP. A three-component force vector cell for *in vitro* quantification of the force exerted by the papillary muscle on the left ventricular wall. Journal of Biomechanics. 1997;**30**:1071-1075

[8] He S, Fontaine AA, Schwammenthal E, Yoganathan AP, Levine RA. Integrated mechanism for functional mitral regurgitation: Leaflet restriction versus coapting force: *In vitro* studies. Circulation. 1997;**96**:1826-1834

[9] Lam JH, Ranganathan N, Wigle ED, Silver MD. Morphology of the human mitral valve. I. Chordae tendineae: A new classification. Circulation. 1970;**41**:449-458

[10] Ormiston JA, Shah PM, Tei C, Wong M. Size and motion of the mitral valve annulus in man. I. A twodimensional echocardiographic method and findings in normal subjects. Circulation. 1981;**64**:113-120

[11] Silverman ME, Hurst JW. The mitral complex. Interaction of the anatomy, physiology, and pathology of the mitral annulus, mitral valve leaflets, chordae tendineae, and papillary muscles. American Heart Journal. 1968;**76**:399-418

[12] Hoffmeier A, Jr S, Scheld HH, Martens S. Cardiac tumors-diagnosis and surgical treatment. Deutsches Ärzteblatt International. 2014;**111**:205-211

[13] Cabrera H, Trindade E, Silva LP, Gamboa C. Heart failure and syncope due to a giant atrial myxoma. Revista Portuguesa de Cardiologia. 2010;**29**:315-319

[14] Nishizaki Y, Yamagami S, Myojin M, Sesoko M, Yamashita H, Suzuki R, et al. A murmur-free giant myxoma discovered incidentally on abdominal ultrasonography. Internal Medicine. 2013;**52**:2529-2531

[15] Manduz S, Katrancioglu N, Karahan O, Yucel O, Yilmaz MB. Diagnosis and follow up of patients with primary cardiac tumours:A singlecentre experience of myxomas. Cardiovascular Journal of Africa. 2011;**22**:310-312

[16] Akhundova A, Samedov F, Cincin A, Tigen K, Ispir S, Ahiskali AR, et al. Giant left atrial myxoma with dual coronary supply presenting with recurrent stroke. Herz. 2015;**40**:318-320

[17] Garatti A, Nano G, Canziani A, Gagliardotto P, Mossuto E, Frigiola A, et al. Surgical excision of cardiac myxomas: Twenty years experience at a single institution. The Annals of Thoracic Surgery. 2012;**93**:825-831

[18] Kumar B, Raj R, Jayant A, Kuthe S. Left atrial myxoma, ruptured chordae tendinae causing mitral regurgitation and coronary artery disease. Annals of Cardiac Anaesthesia. 2014;**17**:133-136

[19] Tas S, Tuncer E, Boyacioglu K, Donmez AA, Bakal RB, Kayalar N, et al. Cardiac myxomas: A 27-year surgical experience. Türk Göğüs Kalp Damar Cerrahisi Dergisi. 2014;**22**:526-533

[20] Lazaros G, Masoura C, Brili S, Stavropoulos G, Kafri G, Stefanadis C. Large left atrial myxoma in an oligosymptomatic young woman. The Hellenic Journal of Cardiology. 2013;**54**:60-63

[21] Diaz A, Di Salvo C, Lawrence D, Hayward M. Left and right ventricular myxoma: An uncommon presentation of a rare tumour. Interactive Cardiovascular and Thoracic Surgery. 2011;**12**:622-623

[22] Nina VJ, Silva NA, Gaspar SF, Rapôso TL, Ferreira EC, Nina RV, et al. Atypical size and location of a right atrial myxoma:A case report. Journal of Medical Case Reports. 2012;**6**:26

[23] Cohen R, Singh G, Mena D, Garcia CA, Loarte P, Mirrer B. Atrial myxoma: A case presentation and review. Cardiology Research. 2012;**3**:41-44

[24] Vazir A, Douthwaite H. Rapidly growing left atrial myxoma - a case report. Journal of Medical Case Reports. 2011;**5**:417

[25] ACCF/AHATask Force on Practice Guidelines. Methodology Manual and Policies From the ACCF/AHA Task Force on Practice Guidelines. American College of Cardiology Foundation and American Heart Association, Inc. cardiosource.org. 2010. Available at: http://assets.cardiosource.com/Methodology_Manual_for_ACC_AHA_Writing_Committees.pdf and http://my.americanheart.org/idc/groups/ahamah-public/@wcm/@sop/documents/downloadable/ucm_319826.pdf. Accessed February 19, 2014

[26] Kamada T, Shiikawa A, Ohkado A, Murata A. A giant left atrial myxoma with severe mitral valve regurgitation: Report of a case. Kyobu Geka. 2003;**56**:152-154

[27] Yamanaka K, Miki S, Kusuhara K, Ueda Y, Okita Y, Tahata T, et al. Left atrial myxoma associated with ruptured chordae tendineae. Kyobu Geka. 1991;**44**:337-339

[28]   Ceviz M, Erkut B, Gürlertop Y, Unlü Y. Giant left atrial myxoma in a patient with mitral insufficiency: Case report. The Heart Surgery Forum. 2004;**7**:E269-E270

[29]   Sharratt GP, Grover ML, Monro JL. Calcified left atrial myxoma with floppy mitral valve. British Heart Journal. 1979;**42**:608-610

[30]   Snir E, Caspi A, Vidne BA. Rupture of chordae tendineae associated myxoma of the left atrium. Scandinavian Journal of Thoracic and Cardiovascular Surgery. 1985;**19**:189-191

[31]   Germing A, Lindstaedt M, Mügge A, Laczkovics A, Fritz M. Severity of mitral regurgitation may be underestimated in the presence of a left atrial myxoma. The Journal of Heart Valve Disease. 2006;**15**:830-832

[32]   Teng YH, Wang CW, Mao CC. Underdiagnosis of the severity of mitral regurgitation in left atrial myxoma. The Journal of Heart Valve Disease. 2010;**19**:806-807

[33]   Bass NM, Sherratt GP. Left atrial myxoma diagnosed by echocardiography, with observations on tumor movement. British Heart Journal. 1973;**35**:1332-1335 http://dx.doi.org/10.1136/hrt.35.12.1332

[34]   Salcedo EE, Cohen GI, White RD, Davison MB. Cardiac tumors-diagnosis and treatment. Current Problems in Cardiology. 1992;**17**:73

[35]   Kostis JB, Moghadam AN. Echocardiographic diagnosis of left atrial myxoma. Chest. 1970;**58**:550-552 http://dx.doi.org/10.1378/chest.58.5.550

[36]   Charuzi Y, Bolger A, Beeder C, Lew AS. A new echocardiographic classification of left atrial myxoma. American Journal of Cardiology. 1985;**55**:614-615 http://dx.doi.org/10.1016/0002-9149(85)90275-9

[37]   Carpentier A. Cardiac valve surgery — The "French correction". The Journal of Thoracic and Cardiovascular Surgery. 1983;**86**:323-337

[38]   Kumar N, Kumar M, Duran CMG. A revised terminology for recording surgical findings of the mitral valve. The Journal of Heart Valve Disease. 1995;**4**:70-75

[39]   Reeder GS. Identification and treatments of complications of myocardial infarction. Mayo Clinic Proceedings 70. 1995;**9**:880-884

[40]   Koukis I, Velissaris T, Pandian A. Left atrial myxoma associated with mitral valve pathology in pregnancy. Hellenic Journal of Cardiology. 2013;**54**:138-142

[41]   Ambrose J, Singh M. "Pathophysiology of coronary artery disease leading to acute coronary syndromes". F1000Prime Reports. 2015;**7**. DOI: 10.12703/P7-08. ISSN 2051-7599. PMC 4311268

[42]   Mouine NN, Asfalou II, Raissouni MM, Benyass AA, Zbir el ME. Giant left atrial myxoma mimicking severe mitral valve stenosis and severe pulmonary hypertension. International Archives of Medicine 2013;**19**:13

[43]   Rajamannan NM, Antonini-Canterin F, Moura L, Zamorano JL, Rosenhek RA, Best PJ, et al. Medical therapy for rheumatic heart disease: Is it time to be proactive rather than reactive? Indian Heart Journal. 2009;**61**(61):14-23

[44] Zheng JJ, Geng XG, Wang HC, Yan Y, Wang HY. Clinical and histopathological analysis of 66 cases with cardiac myxoma. Asian Pacific Journal of Cancer Prevention. 2013;**3**:1743-1746

[45] Gošev I, Paić F, Durić Z, Gošev M, Ivčević S, Jakuš FB, et al. Cardiac myxoma the great imitators: Comprehensive histopathological and molecular approach. International Journal of Cardiology. 2013;**164**:7-20

[46] Yuan SM, Humuruola G. Stroke of a cardiac myxoma origin. Revista Brasileira de Cirurgia Cardiovascular 2015;**30**:225-234

[47] Mitchell RS, Kumar V, Robbins SL, Abbas AK, Fausto N. Robbins basic pathology. 8th edition. Saunders/Elsevier; 2007. pp. 406-408. ISBN 1-4160-2973-7

Cardiac Dyssynchrony as a Pathophysiologic Factor of Functional Mitral Regurgitation: Role of Cardiac Resynchronization Therapy

Barbara Brzezińska and Krystyna Łoboz-Grudzień

Additional information is available at the end of the chapter

Abstract

Functional mitral regurgitation, a common problem in patients with left ventricular systolic dysfunction, has a strong negative impact on prognosis. Beneficial effects of surgical treatment in functional mitral regurgitation are still a matter of debate. Thus, cardiac dyssynchrony, a factor involved in functional mitral regurgitation pathophysiology, may become a therapeutic target in patients with this condition. This part of the book presents the pathophysiology of functional mitral regurgitation as a dynamic process, with particular emphasis on cardiac dyssynchrony, as both a contributor to functional mitral regurgitation and a target for cardiac resynchronization therapy. The underlying mechanisms of success and failure in the resynchronization therapy are discussed, along with therapeutic approaches to symptomatic patients with severe left ventricular dysfunction and significant persistent functional mitral regurgitation.

Keywords: functional mitral regurgitation, left ventricular remodeling, cardiac dyssynchrony, cardiac resynchronization therapy

1. Introduction

Secondary (functional) mitral regurgitation (MR) is a common finding in patients with global left ventricular (LV) dilatation and dysfunction, in both ischemic and non-ischemic cardiomyopathy. This functional disorder of the mitral valve is more common and far more complex than organic MR. In secondary MR, mitral valve is structurally normal (or almost normal) but its geometry and function are disrupted due to an imbalance between closing and tethering

forces secondary to alterations in the geometry and function of the left ventricle. Functional MR can promote progressive LV remodeling. This results in a vicious circle, with both LV dilatation and functional MR acting as self-perpetuating processes. While prognosis is affected only in severe organic MR, even a mild functional MR may significantly worsen the outcome. However, it is unclear whether the unfavorable impact of functional MR on prognosis is independent of underlying LV dysfunction. We still do not know if mitral valve surgery, effective in the treatment of organic diseases of the mitral valve, can be equally beneficial in functional MR, since the surgical correction of valve dysfunction does not reverse the underlying LV pathology. Thus, indications for mitral valve surgery in heart failure (HF) patients with functional MR are not well defined in any currently available guidelines. Also the role of other treatment modalities, such as medical and interventional therapies, still raises controversies because of their limited effectiveness in functional MR management. This is related to both the underlying heart disease and the complexity of functional MR phenomenon. Also, adequate assessment of functional MR mechanisms and severity by means of imaging studies prior to making any therapeutic decisions constitute a challenge for clinicians. Cardiac dyssynchrony is a mechanism that provides a pathophysiologic basis for potential improvement of functional MR after the use of cardiac resynchronization therapy (CRT).

This part of the book presents the pathomechanism of functional MR with particular emphasis on the influence of cardiac dyssynchrony on mitral valve function, as well as the mechanisms of MR improvement after implantation of a CRT device, and prognostic value of both functional MR and its regression in response to CRT in patients with chronic heart failure.

2. Incidence and importance of functional mitral regurgitation in left ventricular dysfunction

Functional MR is a common, but often 'silent,' finding in heart failure patients [1–6]. Reported prevalence of functional MR varies depending on a diagnostic method (angiography, color Doppler echocardiography) and heart failure etiology (ischemic, non-ischemic) [1–5]. The incidence of functional MR after myocardial infarction varies from 20 to 50% but exceeds 50% in patients with non-ischemic dilated cardiomyopathy [4–6]. According to general estimates, nearly a half of heart failure patients may have a functional MR of some degree, and approximately one-third of them may suffer from moderate or severe functional MR [1, 3, 7].

Functional MR is an independent predictor of worse prognosis in patients with either ischemic or non-ischemic etiology of heart failure [3]. In patients with non-ischemic LV dysfunction, functional MR is associated with a two- to three-fold increased risk of heart failure episodes and cardiac mortality [4]. After myocardial infarction the presence of at least moderate functional MR is associated with a 3-fold increased risk of heart failure and a 1.6-fold increased risk of death at the 5-year follow-up [2]. Assessment of mitral valve function is included in routine risk stratification after myocardial infarction.

Functional MR is present in a large proportion of patients eligible for cardiac resynchronization therapy, with the incidence varying slightly from population to population and depending

on the evaluation method. Significant—that is, at least moderate—functional MR is present in about 40% of patients qualified to CRT [8–10]. Nowadays, functional MR no longer disqualifies patients from resynchronization therapy if such treatment is indicated. Furthermore, a decrease in functional MR severity is a determinant of response to CRT [10–12].

3. Difficulties in echocardiographic quantification of functional mitral regurgitation

Adequate evaluation of functional MR requires detailed clinical information (including functional NYHA class), physical examination, electrocardiography, and imaging studies. Echocardiography is essential for the evaluation of mitral valve anatomy and quantification of MR severity [13]. Transthoracic and transesophageal echocardiography may provide complementary clinically useful information, especially in the context of surgical or transcatheter repair feasibility. Usually, transesophageal echocardiography is more suitable for the evaluation of underlying anatomical conditions and identification of functional MR mechanism. However, due to changes in LV loading conditions during transesophageal evaluation (vasodilatory effect of sedation, hypovolemia, or anesthesia), the severity of functional MR may be underestimated; this favors transthoracic echocardiography as a method to quantify mitral regurgitation. Moreover, transthoracic examination is more suitable for the evaluation of other important parameters, such as LV volume, function and sphericity, left atrial size, pulmonary artery pressure, and function of the right ventricle and tricuspid valve. Three-dimensional (3D) echocardiography (either transesophageal or transthoracic) may provide additional information about MR severity, especially with regard to noncircular orifice geometry in functional MR [14]. 3D echocardiography overcomes some limitations of two-dimensional (2D) imaging; for example, it can be used for direct planimetric measurement of *vena contracta* area, a parameter which corresponds directly to the effective regurgitant orifice area (EROA) irrespective of the orifice shape or number of jets. However, both 3D and 2D color Doppler flows tend to overestimate the jet area (volume) due to their known bias in correct assessment of a turbulent stream. Considering all the difficulties previously mentioned, it needs to be stressed that no single parameter (also "quantitative") is sufficient to adequately assess the severity of functional MR and thus, this condition should be evaluated with multiple methods [14].

In practical terms, echocardiographic severity of MR can be graded as mild, moderate or severe. Since available evidence suggests that functional MR of lesser severity may have similar or greater impact on mortality than primary MR [2], distinguishing between moderate and severe MR becomes of vital importance [15]. While severe primary MR is defined as EROA ≥ 40 mm^2 and regurgitant volume ≥ 60 mL, in line with current guidelines, severe secondary MR should be diagnosed whenever EROA ≥ 20 mm^2 and regurgitant volume ≥ 30 mL [13, 15] (**Table 1**) [16]. However, adequate evaluation of functional MR severity in a clinical setting is far more challenging. In functional MR, both regurgitant orifice and jet area depend strongly on the mechanism of mitral regurgitation. Functional MR severity may be overestimated if determined based on the jet size on color Doppler imaging, or underestimated if

	Primary (organic) MR	Secondary (functional) MR
EROA	≥0.4 cm^2	≥0.2 cm^2
Regurgitant volume	≥60 mL	≥30 mL
Regurgitant fraction	≥50%	≥50%
Vena contracta	≥0.7 cm	—
Jet area	Central jet >40% LA or holosystolic eccentric jet	—

Table 1. Quantitative echocardiographic criteria for severe MR in primary and secondary disease of the mitral valve [16].

assessed using other traditional measures of mitral regurgitation such as proximal isovelocity surface area (PISA) and *vena contracta* width [14]. Also the limitations of the volumetric method in the assessment of regurgitant volume and fraction are well-known issues [14]. Furthermore, low inter- and intra-observer agreement between cardiologists reviewing the same dataset was documented [17]. It is now known that due to the limitations inherent to each available method, no single parameter is accurate enough to quantify the degree of MR. Therefore, current guidelines recommend an integrative approach including multiple qualitative and quantitative parameters, along with certain signs and measures of MR severity, such as left ventricular size and function, left atrial size, mitral valve leaflet morphology and motion, mitral filling pattern, pulmonary venous flow pattern and others [13, 16]. If during the first attempt MR is not unequivocally defined as mild or severe, the integrative approach should be used to exclude the severe character of mitral regurgitation.

Functional MR is an evidently dynamic phenomenon. A typical phasic variation in regurgitant volume and orifice, with the maximum values observed in early and late systole and minimum ones in mid-systole (at peak transmitral pressure gradient generated by LV), is documented [18]. This intra-beat variability (referred to as the "loitering pattern") hinders functional MR assessment, which is traditionally carried out in mid-systole. The severity of functional MR may also show a beat-to-beat variability depending on changes in loading conditions and hemodynamic parameters (e.g., during arrhythmia). The dynamic nature of functional MR has particular practical meanings in two situations: during physical exertion and intraoperative assessment. Induction of anesthesia and inotropic agents may significantly reduce MR and thus, may directly affect intraoperative decisions regarding its repair. Owing the dynamic nature of functional MR, in patients whose symptoms at rest are inadequate to assess the severity of mitral regurgitation, more accurate information may be obtained during exercise echocardiography. Exercises contribute to a greater cardiac load and thus, may also trigger dynamic geometric changes in the LV and mitral valve apparatus (even despite the lack of provoked ischemia), which may eventually result in acute "flash pulmonary edema" [19]. This may be a reason behind worse prognosis associated with even a mild functional MR. An exercise-induced increase in EROA by at least 13 mm^2 was shown to correlate with higher morbidity and mortality [20]. Exercise echocardiography may also unmask increasing pulmonary artery pressure and the lack of LV contractile reserve, both being important predictors of the outcome [19, 20]. Finally, exercises may reveal or trigger greater LV dyssynchrony with increased functional MR [21]. Despite some caveats of this approach, current guidelines recommend echocardiographic quantification of secondary MR during exercises, as this may

provide prognostically important information about dynamic characteristics of this condition [13]. Owing to documented limitations of echocardiography in this setting, newer imaging techniques, such as cardiac magnetic resonance and multidetector-row computed tomography, play an increasing role in the evaluation of patients with heart failure and functional MR. Both these techniques provide complementary data, such as true volumetric measures of cardiac chamber size and function, and can be used to assess myocardial viability and scars.

4. Pathophysiology of functional mitral regurgitation

The term "functional mitral regurgitation" refers to a dysfunction of the valve without its primary organic damage. Optimal function of the mitral valve provides nonrestrictive blood flow during diastole and leak tightness during systole. This diastolic and systolic competence is possible due to a synchronous coordination of all components of the mitral valve apparatus, acting under a balanced influence of closing and opening forces. Mitral valve apparatus is an integrated unit consisting of mitral valve itself (formed by two leaflets and mitral annulus) and subvalvular components (chordae tendineae, two papillary muscles, left ventricle and posterior left atrial wall). An effective function of the mitral valve is determined not only by the compatible cooperation between its components but also by their appropriate structural and spatial relations.

4.1. Left ventricular remodeling and dysfunction as a mechanism of functional mitral regurgitation

All changes in LV function and geometry affect functioning of mitral valve through opposing strength vectors: the tethering force (created by displacement of papillary muscles) and the LV-generated leaflet closing force (created by effective contraction causing transmitral pressure gradient) (**Figure 1**) [22]. Global LV dilation results in incomplete mitral leaflet closure and mitral regurgitation, which correlates with LV dysfunction. Local or global dilation of the LV is a prerequisite for incomplete mitral leaflet closure [22]. However, functional MR does not result from LV dilatation per se but from an increase in LV sphericity and resultant posterolateral displacement of the papillary muscles [23, 24]. If functional MR has an ischemic etiology, it does not necessarily need to be preceded by global systolic dysfunction [25]. Regional abnormalities in cardiac wall motion after inferior myocardial infarction may contribute to mitral valve tethering (with systolic tenting of the leaflets), which is strong enough to cause severe mitral regurgitation despite preserved LV ejection fraction (LVEF) [25].

Two main patterns of leaflet tethering can be distinguished in functional mitral regurgitation (**Figure 2**) [26, 27]. The symmetric pattern is characterized by global LV dilation with increased sphericity and predominant apical displacement of both leaflets with central regurgitant jet direction. Also the mitral valve annulus dilates symmetrically, primarily in the septal-lateral direction [26, 27]. This configuration is typical for non-ischemic functional MR (Carpentier type III B symmetric) [27, 28]. The asymmetric pattern is typically resulted from local remodeling of the posterior papillary muscle-bearing wall segment, with posterior tenting of both leaflets and a posteriorly directed asymmetric regurgitant jet (Carpentier type III B asymmetric) [25–28]. While the displacement of posterior papillary muscle is similar regardless of the leaflet tethering pattern, symmetric tethering is characterized by greater posterior and lateral displacement of
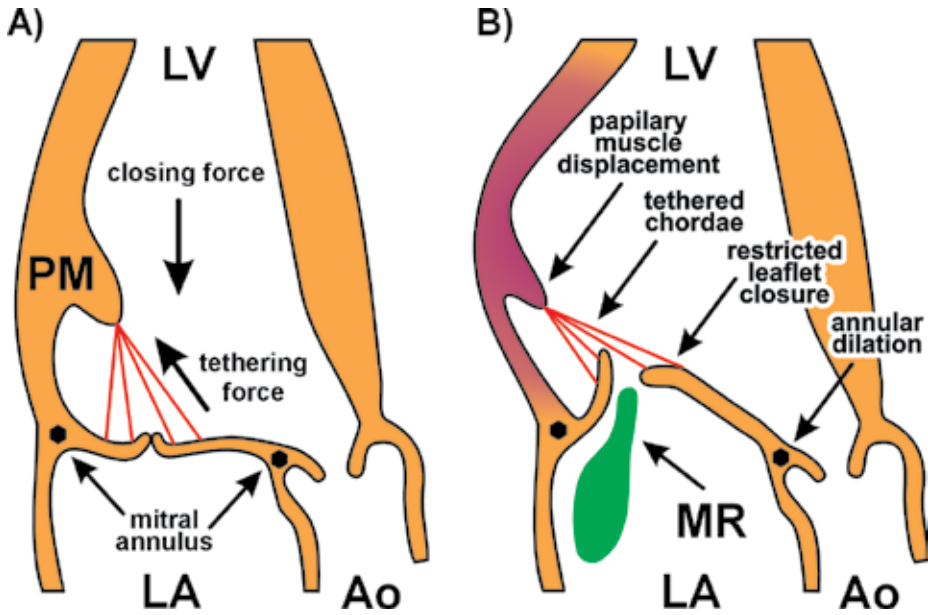
Figure 1. Mechanism of functional mitral regurgitation. (A) Balance of closing and tethering forces acting on mitral leaflets during systole. (B) Disrupted balance of closing and tethering forces due to local LV remodeling (dark shading). LA: left atrium; LV: left ventricle; PM: papillary muscle; Ao: aorta; ME: mitral regurgitation.
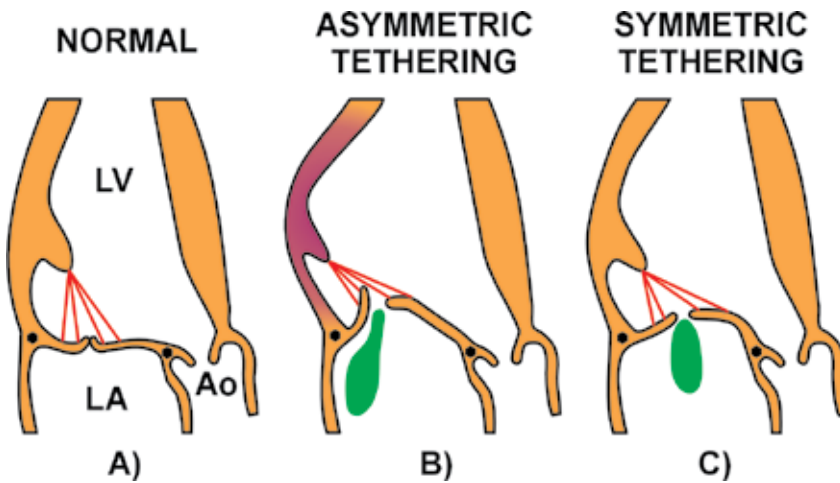
Figure 2. Patterns of leaflet tenting in functional mitral regurgitation. (A) Normal coaptation of mitral leaflets. (B) Asymmetric pattern—predominant posterior displacement of both leaflets with prevent restriction of posterior leaflet and large eccentric regurgitant jet. (C) Symmetric pattern—predominant apical displacement of both leaflets with central regurgitant jet.

anterior papillary muscle and longer inter-papillary distance [27]. Both patterns of leaflet tethering can be observed in ischemic MR [25–27]. The occurrence of the symmetric pattern in ischemic MR is associated with more advanced systolic dysfunction, global remodeling and increased LV sphericity [23, 24, 27]. This pattern is typical for non-ischemic dilated cardiomyopathy [26].

While geometric changes of LV are an essential component of functional MR pathomechanism, it is the tethering distance between the tip of posterior papillary muscle and the anterior pole of mitral annulus ("posterior papillary-fibrosa distance"), which constitutes the final common pathway determining the plane of leaflet coaptation [22, 29]. Mitral annular dilation typically occurs at late stage of ischemic MR [30, 31]. Isolated dilation and flattening of mitral valve annulus are occasionally the cause of severe mitral regurgitation, representing type I in Carpentier's classification [28, 30, 31]. Although atrial fibrillation constitutes a quite frequent cause of functional MR, it rarely results in severe valve dysfunction. Isolated enlargement of the left atrium, with concomitant atrial fibrillation or without, leads to dilatation of mitral annulus and reduced leaflet coaptation [32]. Diastolic MR results from a reversal of atrioventricular pressure gradient during diastole. This form of MR occurs in patients with atrioventricular block, cardiomyopathy and aortic regurgitation, as well as in individuals with long filling periods in atrial tachyarrhythmia [31].

4.2. Cardiac dyssynchrony as a pathophysiologic factor of functional mitral regurgitation

Dyssynchrony, defined as an uncoordinated regional myocardial contraction [33, 34], may manifest as (1) "primary electrical dyssynchrony" (i.e., electrical conduction delay which causes non-uniform timing of myocyte depolarization), (2) abnormalities in excitation-contraction coupling (a surrogate for regional electromechanical coupling is the interval between the onset of QRS complex in ECG and the onset of systolic velocity in spectral pulsed-wave tissue Doppler imaging), or (3) "primary mechanical dyssynchrony" (i.e., a regional delay in onset shortening and in time to peak shortening of LV segments) [34]. Primary electrical dyssynchrony is typical for left bundle branch block (LBBB) and primary mechanical dyssynchrony—for regional ischemia or fibrosis [33, 34]. Currently, QRS duration remains the only clinically significant surrogate for the timing of myocardial contraction and the only criterion amenable for CRT [35, 36]. Clinical significance of "clear" primary mechanical dyssynchrony remains ambiguous [37, 38]. CRT does not provide any benefit (and may be even harmful) in heart failure patients with mechanical dyssynchrony without QRS widening (<130 ms) [38]. Various echocardiographic measures of dyssynchrony turned out not to be a superior selection criterion for CRT [39, 40]. Moreover, unacceptable variability, poor reproducibility and limited practical predictive value of the most echocardiographic parameters of dyssynchrony are documented [41]. Thus, although the predictive value of prolonged QRS also varies from study to study [42, 43], qualification to CRT is still based primarily on this parameter [35, 36].

Functional MR correlates strongly with QRS duration. Left bundle branch block and right ventricular pacing (which produce a conduction abnormality similar to LBBB), but not right bundle branch block or left anterior hemi-block, are strongly associated with functional MR [44]. The relationship between right ventricular pacing and mitral regurgitation indicates that the key determinant of functional MR is a conduction abnormality, rather than the underlying disease causing LBBB [44]. Those findings have important implications for biventricular pacing as a treatment option in heart failure patients with functional MR.

LV dyssynchrony is a less important determinant of functional MR than systolic valvular tenting, which is the strongest predictor of EROA [45]. However, the impact of systolic valvular tenting on functional MR in different subsets of patients with LV dysfunction varies. Mitral valve tenting and local LV remodeling (in the papillary muscle-bearing wall segments), but not regional dyssynchrony, are independent predictors of functional MR degree in ischemic LV dysfunction; these local changes result directly from ischemic lesions. In non-ischemic LV dysfunction, regional dyssynchrony exacerbates functional MR independently of LV geometry but as a factor of lesser importance [45].

5. Effect of cardiac resynchronization therapy on functional mitral regurgitation

Cardiac resynchronization therapy is an established treatment option for patients with advanced chronic heart failure and prolonged QRS duration [35, 36]. The benefits of CRT are attributed mainly to increased efficiency of LV filling and ejection, resulting from the improvement in atrioventricular coupling, intra- and interventricular synchronization [46–48]. CRT can attenuate heart failure symptoms and improve exercise capacity and survival in patients with heart failure and prolonged QRS duration [49–51]. In line with current ESC guidelines, cardiac resynchronization therapy is recommended (class I recommendation) in symptomatic (despite optimal medical therapy) patients with heart failure in sinus rhythm, with LBBB and QRS duration of at least 130 ms, with LVEF ≤ 35%, and in individuals with LV dysfunction (regardless of the NYHA class) who have an indication for ventricular pacing and high degree atrioventricular block [36]. The outcome of cardiac resynchronization therapy is determined by a number of clinical factors, and improvement of functional mitral regurgitation is currently considered as one of the mechanisms underlying the beneficial effect of the treatment.

Echocardiographic studies demonstrate that cardiac resynchronization therapy may correct the pathophysiologic determinants of functional MR. The following mechanisms are considered to mediate the clinical efficacy of CRT.

1. Restoration of the LV and papillary muscle synchronous contraction improves spatial relations and function of the subvalvular apparatus and the mitral valve itself (a decrease in mitral valve tethering force); the effect is specific for this therapeutic method [52, 53].

2. Improved coordination of LV wall contraction and resultant improvement of LV ejection function contribute to an increase in transmitral pressure gradient (greater mitral valve closing force); the effect is specific for this therapeutic method [54, 55].

3. Remote reverse remodeling of the LV with the reduction of LV volume and sphericity induce favorable changes in the geometry of mitral valve apparatus (a decrease in tethering force) and contribute to further improvement in LV systolic function (an increase in mitral valve closing force); the effect is not specific for this therapeutic method and particularly pronounced at the later phase of CRT [53, 55–57].

4. The effect of cardiac resynchronization therapy on mitral valve annular size and function (through the recoordination of contraction in LV basal segments and then through reverse remodeling of the LV) is uncertain [52, 53].

5. Optimization of atrioventricular delay with the restoration of proper timing for atrioventricular synchrony/atrioventricular relaxation contributes to generation of an adequate transmitral pressure gradient during the cardiac cycle and eliminates diastolic MR (if present); this effect is only partially specific for this therapeutic method [58].

5.1. Biphasic response of functional mitral regurgitation to cardiac resynchronization therapy

The improvement of functional MR after the use of cardiac resynchronization therapy has two phases:

1. Immediate, short-term functional MR reduction occurring directly after the implantation of a CRT device. The effect manifests as better-coordinated contraction of the papillary muscle-bearing segment (diminished tethering force) and improvement of LV ejection function (an increase in transmitral pressure gradient—LV dP/dt, which represents the mitral valve closing force) [52–54]. CRT contributes primarily to a decrease in early-systolic MR [59, 60].

2. Late, long-term functional MR reduction occurring weeks to months after the implantation of a CRT device. This phase manifests primarily as reverse remodeling of the LV. A decrease in LV volume and sphericity induces favorable geometric changes in mitral valve apparatus, with the reduction of tethering force. The improvement of LV systolic function is reflected by an increase in closing force [53, 55, 57]. Attenuation of both resting and exercise-induced functional MR usually can be observed in this phase, along with the improvement of cardiopulmonary performance [61].

In fact, the two phases of functional MR improvement may be less distinct. LV reverse remodeling can occur relatively early [10]. Subacute improvement in systolic shape of the LV (lesser sphericity) and subvalvular traction after CRT implementation are also probably related to an increase in LV longitudinal function [56].

Effective CRT reduces the transmitral regurgitant volume in about 40% of patients immediately and in the next 20% of them at a later stage [53]. The sequence of functional MR improvement may depend on a pattern of baseline dyssynchrony. Early and late responders may show a similar extent of LV dyssynchrony; however, the site of latest activation in early responders is mostly inferior or posterior (adjacent to the posterior papillary muscle), whereas in late responders, the latest activation occurs primarily in the lateral wall [53]. Late responders may also show acute improvement in LV end-systolic volume, presumably as an effect of recoordinated and, hence, more effective LV contraction. Acting through the mechanisms described above, CRT can attenuate moderate-to-severe functional mitral regurgitation to a clinically nonsignificant MR in about one-third of heart failure patients. Published data about the association between baseline functional MR and response to CRT are ambiguous [8, 62–64]. The post-CRT improvement of functional MR may be relatively more frequent in patients with greater severity of mitral regurgitation at the baseline. Moreover, an acute or subacute attenuation of functional MR is a predictor of further improvement [8]. Lack of improvement in functional MR in response to CRT is associated with worse prognosis (unfavorable profile of clinical evolution, higher incidence of arrhythmic events and lesser occurrence of LV reverse remodeling [62, 65]). This raises a question about the predictors of functional MR response to CRT.

5.2. Predictors of functional mitral regurgitation improvement in response to cardiac resynchronization therapy

Despite appropriate selection of candidates for CRT, not all of them respond to the treatment. The mechanisms responsible for post-CRT improvement in functional MR are complex. Although QRS duration is the main determinant of primary electrical dyssynchrony and a primary criterion considered during selection of patients for CRT, it is not a good predictor of response to the treatment [42, 43]. Aside from dyssynchrony, the post-CRT improvement in functional MR may also depend on other factors, such as myocardial viability, presence of scar/fibrosis and the extent of LV remodeling at the baseline [10, 66, 67].

Many echocardiographic measures of dyssynchrony do not confirm their value as the predictors of CRT outcomes [39–41]. Inter-ventricular mechanical delay (IVMD, the time difference between right ventricular and left ventricular ejection, determined as the time elapsed since the onset of the QRS to the onset of left ventricular vs. right ventricular ejection, usually measured using pulsed Doppler flow) seems to be a simple and reproducible parameter of dyssynchrony, correlating well with the response to CRT, either LV reverse remodeling or functional MR improvement [10, 41, 68, 69]. Also, speckle-tracking radial strain imaging (time difference in peak septal to posterior wall strain) appears as a relatively simple measure of dyssynchrony, having established a predictive value with regard to CRT outcome [67]. There is no unambiguous evidence regarding the site of the latest activation as an independent predictor of the improvement in functional MR [10, 53]. Myocardial viability (in heart failure with ischemic etiology) and contractile reserve (in non-ischemic cardiomyopathy) are important determinants of CRT effectiveness in terms of functional MR improvement [10, 70–73]. The outcome of CRT may be also associated with the location of contractile reserve (particularly in relation to the papillary muscle-bearing segments and to the paced LV region), as well as with the size of the contractile reserve area [10, 66, 72, 73]. The importance of discordant LV lead position and myocardial scar, especially extensive scar burden, as the predictors of CRT outcomes, is documented [74, 75]. The potential role of myocardial fibrosis stimulates research on biochemical predictors of CRT responses (among them on galactin-3, a protein involved in fibrogenesis) [76].

5.3. Functional mitral regurgitation improvement and left ventricular reverse remodeling in response to CRT

The change in LV end-diastolic volume after the use of cardiac resynchronization therapy proved to be the most powerful independent predictor of death [77]. CRT effectively reversed LV remodeling, both in patients with moderate-to-severe heart failure (NYHA III/IV class) and in individuals with mild heart failure (NYHA I/II class) [49, 50]. The response to CRT may be influenced by the presence of functional mitral regurgitation prior to the implantation of a CRT device and by its persistence despite the treatment. Patients, who do not respond to CRT, present with a significant functional MR more often than the responders [78]. On the other hand, an improvement in pre-existing functional MR contributes to LV reverse remodeling during follow-up after the implantation of a CRT device [60]. The incidence of reverse remodeling, defined as an improvement in LVEF and forward stroke volume, is the highest in patients who show a reduction of total functional MR, intermediate in individuals with mild functional MR or lack thereof at the baseline and the lowest in

persons who do not show an improvement in total functional MR after 3 months of post-CRT follow-up [60]. Correlation between clinical and echocardiographic indices of post-CTR improvement is rather weak [10, 77]. However, the direction and magnitude of LV reverse remodeling correlate with survival, and a 1-year mortality after CRT implementation is predicted by echocardiographic parameters, rather than by clinical indices [77].

Finally, volumetric limitation for functional MR improvement in response to cardiac resynchronization therapy needs to be emphasized. Not only irreversibly damaged ischemic myocytes respond less to CRT, the post-CRT improvement in functional MR is also less likely in patients who present with greater degree of LV dilatation at the baseline. Lesser baseline LV diameters (end-diastolic and end-systolic) and volumes are the independent predictors of functional MR improvement in response to CRT [10, 67, 79–81]. The cut-off value for LV end-diastolic dimension is close to 75 mm [10, 82] and for LV end-systolic dimension index 29 mm/m^2 [67]. Non-responders present a significantly higher baseline LV dilatation. CRT may be insufficient to overcome poor natural history of systolic heart failure but may slow down its progression. The effectiveness of all currently available therapeutic options is limited, and critical enlargement of the left ventricle may trigger the previously mentioned vicious circle of self-perpetuating LV dilatation and functional mitral regurgitation [10, 83, 84].

6. Management of patients with persistent significant functional mitral regurgitation after the use of CRT

Therapeutic targets in patients with functional MR include attenuation of symptoms, lesser number of heart failure hospitalizations, better quality of life and, potentially, survival. At present, the most effective therapies of functional MR are aimed at the underlying LV dysfunction. Therefore, as the first step, optimal medical therapy according to the guidelines for the management of heart failure should be used [36]. As the second step, whenever appropriate, CRT should be implemented in line with the respective guidelines [35, 36]. In patients who remain symptomatic despite optimal medical therapy and CRT (if indicated), mitral valve intervention (surgical or transcatheter repair) should be considered; however, there is no evidence that a reduction of functional MR improves survival [13]. Moreover, the surgery has never clearly been demonstrated to alter the natural history of the primary disease (dilated cardiomyopathy) [85]. Limited empirical data contribute to a lower level of evidence for management recommendations, highlighting the importance of decisions made by the Heart Team. The multidisciplinary Heart Team consisting of imaging experts, heart failure and electrophysiology specialists, interventional cardiologists, and cardiac surgeons should try to reach a consensus on appropriate care. Not only the feasibility of the procedure but also comorbidities, the level of surgical risk, and surgeon experience should be considered [13]. In patients undergoing revascularization, the evaluation and decision to treat (or not to treat) ischemic MR should be made prior to surgery. There is an overall agreement that severe functional MR should be addressed at the time of coronary artery bypass grafting (CABG). The management of moderate functional MR in patients undergoing CABG still raises controversies [86]. The thresholds of functional MR severity are also a matter of debate (as stated earlier). Surgical options in patients with functional MR include mitral valve repair and replacement.

Mitral valve deformation	Coaptation distance ≥1 cm
	Tenting area > 2.5–3 cm^2
	Complex jets originating centrally and posteromedially
	Posterolateral angle >45° (high posterior leaflet tethering)
Local LV remodeling	Interpapillary muscle distance >20 mm
	Posterior papillary-fibrosa distance >40 mm
	Lateral wall motion abnormality
Global LV remodeling	EDD >65 mm, ESD >51 mm (ESV >140 mL) (low likelihood of reverse LV remodeling after repair and poor long-term outcome)
	Systolic sphericity index >0.7

EDD, end-diastolic diameter; ESD, end-systolic diameter; ESV, end-systolic volume; LV, left ventricle.

Table 2. Unfavorable TTE characteristics for mitral valve repair in secondary MR [88].

Mechanical LV-assisted devices and heart transplantation should be considered in the most advanced stage of heart failure.

The controversies regarding an optimal surgical approach should be emphasized [87]. After surgical annuloplasty (undersized complete ring to restore leaflet coaptation), residual or recurrent functional MR is frequently observed (in approximately one-third of the cases) [88]. Valve-sparing mitral valve replacement techniques (leaving the leaflet and subvalvular apparatus intact to preserve the LV function) should be considered in patients with echocardiographic predictors of repair failure (**Table 2**) [88]. The surgery should also be considered in heart failure patients with severe functional MR and LVEF <30% but with an option for CABG and the evidence of myocardial viability. Qualification for surgical treatment of functional MR should be restrained if concomitant revascularization is not indicated [89].

Percutaneous edge-to-edge repair (MitraClip device) for FMR is a low-risk procedure and may be considered in patients during high surgical risk, whenever feasible [90]. The treatment may attenuate symptoms, improve quality of life and promote LV reverse remodeling but is inferior to surgical methods in terms of functional MR reduction. Valve intervention is generally contraindicated in patients with LVEF < 15% [13]. Two investigational extracardiac devices, CorCap (Acorn Cardiovascular) [91] and Coapsys (Myocor, Inc., Maple Grove, Minnesota) [92], which have been used to reshape the LV and thus to reduce the degree of functional MR, remained an interesting experiment. In cases of more advanced LV dysfunction (LVEF ≤ 30%) with no option for CABG, the Heart Team should choose between a palliative treatment of functional MR (surgical or transcatheter procedures, ventricular assist devices, heart transplantation) and a conservative therapy, after careful individual appraisal of the patient [13].

7. Conclusion

Irrespective of heart failure etiology, functional mitral regurgitation has a significant unfavorable impact on prognosis. The benefits of surgical treatment in functional mitral regurgitation

are unclear and thus, resynchronization therapy remains a valuable option in eligible patients. Indications for such treatment should be considered as early as possible, before the development of a severe left ventricular dilatation, a predictor of failure in resynchronization therapy.

Acronyms and abbreviations

CABG	coronary artery bypass grafting
CRT	cardiac resynchronization therapy
EROA	effective regurgitant orifice area
HF	heart failure
LBBB	left bundle branch block
LV	left ventricle
LVEF	left ventricular ejection fraction
MR	mitral regurgitation
NYHA	New York Heart Association
PISA	proximal isovelocity surface area

Author details

Barbara Brzezińska[1]* and Krystyna Łoboz-Grudzień[1,2]

*Address all correspondence to: be.brzezinska@gmail.com

1 Department of Cardiology, T. Marciniak Hospital, Wroclaw, Poland

2 Faculty of Health Science, Wroclaw Medical University, Poland

References

[1] Lamas GA, Mitchell GF, Flaker GC, Smith SC Jr, Gersh BJ, Basta L, Moye L, Braunwald E, Pfeffer MA, Survival and Ventricular Enlargement Investigators. Clinical significance of mitral regurgitation after acute myocardial infarction. Circulation. 1997;**96**:827-833. DOI: 10.1161/01.CIR.96.3.827

[2] Grigioni F, Enriquez-Sarano M, Zehr KJ, Bailey KR, Tajik AJ. Ischemic mitral regurgitation: Long-term outcome and prognostic implications with quantitative Doppler assessment. Circulation. 2001;**103**:1759-1764. DOI: 10.1161/01.CIR.103.13.1759

[3] Trichon BH, Felker GM, Shaw LK, et al. Relation of frequency and severity of mitral regurgitation to survival among patients with left ventricular systolic dysfunction and heart failure. The American Journal of Cardiology. 2003;**91**:538-543. DOI: 10.1016/S0002-9149(02)03301-5

[4] Rossi A, Dini FL, Faggiano P, et al. Independent prognostic value of functional mitral regurgitation in patients with heart failure. A quantitative analysis of 1256 patients with ischemic and non-ischemic dilated cardiomyopathy. Heart. 2011;**97**:1675-1680. DOI: 10.1136/hrt.2011.225789

[5] Bursi F, Enriquez-Sarano M, Nkomo VT, et al. Heart failure and death after myocardial infarction in the community. The emerging role of mitral regurgitation. Circulation. 2005;**111**:295-301. DOI: 10.1161/01.CIR.0000151097.30779.04

[6] Koelling TM, Aaronson KD, Cody RJ, Bach DS, Armstrong WF. Prognostic significance of mitral regurgitation and tricuspid regurgitation in patients with left ventricular systolic dysfunction. American Heart Journal. 2002;**144**:524-529. DOI: 10/1067/mhj.2002.12357

[7] van Bommel RJ, Marsan NA, Delgado V, et al. Cardiac resynchronization therapy as a therapeutic option in patients with moderate-severe functional mitral regurgitation and high operative risk. Circulation. 2011;**124**:912-919. DOI: 10.1161/CIRCULATIONAHA.110.009803

[8] Di Biase L, Auricchio A, Mohanty P, et al. Impact of cardiac resynchronization therapy on the severity on mitral regurgitation. Europace. 2011;**13**:829-838. DOI: 10.1093/europace/eur047

[9] Cabrera-Bueno F, Molina-Mora MJ, Alzueta J, et al. Persistence of secondary mitral regurgitation and response to cardiac resynchronization therapy. European Journal of Echocardiography. 2010;**11**:131-137. DOI: 10.1093/ejechocard/jep184

[10] Brzezińska B, Łoboz-Grudzień K, Wita K, et al. Predictors of functional mitral regurgitation improvement during a short-term follow-up after cardiac resynchronization therapy. Kardiologia Polska. 2016;**74**(7):665-673. DOI: 10.5603/KP.a2016.0005

[11] Boriani G, Gasparini M, Landolina M, et al. Impact of mitral regurgitation on the outcome of patients treated with CRT-D: Data from the InSync ICD Italian Registry. Pace. 2012;**35**:146-154. DOI: 10.1111/j.1540-8159.2011.03280.x

[12] Upadhyay GA, Chatterjee NA, Kandala J, et al. Assessing mitral regurgitation in prediction of clinical outcome after cardiac resynchronization therapy. Heart Rhythm. 2015;**12**(6):1201-1208. DOI: 10.1016/j.hrthm.2015.02.022

[13] Baumgartner H, Falk V, Bax JJ, et al. 2017 ESC/EACTS Guidelines for the management of valvular heart disease: The Task Force for the management of valvular heart disease of the European Society of Cardiology (ESC) and the European Association for Cardio-Thoracic Surgery (EACTS). European Heart Journal. 2017;**38**:2739-2791. DOI: 10.1093/eurheartj/ehx391

[14] Grayburn PA, Weissman NJ, Zamorano JL. Quantification of mitral regurgitation. Circulation. 2012;**126**:2005-2017. DOI: 10.1016/j.amjcard.2013.07.047

[15] Grayburn PA, Carabello B, Hung J, et al. Defining 'severe' secondary mitral regurgitation. Emphasizing an integrated approach. Journal of the American College of Cardiology. 2014;**64**:2792-2780. DOI: 10.1016/j.jacc.2014.10.016

[16] Nishimura RA, Otto CM, Bonow RO, et al. 2014 AHA/ACC guideline for the management of patients with valvular heart disease, a report of the American Collage of Cardiology/American Heart Association Task Force on Practice Guidelines. Journal of the American College of Cardiology. 2014;**63**:e57-e185. DOI: 10.1016/j.jacc.2014.02.536

[17] Biner S, Raphique A, Rafii F, et al. Reproducibility of proximal isovelocity surface area, vena contracta, and regurgitant jet area for assessment of mitral regurgitation severity. Journal of the American College of Cardiology. 2010;**3**:235-243. DOI: 10.1016/j.jcmg.2009.09.029

[18] Schwammenthal E, Chen C, Benning F, et al. Dynamics of mitral regurgitation flow and orifice area; physiologic application of the proximal flow convergence method: Clinical data and experimental testing. Circulation. 1994;**90**:307-322. DOI: 10.1161/01.CIR.90.1.307

[19] Pierard L, Lancellotti P. The role of ischemic mitral regurgitation in the pathogenesis of acute pulmonary edema. The New England Journal of Medicine. 2004;**352**:1627-1634. DOI: 10.1056/NEJMoa040532

[20] Lancellotti P, Transfontaines P, Toussaint AC, et al. Prognostic importance of exercise-induced changes in mitral regurgitation in patients with chronic ischemic left ventricular dysfunction. Circulation. 2003;**108**:1713-1717. DOI: 10.1161/01.CIR.0000087599.49332.05

[21] Lancellotti P, Stainier PY, Lebois F, Pierard LA. Effect of dynamic left ventricular dyssynchrony on dynamic mitral regurgitation in patients with heart failure due to coronary artery disease. The American Journal of Cardiology. 2005;**96**:1304-1307. DOI: 10.1016/j.amjcard.2005.06.077

[22] Otsuji Y, Handschumacher MD, Schwammenthal E, et al. Insight from tree-dimensional echocardiography into the mechanism of functional mitral regurgitation: Direct in vivo demonstration of altered leaflet tethering geometry. Circulation. 1997;**96**:1999-2008. DOI: 10.1161/01.CIR.96.6.1999

[23] Kono T, Sabbah HN, Rosman H, et al. Left ventricular shape is the primary determinant of functional mitral regurgitation in heart failure. Journal of the American College of Cardiology. 1992;**20**:1594-1598. DOI: 10.1016/0735-1097(92)90455-V

[24] Sabbah HN, Rosman H, Kono T, et al. On the mechanism of functional mitral regurgitation. American Journal of Cardiology. 1993;**72**:1074-1076. DOI: 10.1016/0735-1097(94)00426-Q

[25] Kumanohoso T, Otsuji Y, Yoshifuku S, et al. Mechanism of higher incidence of ischemic mitral regurgitation in patients with inferior myocardial infarction: Quantitative analysis of left ventricular and mitral valve geometry in 103 patients with prior myocardial infarction. The Journal of Thoracic and Cardiovascular Surgery. 2003;**125**:135-143. DOI: 10.1067/mva.2003.78

[26] Yiu SF, Enriquez-Sarano M, Tribouilloy C, et al. Determinants of the degree of functional mitral regurgitation in patients with systolic left ventricular dysfunction. A quantitative clinical study. Circulation. 2000;**102**:1400-1406. DOI: 10.1161/01.CIR.102.12.1400

[27] Agricola E, Oppizzi M, Maisano F, et al. Echocardiographic classification of chronic ischemic mitral regurgitation caused by restricted motion according to tethering pattern. European Journal of Echocardiography. 2004;**5**:326-334. DOI: 10.1016/j.euje.2004.03.001

[28] Carpentier A. Cardiac valve surgery: The "French correction." The Journal of Thoracic and Cardiovascular Surgery. 1983;**86**:323-337

[29] Otsuji Y, Levine RA, Takeuchi M, et al. Mechanism of ischemic mitral regurgitation. Journal of Cardiology. 2008;**51**:145-156. DOI: 10.1016/j.jjcc.2008.03.005

[30] Boltwood CM, Tei C, Wong M, et al. Quantitative echocardiography of the mitral complex in dilated cardiomyopathy: The mechanism of functional mitral regurgitation. Circulation. 1983;**68**:498-508. DOI: 10.1161/01.CIR.68.3.498

[31] Nof E, Glikson M, Bar-Lev D, et al. Mechanism of diastolic mitral regurgitation in candidates for cardiac resynchronization therapy. The American Journal of Cardiology. 2006;**97**(11):1611-1614. DOI: 10.1016/j.amjcard.2005.12.064

[32] Gertz ZM, Raina A, Saghy L, et al. Evidence of atrial functional mitral regurgitation due to atrial fibrillation: Reversal with arrhythmia control. Journal of the American College of Cardiology. 2011;**58**:1474-1781. DOI: 10.1016/j.jacc.2011.06.032

[33] Task FM, Vardas PE, Auricchio A, et al. Guidelines for cardiac pacing and cardiac resynchronization therapy: The Task Force for Cardiac Pacing and Cardiac Resynchronization Therapy of the European Society of Cardiology. Developed in collaboration with the European Heart Rhythm Association. European Heart Journal. 2007;**28**:2256-2295. DOI: 10.1093/eurheartj/ehm305

[34] Smiseth OA, Russell K, Skulstad H. The role of echocardiography in quantification of left ventricular dyssynchrony: State of the art and future directions. European Heart Journal—Cardiovascular Imaging. 2012;**13**:61-68. DOI: 10.1093/ejechocard/jer243

[35] Brignole M, Auricchio A, Baron-Esquivias G, et al. ESC Guidelines on cardiac pacing and cardiac resynchronization therapy. The Task Force on cardiac pacing and resynchronization therapy of the European Society of Cardiology (ESC). Developed in collaboration with the European Heart Rhythm Association. European Heart Journal. 2013, 2013;**34**:2281-2329. DOI: 10.1093/eurheartj/eht150

[36] Ponikowski P, Voors AA, Anker DA, et al. ESC Guidelines for the diagnosis and treatment of acute and chronic heart failure. The Task Force for the diagnosis and treatment of acute and chronic heart failure of the European Society of Cardiology (ESC). Developed with the special contribution of the heart failure association (HFA) of the ESC. European Heart Journal. 2016;**37**:2129-2200. DOI: 10.1093/eurheartj/ehw128

[37] D'Andrea A, Mele D, Nistri S, et al. The prognostic impact of dynamic ventricular dyssynchrony in patients with idiopathic dilated cardiomyopathy and narrow QRS. European Heart Journal. Cardiovascular Imaging. 2013;**14**:183-189. DOI: 10.1093/ehjci/jes154

[38] Ruschitzka F, Abraham WT, Singh JP, et al. EchoCR TSG. Cardiac-resynchronization therapy in heart failure with narrow QRS complex. The New England Journal of Medicine. 2013;**369**:1395-1405. DOI: 10.1056/NEJMoa1306687

[39] Hawkins NM, Petrie MC, Burgess MI, et al. Selecting patients for cardiac resynchronization therapy: The fallacy of echocardiographic dyssynchrony. Journal of the American College of Cardiology. 2009;**53**:1944-1959. DOI: 10.1016/j.jacc.2008.11.062

[40] Fornwalt BK, Sprague WW, BeDell P, et al. Agreement is poor among current criteria used to define response to cardiac resynchronization therapy. Circulation. 2010;**121**:1985-1991. DOI: 10.1161/CIRCULATIONAHA.109.910778

[41] Chung ES, Leon AR, Tavazzi L, et al. Results of the predictors of response to CRT (PROSPECT) Trial. Circulation. 2008;**117**:2608-2616. DOI: 10.1161/CIRCULATIONAHA. 107.74312

[42] Mollema SA, Bleeker GB, van der Wall EE, et al. Usefulness of QRS duration to predict response to cardiac resynchronization therapy in patients with end-stage heart failure. The American Journal of Cardiology. 2007;**100**:1665-1670. DOI: 10.1016/j.amjcard.2007.06.071

[43] Gervais R, Leclercq C, Shankar A, et al. Surface electrocardiogram to predict outcome in candidates for cardiac resynchronization therapy: A sub-analysis of the CARE-HF trial. European Journal of Heart Failure. 2009;**11**:699-705. DOI: 10.1093/eurjhf/hfp074

[44] Erlebacher JA, Barbarash S. Intraventricular conduction delay and functional mitral regurgitation. The American Journal of Cardiology. 2001;**88**(A7):83-86. DOI: 10.1016/S0002-9149(01)01595-8

[45] Agricola E, Oppizzi M, Galderisi M, et al. Role of regional mechanical dyssynchrony as a determinant of functional mitral regurgitation in patients with ventricular systolic dysfunction. Heart. 2006;**92**:1390-1395. DOI: 10.1136/hrt.2005.082115

[46] Nishimura RA, Hayes DL, Holmes DR Jr, et al. Mechanism of hemodynamic improvement by dual-chamber pacing for severe left ventricular dysfunction: An acute Doppler and catheterization hemodynamic study. Journal of the American College of Cardiology. 1995;**25**:281-288. DOI: 10.1016/0735-1097(94)00419-Q

[47] Auricchio A, Stellbrink C, Block M, et al. Effect of pacing chamber and atrioventricular delay on acute systolic function of paced patients with congestive heart failure. Circulation. 1999;**99**:2993-3001. DOI: 10.1161/01.CIR.99.23.2993

[48] Nelson GS, Curry CW, Wyman BT, et al. Predictors of systolic augmentation from left ventricular preexcitation in patients with dilated cardiomyopathy and intraventricular conduction delay. Circulation. 2000;**101**:2703-2709. DOI: 10.1161/01.CIR.101.23.2703

[49] St John Sutton MG, Plappert T, Abraham WT, et al. Effect of cardiac resynchronization therapy on left ventricular size and function in chronic heart failure. The Multicenter InSync Randomized Clinical Evaluation (MIRACLE) Study Group. Circulation. 2003;**107**:1985-1990. DOI: 10.1161/01.CIR.0000065226.24159.E9

[50] Linde C, Abraham WT, Gold MR, et al. Randomized trial of cardiac resynchronization therapy in mildly symptomatic heart failure patients and in asymptomatic patients with left ventricular dysfunction and previous heart failure symptoms. The REVERSE study group. Journal of the American College of Cardiology. 2008;**52**:1834-1843. DOI: 10.1016/j.jacc.2008.08.027

[51] Cazeau S, Leclercq C, Lavergne T, et al. Effects of multisite biventricular pacing in patients with heart failure and intraventricular conduction delay. The New England Journal of Medicine. 2001;**344**:873-880. DOI: 10.1056/NEJM200103223441202

[52] Kanzaki H, Bazaz R, Schwartzman D, et al. A mechanism for immediate reduction in mitral regurgitation after myocardial infarction. Journal of the American College of Cardiology. 2004;**44**:1619-1625. DOI: 10.1016/j.jacc.2004.07.036

[53] Ypenburg C, Lancellotti P, Tops LF, et al. Mechanism of improvement in mitral regurgitation after cardiac resynchronization therapy. European Heart Journal. 2008;**29**:757-765. DOI: 10.1093/eurheartj/ehn063

[54] Breithardt OA, Sinha AM, Schwammenthal E, et al. Acute effects of cardiac resynchronization therapy on functional mitral regurgitation in advanced systolic heart failure. Journal of the American College of Cardiology. 2003;**41**:765-770. DOI: 10.1016/S0735-1097(02)02937-6

[55] Solis J, McCarthy D, Levine RA, et al. Mechanism of decrease in mitral regurgitation after cardiac resynchronization therapy: Optimization of the force-balance relationship. Circulation. Cardiovascular Imaging. 2009;**2**:444-450. DOI: 10.1161/CIRCIMAGIN. 108.823732

[56] Vinereanu D, Turner M, Bleasdale R, et al. Mechanisms of reduction of mitral regurgitation by cardiac resynchronization therapy. Journal of the American Society of Echocardiography. 2007;**20**:54-62. DOI: 10.1016/j.echo.2006.07.002

[57] Porciani MC, Macioce R, Demarchi G, et al. Effects of cardiac resynchronization therapy on the mechanisms underlying functional mitral regurgitation in congestive heart failure. European Journal of Echocardiography. 2006;**7**:31-39. DOI: 10.1016/j.euje.2005.03.008

[58] Bordachar P, Garrigue S, Laffite S, et al. Intraventricular and intra-left ventricular electromechanical delays in right ventricular paced patients with heart failure: Implications for upgrading to biventricular stimulation. Heart. 2003;**89**:1401-1405. DOI: 10.1136/heart.89.12.1401

[59] Fukuda S, Grimm R, Song JM, et al. Electric conduction disturbance effects on dynamic changes of functional mitral regurgitation. Journal of the American College of Cardiology. 2005;**46**:2270-2276. DOI: 10.1016/j.jacc.2005.08.037

[60] Liang YJ, Zhang Q, Fung JWH, et al. Impact of reduction in early- and late-systolic functional mitral regurgitation on reverse remodeling after cardiac resynchronization therapy. European Heart Journal. 2010;**31**:2359-2368. DOI: 10.1093/eurheartj/ehq134

[61] Madaric J, Vanderheyden M, Van Laethem C, et al. Early and late effect of cardiac resynchronization therapy on exercise-induced mitral regurgitation: Relationship with left ventricular dyssynchrony, remodeling and cardiopulmonary performance. European Heart Journal. 2007;**28**:2134-2141. DOI: 10.1093/eurheartj/ehm126

[62] Cabrera-Bueno F, Pinilla JMG, Hernandez JP, et al. Repercussion of functional mitral regurgitation on reverse remodeling in cardiac resynchronization therapy. Europace. 2007;**9**:757-761. DOI: 10.1093/europace/eum122

[63] Van Bommel RJ, Borleffs CJW, Ypenburg C, et al. Morbidity and mortality in heart failure patients treated with cardiac resynchronization therapy: Influence of pre-implantation characteristics on long-term outcome. European Heart Journal. 2010;**31**:2783-2790. DOI: 10.1093/eurheartj/ehq252

[64] Verhaert D, Popovic ZB, De S, et al. Impact of mitral regurgitation on reverse remodeling and outcome in patients undergoing cardiac resynchronization therapy. Circulation. Cardiovascular Imaging. 2012;**5**:21-26. DOI: 10.1161/CIRCIMAGIN.111.966580

[65] Kwon DH, Kusunose K, Obuchowski NA, et al. Predictors and prognostic impact of progressive ischemic mitral regurgitation in patients with advanced ischemic cardiomyopathy—A multimodality study. Circulation. Cardiovascular Imaging. 2016;**e004577**:9. DOI: 10.1161/CIRCIMAGIN.115.004577

[66] Senechal M, Lancellotti P, Magne J, et al. Impact of mitral regurgitation and myocardial viability on left ventricular reverse remodeling after cardiac resynchronization therapy in patients with ischemic cardiomyopathy. The American Journal of Cardiology. 2010;**106**:31-37. DOI: 10.1016/j.amjcard.2010.02.012

[67] Onishi T, Onishi T, Marek JJ, et al. Mechanistic features associated with improvement in mitral regurgitation after cardiac resynchronization therapy and their relation to long-term patient outcome. Circulation. Heart Failure. 2013;**6**:685-693. DOI: 10.1161/CIRCHEARTFAILURE.112.000112

[68] Gorcsan IIIJ, Abraham T, Agler DA, et al. Echocardiography for cardiac resynchronization therapy: Recommendations for performance and reporting—A report from American Society of Echocardiography Dyssynchrony Writing Group endorsed by the Heart Rhythm Society. Journal of American Society of Echocardiography. 2008;**21**(3):191-213. DOI: 10.1016/j.echo.2008.01.003

[69] Stockburger M, Fateh-Moghadam S, Nitardy A, et al. Baseline Doppler parameters are useful predictors of chronic left ventricular reduction in size by cardiac resynchronization therapy. Europace. 2008;**10**:69-74. DOI: 10.1093/europace/eum269

[70] Altman R, McCarthy D, Chen-Tournoux A, et al. Usefulness of low-dose dobutamine echocardiography to predict response and outcome in patients undergoing cardiac resynchronization therapy. The American Journal of Cardiology. 2011;**108**:253-257. DOI: 10.1111/j.1540-8175.2009.00962.x

[71] Gasparini M, Muto C, Iacopino S, et al. Low-dose dobutamine test associated with interventricular dyssynchrony: A useful tool to identify cardiac resynchronization therapy responders: Data from the LODO-CRT phase 2 study. American Heart Journal. 2012;**163**:422-429

[72] Lim P, Bars C, Mitchell-Heggs L, et al. Importance of contractile reserve for CRT. Europace. 2007;**9**:739-743. DOI: 10.1093/europace/eum117

[73] Mizia-Stec K, Wita K, Mizia A, et al. Preserved contractile reserve in a dobutamine test for the prediction of a response to resynchronization therapy in ischaemic and non-ischaemic cardiomyopathy: A multicenter ViaCRT study. International Journal of Cardiology. 2014;**172**:476-477. DOI: 10.1016/j.ijcard.2013.12.204

[74] Delgado V, van Bommel RJ, Bertni M, et al. Relative merits of left ventricular dyssynchrony, left ventricular lead position, and myocardial scar to predict long-term survival of ischemic heart failure patients undergoing cardiac resynchronization therapy. Circulaction. 2011;**123**:70-78. DOI: 10.1161/CIRCULATIONAHA.110.945345

[75] Adelstein EC, Tanaka H, Soman P, et al. Impact of scar burden by single-photon emission computed tomography myocardial perfusion imaging on patients outcomes following cardiac resynchronization therapy. European Heart Journal. 2011;**32**:93-103. DOI: 10.1093/eurheart/ehq389

[76] Beaudoin J, Singh JP, Szymonifka J, et al. Novel heart failure biomarkers predict improvement of mitral regurgitation in patients receiving cardiac resynchronization therapy—The BIOCRT Study. The Canadian Journal of Cardiology. 2016;**32**(12):1478-1484. DOI: 10.1016/j.cjca.2016.05.013

[77] Yu CM, Bleeker GB, Fung JW, et al. Left ventricular reverse remodeling but not clinical improvement predicts long-term survival after cardiac resynchronization therapy. Circulation. 2005;**112**:1580-1586. DOI: 10.1161/CIRCULATIONAHA.105.538272

[78] Cleland JG, Daubert JC, Erdmann E, et al. The effect of cardiac resynchronization on morbidity and mortality in heart failure. The New England Journal of Medicine. 2005;**352**:1539-1549. DOI: 10.1056/NEJMoa050496

[79] Stellbrink C, Breithardt OA, Franke A, et al. Impact of cardiac resynchronization therapy using hemodynamically optimized pacing on left ventricular remodeling in patients with congestive heart failure and ventricular conduction disturbances. Journal of the American College of Cardiology. 2001;**38**:1957-1965. DOI: 10.1016/S0735-1097(01)01637-0

[80] Carluccio E, Biagioli P, Alunni G, et al. Presence of extensive LV remodeling limits the benefits of CRT in patients with intraventricular dyssynchrony. Journal of the American College of Cardiology. 2011;**4**:1067-1076. DOI: 10.1016/j.jcmg.2011.07.006

[81] Tayal B, Sogaard P, Delgado-Montero A, et al. Interaction of left ventricular remodeling and regional dyssynchrony on long-term prognosis after cardiac resynchronization therapy. Journal of the American Society of Echocardiography. 2017;**30**:244-250. DOI: 10.1016/j.echo.2016.11.010

[82] Diaz-Infante E, Mont L, Leal J, et al. Predictors of lack of response to resynchronization therapy. The American Journal of Cardiology. 2005;**95**:1436-1440. DOI: 10.1016/j.amjcard.2005.02.009

[83] Brzezińska B, Łoboz-Grudzień K, Sokalski L. Patterns of post-MI left ventricular volume changes: Clinical implications. Kardiologia Polska. 2007;**65**:1190-1198

[84] Cleland JG, Tavazzi L, Daubert JC, et al. CRT. Cardiac resynchronization therapy. Are modern myths preventing appropriate use? Journal of the American College of Cardiology. 2009;**53**:608-611. DOI: 10.1016/j.jacc.2008.10.040

[85] Calafiore AM, Iaco AL, Gallina S, et al. Surgical treatment of functional mitral regurgitation. International Journal of Cardiology. 2013;**166**:559-571. DOI: 10.1016/j.ijacard.2012.05.027

[86] Michler RE, Smith PK, Parides MK, et al. Two-years outcomes of surgical treatment of moderate ischemic mitral regurgitation. The New England Journal of Medicine. 2016;**374**:1932-1941. DOI: 10.1056/NEJMoa1602003

[87] Acker MA, Parides MK, Perrault LP, et al. Mitral-valve repair versus replacement for severe ischemic mitral regurgitation. The New England Journal of Medicine. 2014;**370**: 23-32. DOI: 10.1056/NEJMoa1312808

[88] Lancellotti P, Tribouilloy C, Hagendorff A, et al. Scientific Document Committee of the European Association of Cardiovascular Imaging. Recommendations for echocardiographic assessment of native valvular regurgitation: An executive summary from European Association of Cardiovascular Imaging. European Heart Journal. Cardiovascular Imaging. 2013;**14**:1611-1644. DOI: 10.1093/ehjci/jet105

[89] Wu AH, Aaronson KD, Bolling SF, Pagani FD, et al. Impact of mitral valve annuloplasty on mortality risk in patients with mitral regurgitation and left ventricular systolic dysfunction. Journal of the American College of Cardiology. 2005;**45**:381-387. DOI: 10.1016/j.jacc.2004.09.073

[90] Maisano F, Franzen O, Baldus S, et al. Percutaneous mitral valve interventions in the real world: Early and 1-year results from the ACCESS-EU, a prospective, multicenter, nonrandomized postapproval study of the MitraClip therapy in Europe. Journal of the American College of Cardiology. 2013;**62**(12):1052-1061. DOI: 10.1016/j.jacc.2013.02.094

[91] Mann DL, Kubo SH, Sabbah HN, et al. Beneficial effects of the CorCap cardiac support device: Five-year results from the Acorn Trial. The Journal of Thoracic and Cardiovascular Surgery. 2012;**143**:1036-1042. DOI: 10.1016/j.jtcvs.2011.06.014

[92] Grossi EA, Patel N, Woo J, Goldberg JD, et al. Outcomes of the RESTOR-MV trial (Randomized Evaluation of a Surgical Treatment for Off-Pump Repair of the Mitral Valve). Journal of the American College of Cardiology. 2010;**56**:1984-1993. DOI: 10.1016/j.jacc.2010.06.051

Mitral Valve Prolapse in Pregnancy: Modern Concept

Ignatko Irina Vladimirovna,
Strizhakov Leonid Alexandrovich,
Rodionova Alexandra Mihailovna and
Martirosova Alina Lorisovna

Additional information is available at the end of the chapter

Abstract

This chapter presents the recent literature data data on the problems of etiopathogenesis, cardiac, and obstetric risk of mitral valve prolapsus, as well as the tactics of patients with this pathology. Modern views on the role of genomic, genetic disorders, and metabolomics in violations valvular structures in the etiology and pathogenesis of clinical manifestations of the mitral valve prolapsus. In addition, the data on the peculiarities of pregnancy and childbirth in women with mitral valve prolapsus (miscarriage, cervical incompetence, preeclampsia, fetal growth restriction, placental insufficiency, labor anomaly, and postpartum hemorrhage) are studied. However, ambiguous and sometimes conflicting data on the relationship and the incidence of these complications with mitral valve prolapsus require further research to determine the set of diagnostic and preventive measures.

Keywords: mitral valve prolapse, mitral regurgitation, mitral valve prolapsus classification, diagnostic imaging techniques, preeclampsia, anomalies of labor activity

1. Introduction

In recent years, the importance of extragenital pathology in severe maternal morbidity and mortality has increased significantly worldwide [1–3]. The role of diseases of the cardiovascular system in the complications of pregnancy and the frequency of perinatal complications are increasing [4, 5]. In addition, often in the genesis of diseases of internal organs in a pregnant woman is the genetic conditioned systemic disorders of histogenesis, in particular connective

tissue dysplasia [5–7]. The prolapse of the mitral valve is one of the most common and studied visceral manifestations of connective tissue dysplasia (CTD). Connective tissue dysplasia (DST) is the disorder of the connective tissue of polygenic multifactorial nature, combined into phenotypes on the basis of the commonness of external and/or visceral features [6]. CTD is characterized by defects in fibrous structures and the basic substance, leading to a disorder of homeostasis at the tissue, organ, and organism levels in the form of various morphofunctional disturbances of visceral and locomotor organs.

Interest in the study of MVP is due primarily to its relatively high frequency in the general population and among young women of reproductive age, as well as possible complications—sudden death, arrhythmias and congestive disorders of the heart, infectious endocarditis, and thromboembolic disorders. However, previously reported MVP complications such as stroke, disautonomy (postural orthostatic tachycardia syndrome (POTS)), panic attacks, feelings of fear, and transient ischemic attacks [8] are not currently considered in connection with the MVP itself [9]. In the majority of women, no cardiovascular pathology has been detected in 10 years after the diagnosis of MVP [3].

2. Definition

Primary mitral valve prolapsus (MVP) related to small (minor) cardiac abnormalities (MCA) is considered to be one of the most common heart valve anomalies. Mitral valve prolapsus (MVP) represents a range of valvular abnormalities that allow one or both mitral valve leaflets to extend above the plane that separates the atria and the ventricle.

MVP is such a pathology of the valve apparatus (some redundancy of it), in which one or both mitral valve flaps bend ("sag," prolapse) upward and posteriorly above the plane separating the atria and ventricles (above the valvular ring plane) during systole [10–12]. The valves can remain connected or can be separated, which leads to a different degree of regurgitation (**Figure 1**).

The more pronounced prolapse can be caused by myxomatous degeneration of mitral valve flaps. An anomaly of the mitral valve may be an isolated visceral manifestation of CTD, but it can also be a part of dysplastic syndromes. MVP (and sometimes the tricuspid valve prolapse) can be associated with other intracardiac anomalies, in particular, an interstitial septal defect [3, 5].

The average frequency of MVP in the population is 3–10% with a widespread frequency according to literature data, depending on population factors (gender, age, race) [6, 13, 14], as well as the diagnostic method and diagnostic criteria [10, 11].

Individuals with classic MVP (leaflet thickness of ≥5 mm; 1.3%) and non-classic MVP (leaflet thickness of <5 mm; 1.1%) had similar age and sex distributions. MVP prevalence was similar in three ethnic groups (2.7% in South Asian, 3.1% in European, and 2.2% in Chinese) [10]. MVP patients were leaner and had a greater degree of mitral regurgitation (MR) than the general population [6, 7]. MVP may be slightly more common in women than in men. The
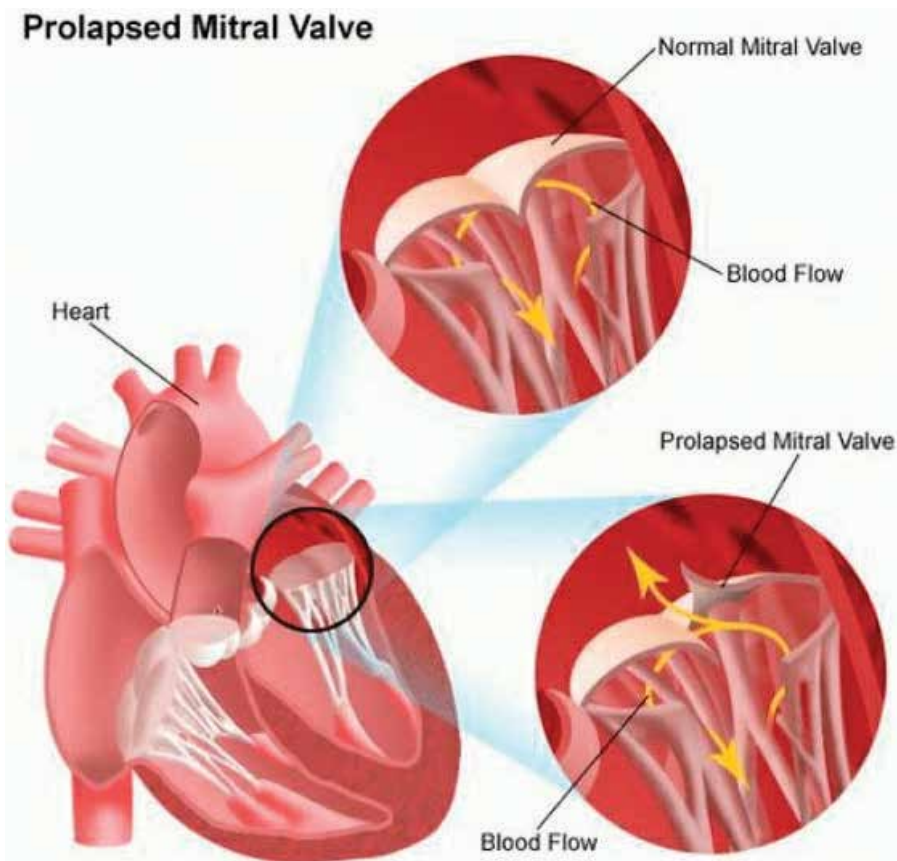
Figure 1. Mitral valve prolapse.

majority of patients with MVP have mitral regurgitation (MR), but most patients with MVP (approximately 75%) have mild, trace, or no MR [1]. Severe MR is uncommon, identified in 4% of patients with MVP. Unlike adults, mitral valvulopathy (MVP) with Marfan syndrome in newborns can be accompanied by severe regurgitation and functional disorders of the contractile activity of the heart leading to congestive heart failure [15]. Most often among all population groups (17–38%), MVP is noted in women of reproductive age [10, 16]. According to the REPLICA study (mitral valve prolapse prevalence among young people), MVP is detected more often—in 4.3% of cases [17].

Therapists working in obstetrics consider MVP the most common heart anomaly in pregnant women [18]. The proportion of MVP in the structure of small heart anomalies in pregnant women is 60.8% [19]. In the recent past, this pathology was considered to be so frequent, especially among young women, that a number of authors proposed to consider MVP as a variant of the normal structure of the mitral valve [20]. However, the standardization of echocardiographic criteria and a better understanding of the structure of the valvular apparatus led to a significant decrease in the frequency of the detection of true MVP, which is 0.5–3.0% in the population and 1% in women of all age groups with a maximum frequency—in reproductive age. A large

retrospective study, during which 16,185 echocardiograms were analyzed, performed according to clinical indications in the Consultative-Diagnostic Center of National Medical Research Center of V.A. Almazov (St. Petersburg, Russia) from 2008 to 2011, also showed a low prevalence of MVP and in the Russian population—1.3% [21].

3. Classification

For the first time, mitral valve prolapse was described by J.B. Barlow et al. in 1963.

There are multiple ways of classifying MVP, underscoring the heterogeneity of this disorder:

- Etiologically, MVP is classified as primary (degenerative disease in the absence of identifiable connective tissue disease, sporadic, or familial) versus secondary MVP (associated with an identifiable disorder such as Marfan syndrome).

- Clinically, MVP can be classified as syndromic when extracardiac manifestations are present (e.g., pectus excavatum) versus non-syndromic, isolated MVP.

- MVP is also classified by the severity of the abnormal movement of the valve. The leaflets are described as billowing when the tips of leaflets remain in the left ventricle (LV) versus flail when the tip(s) of one (or both) leaflets prolapses into the left atrium (LA).

- Morphologically, MVP is classified as classic (also known as Barlow's syndrome with markedly and diffusely thickened leaflets (≥5 mm) with bileaflet prolapse) versus non-classic (with limited or absent thickening (thickness <5 mm) and segmental prolapse).

- Doppler echocardiography can also distinguish MVP without mitral regurgitation (MR) from MVP with MR.

The 2014 American Heart Association/American College of Cardiology guidelines for the management of patients with valvular heart disease separate mitral regurgitation by a mechanism into primary (disease of one or more valve components including leaflets, chordae tendineae, papillary muscles, or annulus) and secondary (disease of the left ventricle) [22]. In this classification, primary disease includes all forms of MVP along with other causes of MR involving the components of the valve (e.g., calcific degeneration, cleft mitral valve, leaflet perforations, etc.). Isolate primary (congenital, idiopathic) and secondary prolapse develops against the background of the already existing diseases of the cardiovascular system. Primary prolapse of the mitral valve is a hereditary violation of the formation of the connective tissue [6, 7, 10, 11]. It should be noted that in the MVP structure, the primary occurs much more often. The share of the secondary accounts for only 5% of the total number of observations. Clinically anatomically, MVP is a syndrome that accompanies many nosological forms [10, 15, 16].

Currently, there are several MVP variants [23]:

1. pleiotropic manifestation of some classified hereditary disorders of the connective tissue (syndromes Marfan, Ehlers-Danlo, etc.). Thus, the combination of MVP with aortic

dilatation and signs of connective tissue dysplasia of seven or more points gives reason to consider it as associated with the Marfan syndrome. However, it should be emphasized that only 1–2% of patients with MVP have one of the monogenic undifferentiated disorders of the connective tissue [6];

2. independent clinically and prognostically significant syndrome: primary familial mitral valve prolapse (MIM 157700), primary myxomatous mitral valve prolapse (MIM 607829 or 610,840). In the absence of signs of one of the monogenic NNST, in the case of detection of MVP with hemodynamically significant mitral regurgitation and/or myxomatous degeneration of the valves in persons with a young age, it is possible to speak with a high probability of the presence of a clinically significant primary MVP. To diagnose genetically determined primary MVP, it is not possible to restrict only echocardiography to a study, but it is necessary to take into account the results of a family survey, the phenotypic data, and the clinical picture of the disease. For evaluation of MVP, its combination with the signs of dysplasia of the connective tissue or the absence thereof is also important. The combination of MVP with clinical symptomatics allows talking about the syndrome of MVP. It is characterized by vegetative dysfunction, arterial hypotension and orthostatic failure, cardiac rhythm disturbances, and repolarization disorders on the ECG [6];

3. the minor heart anomaly, often accompanying other classified and unclassified dysplastic syndromes.

With the exclusion of MVP syndrome, prolapse of the valves without their thickening and significant mitral regurgitation can be regarded as one of the variants of a small heart anomaly, the number of which, as is well known, closely correlates with the number of external signs of dysembryogenesis detected [24].

4. Etiopathogenesis

To explain the causes of primary prolapse of the mitral valve, several theories have been proposed. Proponents of the "myocardial" theory in the histological study of the myocardium found interstitial fibrosis and hypertrophy of myofibrils in patients with mitral valve prolapse and in electron microscopy—degenerative changes in mitochondria, endocardium thickening [25, 26].

The revealed changes allowed to make an assumption about the similarity of morphological changes with mitral valve prolapse and dilated cardiomyopathy. However, after conducting a complex echocardiographic, radionuclide, and angiographic study, the hypothesis of the cardiomyopathic etiology of the primary prolapse of the mitral valve has not been confirm [6, 26]. The theory of the "rheumatic" nature of the prolapse of the mitral valve was also common. This point of view is confirmed by information about a greater frequency of prolapse in patients with rheumatism. Supporters of this theory explained the mechanism of prolapse of the valves with partial chord separation as a result of inflammatory changes in the endocardium [5, 27]. There are also data indicating the possible involvement of a viral infection in the

development and progression of mitral valve prolapse [28]. However, modern protocols for management of patients with MVP do not provide for antibiotic prophylaxis [3].

At the basis of the development of secondary MVP lies the violation of myocardial contractility of the left ventricle and dysfunction of the papillary muscles. It develops under the following pathological conditions: inflammatory processes (myocarditis), cardiomyopathy, myocardial dystrophy [10, 16], ischemic heart disease, a decrease in tissue elasticity as a result of left ventricular contraction asymmetry and papillary muscle ischemia and tendon chords, violation of autonomic innervation and impulse conduction in myocarditis, extrasystole, WPW syndrome, with neuroses and hysteria. Also, the cause of secondary MVP can serve as a blunt trauma to the heart [22].

Most researchers are supporters of the "valve" theory. This theory presupposes the presence of a genetically determined collagen defect, which leads to the "weakness" of the connective tissue of the mitral valve flaps and their prolapse into the atrial cavity. Three gene loci are described on 16, 11, and 13 chromosomes, but the genetic defects underlying them are not known to date. The recessive form of MVP associated with the X chromosome is known as myxomatous dystrophy of the heart valves, and mutations of the gene for the pathogen have recently been identified [6].

There are several possible pathogenetic mechanisms that can explain the onset of MVP. According to some data, the role of magnesium deficiency in the development of MVP is great. The lack of magnesium reduces the activity of magnesium-dependent adenylate cyclase, which ensures the removal of defective collagen [29] and affects the ability of fibroblasts to produce collagen [16]. In addition to the direct participation of magnesium ions in the processes of collagen formation, the role of magnesium in the functioning of the vegetative nervous system is undoubtedly important, since a deficiency of magnesium ions promotes an increase in the level of catecholamines of the blood plasma, that is, the development of hyper-catecholaminemia, changes in the tone of the papillary muscles, and the formation of MVP.

5. Clinical picture

Symptoms attributed to mitral valve prolapsus (MVP) cannot clearly be explained by the degree of prolapse or mitral regurgitation. However, autonomic or neuroendocrine dysfunction has been suggested as a possible cause of the nonspecific symptoms in many patients with MVP. Patients with MVP tend to exhibit the following findings when compared to controls [3, 4]:

- elevated urine and plasma catecholamine levels;

- an exaggerated heart rate response to phenylephrine;

- a less than expected bradycardiac response to the dive reflex;

- the reproduction of symptoms with isoproterenol infusion.

The specificity of these findings for MVP is uncertain. One study found a series of abnormalities in patients with symptoms of autonomic dysfunction, which did not correlate with the presence or absence of MVP [5].

An association between panic disorder and MVP has also been suggested by several studies, including a meta-analysis [6]. However, these studies have been criticized because of inconsistencies in the diagnostic criteria used for both panic disorder and MVP and the use of imperfectly matched controls. In addition, panic disorder and MVP are both common illnesses with similar age and gender distributions, suggesting that their association may only be a coincidence.

The clinical manifestations of prolapsus of the mitral valve differ in variety [5, 6]. At the same time, most researchers note the polymorphism of the clinical picture [3, 17]. Data on the frequency of clinical symptoms and the pathogenetic mechanisms of their formation are contradictory [3, 10, 11, 13]. However, the recognition of prolapsus is accompanied by a fairly clear and definite clinical picture. It is proposed to isolate clinically and morphologically significant MVP syndromes:

1. the pain syndrome in the left half of the chest (32.3–65%) [6, 10, 17]. At the same time, the mechanisms of the formation of the pain syndrome remain controversial. Currently, the most common explanations of pathogenetic mechanisms of pain syndrome are local myocardial ischemia as a result of tension of papillary muscles, microthrombemia in the zone located between the left atrium and the back wall of the mitral valve, a decrease in the diastole duration as a result of an increase in the heart rate, and sinus tachycardia in response to stress or physical exertion [3];

2. the syndrome of disturbance of vegetative regulation of heart rhythm (25.8–79%). The complaints about the heartbeat and interruptions in the work of the heart are noted in individuals in cases [30]. There was no consensus on the mechanism of cardiac rhythm disturbance and repolarization process disturbances in these patients, the role of abnormal traction of papillary muscles, the presence of late ventricular potentials, myxomatous degeneration of dilated valves, and dysfunction of the autonomic nervous system was discussed [10, 17];

3. the hyperventilation syndrome (dyspnea—15.6–31.5%). Domestic authors with mitral valve prolapse noted the presence of a feeling of lack of air and obstacles in the way of inhaled air, the need to periodically make deep sighs, and a feeling of dissatisfaction with inspiration [6]. The main pathogenetic mechanism is disautonomy [10];

4. the hemorrhagic syndrome: nasal bleeding, tendency to easy formation of bruises, bleeding gums, prolonged bleeding after removal of the teeth, prolonged and (or) profuse menstruation. The tendency to easy bruising and nasal bleeding can be explained by the presence of disturbances in the hemostasis system in patients with MVP—a change in the aggregation function of platelets, a decrease in the activity of von Willebrand factor in the blood plasma, and a disruption of the final stage of blood coagulation [31]. As is known, hemorrhagic syndrome is one of the manifestations of mesenchymal dysplasia, which explains its presence in patients with prolapse of the mitral valve;

5. the vascular disorders in the limbs of persons with mitral valve prolapse (68.8%), which are presented in the form of vascular necklace, Raynaud's syndrome, changes in the color of the limbs, idiopathic pastosity, or swelling [6]. Lipothymia is a complex of sensations that preceded the loss of consciousness noted in the work of T.M. Dominitskaya (1998) in 69.0% of patients with mitral valve prolapse in combination with abnormally located chord and in 51.0% of persons with abnormally located chord with orthostatic load, emotional stress, prolonged stay in a vertical position, and in stuffy rooms [32];

6. the vegetative crises (sympathetic-adrenal, vago-insular, mixed). These are the most striking manifestations of MVP;

7. the mental disorders: neurasthenia, anxiety disorders, anxiety-phobic disorders, mood disorders. When assessing the results of a comprehensive psychological examination, it was found that in persons with mitral valve prolapse, there are a number of distinguishing features from healthy people: inadequate self-esteem (32.1%), low level and inadequacy of attitudes (50.9%), high situational anxiety (32.7%), low emotional stability (39.0%), and a decrease in the dynamic indicators of mental activity [6].

Along with the widespread point of view about the propensity of patients with mitral valve prolapse to hypotension, recently there have been isolated reports of the presence of arterial hypertension in patients with prolapse of the mitral valve [5]. The possibility of hereditary predisposition to arterial hypertension, mixed with hereditary pathology of connective tissue, is not excluded.

However, not all authors agree with the presence of MPV syndrome with the above-described clinical symptoms [3], believing that PMC is only an anatomical feature of the valve structure, if it is not a manifestation of the Martha syndrome. Clinical manifestations of approximately equal frequency are observed in women with and without EchoCG signs of MPV.

6. Diagnostics

It should be emphasized that the main method of diagnosis of mitral valve prolapse is currently two-dimensional echocardiography. However, certainly, it is necessary to take into account the history of the patient, including the family history, the presence of concomitant markers of connective tissue dysplasia, the presence of clinical manifestations of prolapse MV, including relatives, clarify the family thrombotic anamnesis or the presence of sudden deaths in relatives.

In most cases, the diagnosis of prolapse MV in pregnant women is established even before its onset. However, in a part of young primitive women—MVP—a random echocardiographic finding requires a careful evaluation of clinical and anamnestic risk factors in each pregnant woman [5, 33].

6.1. Cardiac examination

The most common auscultatory features of mitral valve prolapse are the non-ejection click (single or multiple) and the murmur of mitral regurgitation. The click is thought to be caused by snapping of the mitral chordae during systole when the valve bows into the atrium. The click is mobile, meaning its timing varies with maneuvers that change the left ventricular volume, occurring earlier in systole with sitting, standing, or other interventions that reduce ventricular size, or later with those interventions that increase the chamber size such as squatting (movie 4 and movie 5) [34]. An MVP click should be differentiated from the aortic or

pulmonary ejection clicks (occurring early in systole, at the foot of the carotid upstroke) and from other cardiac sounds (split first or second heart sounds, pericardial sounds, atrial septal aneurysm clicks).

With a routine clinical examination and auscultation of cardiac tones, a systolic click is heard between the I and II heart tones, together or without middle diastolic or late systolic murmur, which is a characteristic symptom. The presence of these auscultative data may vary depending on the position of the body of the pregnant woman or the degree of her hydration. Similar auscultative changes can occur in healthy women during pregnancy, varying in the time of click occurrence and in mitigating or shortening the time of noise, and when series of echocardiographic studies in the presence of MPV in some women EchoCG signs of it disappear [6].

6.2. Diagnostic imaging techniques

In most pregnant women who do not show any other clinical signs, so in the absence of significant regurgitation in *echocardiography*, women should talk about the safety of pregnancy and childbirth, as well as the absence of a negative effect on the fetus of this condition [3]. MVP is diagnosed at the maximum systolic displacement of the mitral valve flaps beyond the ring line in the parasternal longitudinal position by more than 2 mm. The use of the parasternal longitudinal section for the diagnosis of MVP is due to the peculiarities of the shape of the mitral valve ring, while the isolated displacement of the anterior valve beyond the ring line seen in the four-chamber apex position is the main cause of its overdiagnosis. In echocardiographic conclusion, it is necessary to indicate the depth of prolapse, the length and thickness of each of the valves, and the degree of mitral regurgitation [6, 12] (**Figure 2**).

The normal length of the front leaf is 21–24 mm, the rear is 12–14 mm. Depending on the thickness of the leaf, the classic MPV is distinguished, with a valve thickness of more than 5 mm in diastole (reflects the presence of myxomatous degeneration of the valves) and non-classical MPV—with a thickness of less than 5 mm.

The determination of the degree of mitral regurgitation is currently conducted according to the recommendations of the ANA/ACC [6]. For this purpose, the following qualitative indices are used: the diameter of the vein of the regurgitation jet (vena contracta), the volume of regurgitation, and the area of the regurgitation opening calculated according to the area of the proximal equal-velocity surface (PISA). Specific for MPV is the mitral regurgitation that occurs at the end of the systole; it is usually high speed and eccentric.

The evaluation of LV systolic function is also an important component of EchoCG study. It is an important prognostic factor in patients with MVP and severe MH [6, 12]. There is evidence of worsening of LV systolic function in young patients with MVP and without significant mitral regurgitation [35].

The development of 3D technology, especially real-time 3D-TEE, provides excellent rendering of the mitral valve complex. Live 3D-TEE has become routine in pre/intraoperative imaging of the mitral valve and in percutaneous mitral valve interventions. 3D-TEE efficiently identifies
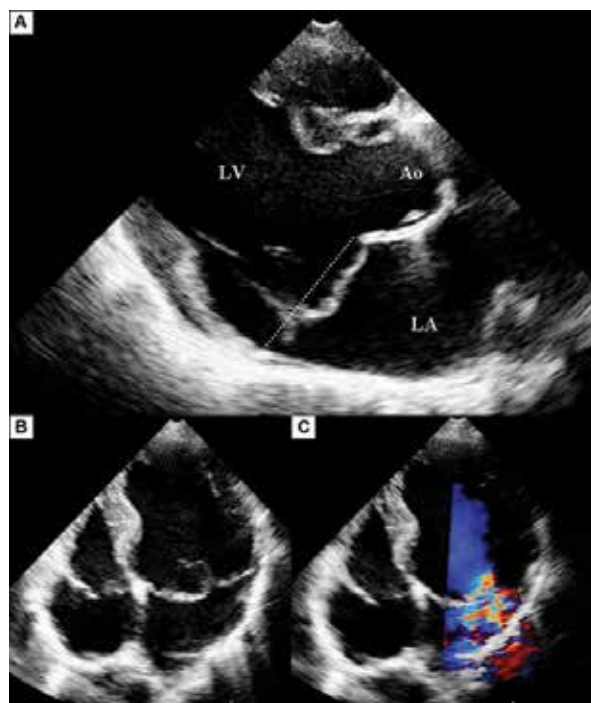
Figure 2. Echocardiography in mitral valve prolapse.

correct location of prolapse and flail segments, and by reconstruction of the 3D image from the left atrial view (surgical view), information is easily communicated to the surgical team. In a study comparing 2D TEE with 3D-TEE, both expert and less experienced echocardiographers more accurately described the mitral valve pathology using 3D-TEE (with surgical pathology as the reference), with less experienced interpreters gaining a significantly greater advantage from using 3D-TEE [36]. 3D-TEE is the key imaging modality for guidance of percutaneous mitral valve repair with the MitraClip system.

With increased use of 3D-TEE, cleft-like indentations of the posterior mitral leaflet are more frequently recognized and may be present in up to one-third of patients with myxomatous MVP [36]. Appropriate recognition of cleft-like indentation is important when planning surgical or percutaneous mitral valve repair. However, it must be emphasized that not all cleft-like indentations apparent on 3D reconstruction are associated with mitral regurgitation (i.e., many are "non-functional" clefts, being visible only during diastole, which do not require a repair). The best approach to determine the significance of cleft-like indentation is to examine the mitral valve anatomy from the left ventricular en-face view, in both 3D and 3D color.

3D-TEE also allows insights into the dynamic mitral annulus function, with early-systolic area contraction and saddle-shape deepening contributing to mitral competency. The mitral annulus in MVP is also dynamic but considerably different from normal patients, with loss of early-systolic area contraction and diminished saddle-shape deepening despite similar magnitude of ventricular contraction, suggestive of ventricular-annular decoupling [36]. With the rapid development of percutaneous interventions for mitral regurgitation, accurate

assessment of the mitral valve anatomy (annulus area and perimeter, inter-commissural and septal-lateral diameters) becomes increasingly important. These can be reliably measured by both 3D echocardiography and computed tomography (CT).

While 2D and 3D imaging techniques allow identification of anatomical substrate, Doppler echocardiographic techniques are key to estimating the severity of MR. The criteria used to diagnose severe MR are discussed separately.

MR severity should be quantitated in all patients with a visual appearance of greater than mild MR on color Doppler. Formal quantification of mitral valve severity not only minimizes errors intrinsic to color Doppler visual quantification of severity but also provides essential information about a patient's individual risk. Quantitative measures of MR (regurgitant volume and orifice) are essential predictors of outcome [36] as confirmed in two independent prospective studies totaling more than 1000 patients followed long term.

In a dynamic echocardiographic study in pregnant women with prolapse of the mitral valve of women, there are stable sizes of the left chambers of the heart, as well as the thickness of the left ventricular myocardium and the interventricular septum throughout the period of pregnancy and in the postpartum period [5]. With an increase in the period of pregnancy from the first to third trimester, there is a natural increase in the frequency of a greater degree of prolapse of the mitral valve and to a lesser extent the degree of mitral regurgitation.

In accordance with the generally accepted approaches, the stratification of the risk of cardiovascular complications and death in patients with MVP should be based, first of all, on the evaluation of the severity of mitral regurgitation and the thickness of the mitral valve leaf [5, 6, 33]. The latter characterizes the presence and severity of their myxomatous degeneration. With a leaf thickness of 5 mm or more, the total probability of sudden death, endocarditis, and cerebral embolism, the likelihood of developing mitral insufficiency, rupture of chords, and ventricular arrhythmias in such patients can be attributed to the high-risk group [6, 10, 12, 13, 37].

The degree of risk was determined in the presence and severity of a number of factors: the auscultatory pattern, the degree of prolapse, the severity of myxomatic degeneration of the valves, mitral regurgitation, age, fibrillation of pre-arthies, chronic heart failure, hypertension, and others [38].

Most patients with MVP, without signs of MR and mild MR, can be classified as low risk with a favorable prognosis [3, 10, 15]. Life expectancy at them corresponds to that in the general population [20]. The unfavorable course of MVP is the increase in MR, leading to dilatation of the LV and LP, development of atrial fibrillation, LV systolic dysfunction, and chronic heart failure. The onset and rapid progression of MP may be due to the rupture of myxomatologically altered chords [6].

The presence of altered valves with MVP increases the risk of infectious endocarditis, although overall its probability in the population of patients with MVP is low [39]. Thromboembolism of cerebral vessels is the main cause of neurologic symptoms (transient ischemic attacks and strokes) in patients with MVP, and the risk of embolism is higher than in the general population [3, 6, 10]. Sudden death is a rare complication of primary MVP (less than 2% of cases with prolonged follow-up, with an annual mortality of less than 1%). The main cause of sudden

cardiac death in MVP is ventricular tachyarrhythmias, which are especially common in family MVP forms [3, 10]. In a number of cases in the presence of pain in the left half of the chest, in women, there is an inversion of the T-wave on the ECG, especially in the II and III thoracic leads, even in the presence of normal coronary angiography. When conducting a treadmill test, it is also possible to detect the depression of the ST segment, indistinguishable from that of myocardial ischemia.

7. Mitral valve prolapsus and pregnancy

The features of the course of pregnancy and childbirth in women with DST are not sufficiently studied. Pathology of pregnancy is much more common in women with MVP and CTD than in healthy women—85.5 versus 53.3%.The threat of spontaneous abortion and miscarriage occurs in 50% of women with MVP, and the threat of premature birth is observed six times more often than in healthy pregnant women [13]. The main reason for the habitual miscarriage of pregnancy in this group of patients is cervical insufficiency [16]. In women with MVP and CTD, the threat of interruption of pregnancy up to 20 weeks is in almost one-third of cases, the threat of premature birth—in 17.2%, pregnancy ended in premature births of 4.6% [40]. The threat of spontaneous termination of pregnancy in the first trimester was noted in every third patient with MVP, in the II trimester—in 25.9% of patients with MVP; in the third trimester—in 15.5% [33]. The 9.6% of women with habitual miscarriage have MVP [41, 42].

The pregnancy in patients with MVP and undifferentiated connective tissue dysplasia is accompanied by an increase in the frequency of the threat of interruption in the first trimester of pregnancy—OR 1.7, hyperemesis gravidarum—OR 1.8, the threat of interruption in the second trimester of pregnancy—2.5%, premature births—OR 3.2, and polyhydramnios—OR 2.7. The course of labor is complicated by cervical rupture—OR 1.8 and weakness of labor activity—OR 3.7 [7].

The most common complication of the second half of pregnancy in women with MVP is preeclampsia—51.7% [16, 43], and the course of labor in these patients is characterized by frequent complications [16, 40, 43]. It is known that preeclampsia ranks two to three in the structure of causes of maternal mortality [33, 44–47] and is one of the main causes of premature birth and perinatal fetal death. Every fifth child born to a mother with preeclampsia, to some extent, deviations in physical and psycho-emotional development are observed [7].

Another complication, no less important for obstetrics—preterm rupture of placental membranes and outflow of amniotic fluid—in women with MVP is observed in 40.0–51.6% of cases [7, 29, 43, 48]. The frequency of premature and early outflow of amniotic fluid in pregnant women with MVP is 38.1%.

Among the characteristics of the course of labor associated with MVP, the relationship with the rapid course of labor is described, and with a severe degree of MVP, the rate of fast and rapid delivery in primiparas reaches 50%, and for weakly expressed symptoms of MVP is about 12%.

In women older than 30 years, WLA occurs two times more often than in women at the age of 20–25. WLA leads to a prolonged course or complete stopping of labor, the appearance of signs of distress syndrome of the fetus, which causes operative delivery. In the structure of an emergency cesarean section, the WLA occupies the second to third place, reaching 37%.

The investigation of the causes of WLA concerns mainly the issue of the state of the myometrium without sufficient attention to the general anamnestic and clinical signs inherent in the MVP, although the causative factors of the WLA may indicate the possible involvement of MVP in the pathogenesis of an abnormality of labor [16].

The study of the features of the course of pregnancy and childbirth of women with small and large signs of MVP and CTD made it possible to establish that anomalies of labor in the first stage of childbirth appeared in 85.2% of women giving birth, compared to 33.9% in the control group without CDT. Cesarean section in the main group was performed in 12% of pregnant women and only in 4% of patients in the control group. Hypotonic bleeding in the III stage of labor took place in 7.3% of mothers with MVP and CTD and were absent in the control group. The discrepancy of the pubic joint was diagnosed in 7.2% of women with MVP and CTD and was not detected in the control group.

The birth traumatism of newborns from mothers with MVP and CTD was diagnosed in 34.4% of cases compared with 3.4% in the control group. This study showed that patients with generalized manifestations (involvement of three or more organs in the connective tissue defect) of MVP and CTD even in the absence of severe forms of this pathology constitute a high-risk group for the formation of obstetric and neonatal pathology.

The frequent occurrence of MVP and CDT in pediatric practice, the pronounced clinical polymorphism, and multiple organ changes make the problem relevant from the point of view of differential diagnostics and complex therapy.

Hemodynamic changes that develop during pregnancy, during childbirth, and in the postpartum period (primarily changes in bcc and cardiac ejection) cannot but affect the current of the woman's cardiovascular diseases. As well as diseases of the heart and blood vessels can adversely affect the course of pregnancy. Changes in hemodynamics in the mother have a negative effect on uteroplacental blood circulation, which in some cases may lead to the development of placental insufficiency, fetal growth retardation (FGR), and premature birth [4, 7, 16]. The central hemodynamics in women with mitral valve prolapse in the III trimester is characterized by an increase in the overall peripheral resistance of the vessels against a background of a decrease in volume indices, which indicates the voltage of the compensatory-adaptive mechanisms of the cardiovascular system [33].

The features of hemodynamics (heart rate, peripheral resistance of blood vessels, changes in blood pressure) are due to changes in the activity of the sympathoadrenal system. The pregnant women with MVP showed a significant decrease in MI and BV, as well as CI and BI as compared to those in women without MVP with a physiological pregnancy. Perhaps, the reduction of these indicators is due to a decrease in the contractility of the myocardium and a decrease in the activity of the sympathoadrenal system. Formation in the first trimester of

the hypokinetic type of central maternal hemodynamics with a reduced peripheral vascular resistance is one of the leading pathogenetic mechanisms of the development of preeclampsia and placental insufficiency (fetal hypoxia and IUGR) [4, 33].

The main clinical manifestation of placental insufficiency in patients with MVP is chronic intrauterine fetal hypoxia (7.33), which is detected in 34.5% of pregnant women, which is significantly higher than in women without MVP (13.2%). Dopplerometric examination of blood flow velocities revealed a violation of both placental and uterine-placental blood flow. In 11.2% of pregnant women with MVP on the background of chronic intrauterine fetal hypoxia, the fetal growth retardation (FGR) syndrome was detected, and in 84.4%—on the background of preeclampsia. In the development of placental insufficiency, the main and often initial causes are hemodynamic microcirculatory disorders. The factors that are genetically determined, exist in the maternal organism initially, also play a role in the formation of placental insufficiency, while the process of collagen formation has a certain role [7].

In the presence of a syndrome of non-differentiated dysplasia of connective tissue, the mother has the prerequisites for the birth of children with small developmental anomalies and congenital heart defects (MVP, TVP, left ventricular abnormal chords, patent foramen ovale, open arterial duct, atrial and interventricular septal defect). In children born from mothers with MVP, minor heart anomalies were detected in 16.4% [49].

The more significant clinical manifestations and a higher incidence of obstetric and perinatal complications are noted when MVP is combined with other intracardiac anomalies. Thus, in pregnant women with mitral valve prolapse and in combination with abnormally located chord and congenital heart disease (atrial septal defect), there is a significant increase in cardiac clinical symptoms from the first to the third trimester of pregnancy [5].

The postpartum period is characterized by a significant "positive" dynamics of ultrasound indicators of the degree of prolapse of the mitral valve and the degree of mitral regurgitation: they decrease reliably, even in comparison with the data during echocardiography in the first trimester of pregnancy. Thus, according to literature data [3, 5, 7, 10, 16, 41, 49, 50], women with MVP and other connective tissue anomalies of heart development are considered to be at high risk for complications of pregnancy, childbirth, and perinatal morbidity.

8. Conclusion

In connection with this, the following measures should be taken:

1. systematic prenatal supervision by an obstetrician and a cardiologist as during pregnancy, and at the stage of pregravid preparation;

2. in every trimester of pregnancy, it is necessary to carry out echocardiography, ECG, daily ECG monitoring;

3. investigation of the magnesium content in biological fluids and the detection of its deficiency in the appointment of magnesium preparations;

4. in case of complications of pregnancy and (or) complaints from the cardiovascular system—hospitalization;

5. systematic control of the fetus with the use of Doppler, cardiotocography, ultrasound in the detection of abnormalities timely correction;

6. labor is preferred to lead through the natural birth canal with adequate analgesia, under cardiac monitoring of the fetus and contractive activity of the uterus, prevention of abnormalities of labor. Cesarean section—according to obstetric indications;

7. examination of newborns with the help of echocardiography and consultation with a cardiologist and neurologist;

8. control echocardiography of a woman to determine the degree of prolapse of the mitral valve after delivery [33].

However, this algorithm is the opinion of only domestic obstetricians. According to data of some authors [3, 10], the complicated course of pregnancy and the increase in clinical symptoms in women with MVP are extremely rare. Women are primarily advised to avoid stressful situations, drinking coffee, strong tea, alcohol and tobacco, and using β-mimetics. Therapy is required only in the presence of arrhythmia (often tachycardia and extrasystoles). In this case, β-blockers are the drugs of choice. An interesting one is the recommendation of antibiotic prophylaxis in the presence of MVP and delivery with cesarean section in order to avoid infective endocarditis, but it is also controversial. The risk of serious complications in women with uncomplicated MVP younger than 45 years old is 0.2% per year.

Thus, the data presented earlier indicate a number of conflicting views on the etiology, classification, pathogenetic features of the mitral valve prolapsed, and the significance of its presence in the formation of various obstetric and perinatal complications. At present, it is urgent to continue research into the complex effects of nondifferentiated connective tissue dysplasia (NCTD) and MVP on the course of pregnancy, postpartum and neonatal delivery, analysis of current classifications of NCTD and pathogenetic (including genetic factors) of MVP features, and the definition of their importance in the development of obstetric complications.

Author details

Ignatko Irina Vladimirovna*, Strizhakov Leonid Alexandrovich,
Rodionova Alexandra Mihailovna and Martirosova Alina Lorisovna

*Address all correspondence to: iradocent@mail.ru

First Moscow State Medical University, I. M. Sechenov (Sechenov University), Moscow, Russia

References

[1]   Cunningham FG, Lenovo KJ, Bloom SL, Hauth JC, Rouse DJ, Spong CY. Medical and surgical complication. In: William's Obstetrics. 23rd ed, Section 8 ed. Vol. 2010. McGraw-Hill. pp. 912-1235

[2]   James D, Steer PJ, Weiner CP, Gonik B. Chapter 1. Global maternal and perinatal health issues. In: High Risk Pregnancies: Management Options. 4th ed. PA: Elsevier Saunders; 2010. pp. 1-7

[3]   Creasy RK, Resnik R, Iams JD. Maternal-fetal medicine. Principles and Practice. Chapter 52. In: Cardiac Diseases. PA: Elsevier Saunders; 2014. pp. 852-878

[4]   Strizhakov AN, Timokhina EV, Ignatko IV, Belotserkovtseva LD. Pathophysiology of the Fetus and Placenta. Moscow: GEOTAR-Media; 2015. p. 176

[5]   Kamovich TE. Clinical and diagnostic features in the prolapse of mitral valve in women during pregnancy and in the postpartum period [Dissertation Candidate of Medical Sciences]. Ryazan; 2004. p 123

[6]   Hereditary Disorders of Connective Tissue. Russian Recommendations. Developed by the expert committee of the All-Russian Scientific Society of Cardiology. Moscow. 2012. 76 pp

[7]   Amiraslanov E Yu. Forecasting Obstetric Complications in Patients with Non-differentiated Connective Tissue Dysplasia. Moscow; 2014. 140 p

[8]   Perloff JK, Child JS, Edwards JE. New guidelines for the clinical diagnosis of mitral valve prolapse. The American Journal of Cardiology. 1986;**57**:1124-1129

[9]   Gilon D, Buananno FS, Leavitt M, et al. Lack of evidence of an association between mitral-valve prolapse and stroke in young patients. The New England Journal of Medicine. 1999;**341**:8-14

[10] James D, Steer PJ, Weiner CP, Gonik B. High risk pregnancy. Management Options. In: Chapter 36. Cardiac Diseases. 4th ed. PA: Elsevier Saunders; 2011. pp. 627-657

[11] Zemtsovsky EV. Dysplastic Phenotypes. Dysplastic heart: An analytical review. St. Petersburg; 2007. 80 p

[12] Zatikyan EP. Mitral valve prolapse: Diagnosis, clinic and functional manifestations. The nature of the change in the data of functional research methods during pregnancy. Sonoace International. 1999;**5**:34-41

[13] Trochu JN, Kyndt F, Schott JJ. Clinical characteristics of a familial inherited myxomatous valvular dystrophy mapped to Xq28. Journal of the American College of Cardiology. 2000;**35**(7):1890-1897

[14] Theal M, Sleik K, Anand S. Prevalence of mitral valve prolapse in ethnic group. Canadian Journal of Cardiology. 2004;**5**(20):511-555

[15] Cook JR, Carta L, Galatioto J, Ramirez F. Cardiovascular manifestation in Marfan syndrome and related diseases; multiple genes causing similar phenotypes. Clinical Genetics. 2015;**87**:11-20

[16] Klemenov AV, Alekseeva OP, Tkacheva ON. Features of the course of pregnancy in women with undifferentiated connective tissue dysplasia. Problemy reprodukzii. 2005;**3**:85-88

[17] Zemtsovsky EV, Malev EG. Small Heart Abnormalities and Dysplastic Phenotypes. SPb: Publishing House "IVESEP" 2011. p. 160

[18] Shekhtman MM. Manual on extragenital pathology in pregnant women. M: Triad-X; 2008. 816

[19] Ghia YT. Maternal congenital heart disease and pregnancy outcome. Journal of Obstetrics and Gynaecology Research. 1996;**2**(22):185-191

[20] Devereux RB, Perloff JK, Reichek N. Mitral valve prolapse. Circulation. 1976;**54**:3-6

[21] Malev EG, Zemtsovsky EV. The prevalence of mitral valve prolapse in the Russian population. Bulletin of the Federal Center of Heart, Blood and Endocrinology. V.A. Almazov. 2011;**4**:25-30

[22] Eliseeva IV. Clinico-functional features of the somatic state and the course of labor in women with prolapse of the mitral valve. Clinical Medicine. 2003;**3**:22-24

[23] Zemtsovsky EV. The Prolapse of the Mitral Valve. SPb: Society "Knowledge" of St. Petersburg and the Leningrad Region; 2010. p. 160

[24] Yagoda AV, Gladkikh NN. Small HeaRt Anomalies. Stavropol: Izd-vo StGMA; 2005. p. 248

[25] Yokota Y, Kumaki T, Fukuzaki H. Clinical and exercise echocardiographic findings in patients with mitral valve prolapse. Japanese Circulation Journal. 1990;**54**:62-70

[26] Marlin-Neto JA, Mattar-Junior L, Maciel BC, et al. Funacao ventricular no prolapse de valva mitral: efeitos do bloqueio betaadrenergico com e sem atividade simpatomimetica intrinseca. Arquivos Brasileiros de Cardiologia. 1989;**52**:247-252

[27] Lembo NJ, DeU'Italia LJ, Crawford MH. Mitral valve prolapse in patients with prior rheumatic fever. Circulation. 1988;**77**:830-836

[28] Mitrofanova LB, Karev VE, Shlyakhto EV, Kovalsky GB. Mesenchymal dysplasia of the heart valves, cystic mediaronecrosis of the aorta and herpetic infection. Archive of Pathology. 2005;**5**(67):20-23

[29] Gromova O. Molecular mechanisms of magnesium action on connective tissue dysplasia. Journal for practicing doctors. Connective Tissue Dysplasia. 2008;**1**:23-32

[30] Nedostup AV, Wein AM, Solovyova AD. The state of autonomic regulation in patients with mitral valve prolapse and sinus node dysfunction. Clinical Medicine. 1996;**3**:35-39

[31] Suhanova GA. Identification and correction of hemostasis disorders in mesenchymal dysplasia: Author's Abstract [Dissertation Candidate of Medical Sciences]. Barnaul; 1993. p 23

[32] Domnitskaya TM, Dyachenko AV, Kupriyanova OO, Domnitsky MV. Clinical evaluation of the use of magnesium orotate in young people with dysplasia syndrome of connective tissue of the heart. Cardiology. 2005;**45**(3):76-81

[33] Bakashvili Sh.B. A differentiated approach to the tactics of pregnancy management in women with mitral valve prolapse. Author's Abstract [Dissertation Candidate of Medical Sciences]. Moscow; 2010. p 23

[34] Milkovskaya-Dimitrova T. Diagnostic criteria for connective tissue dysplasia. Pediatrics (Sofia). 1982;**21**:127-136

[35] Malev E, Zemtsovsky E, Reeva S, et al. Cardiomyopathy in mitral valve prolapse. European Journal of Echocardiography. 2011;**12**(Suppl 2):ii63

[36] Pislaru S, Enriquez-Sarano M. Definition and Diagnosis of Mitral Valve Prolapse. UpToDate, 2018

[37] Fomin VV. The state of myocardial contractility of the left and right ventricles with mitral valve prolapse. Author's Abstract [Dissertation Candidate of Medical Sciences]. Moscow; 2004. p 23

[38] Storozhakov GI, Vereshchagina GS, Malysheva NV. Risk stratification and choice of clinical tactics in patients with mitral valve prolapse. Serd. lack. 2001;**6**(2):287-290

[39] Devereux RB, Frary CJ, Kramer-Fox R, Roberts RB, Ruchlin HS. Cost-effectiveness of infective endocarditis prophylaxis for mitral valve prolapse with or without a mitral regurgitant murmur. The American Journal of Cardiology. 1994;**74**:1024-1029

[40] Smolnova T.Yu. Phenotypic Symptom Complex of Connective Tissue Dysplasia in Women. Wedge. Honey. 2003;**8**:42-47

[41] Tetruashvili N. Analysis of the causes of the usual early loss of pregnancy. Doctor. 2008;**8**:54-57

[42] Strizhakov AN, Timokhina EV, Pitskhelauri EG, Belousova VS, Yakushina NI. Preeclampsia today: Pathogenesis and the ability to predict and treat. Questions of Gynecology, Obstetrics and Perinatology: 2016;**15**(3): 24-31

[43] Romero R, Friel LA, Velez Edwards DR, Kusanovic JP, Hassan SS, Mazaki-Tovi S, et al. A genetic association study of maternal and fetal candidate genes that predispose to preterm prelabor rupture of membranes (PROM). American Journal of Obstetrics & Gynecology. 2010;**203**(4):361 e1-361; e30

[44] Disse S. Mapping of the first locus for autosomal dominant myxomatous mitral valve prolapse to chromosome 16p11.2-p.12.1. American Journal of Human Genetics. 1999;**65**(5): 1242-1251

[45] Biery NJ. Revised genomic organization of FBN1 and significance for regulated gene expression. Genomics. 1999;**56**(1):70-77

[46] Rabkin E. Activated interstitial myofibroblasts express catabolic enzymes and mediate matrix remodeling in myxomatous heart valves. Circulation. 2001;**104**(21):2525-2532

[47] Milewicz DM, Urban Z, Boyd C. Genetic disorders of the elastic fiber system. Matrix Biology. 2000;**19**(6):471-480

[48] Chen C, Hill LD, Schubert CM, Strauss JR 3rd, Matthews CA. Is laminin gamma-1 a candidate gene for advanced pelvic organ, prolapse? American Journal of Obstetrics and Gynecology. 2010;**202**:5-10

[49] Nikiforova OK, Kozinova OV, Zaretskaya NV. Small developmental anomalies in newly born children born from women with hereditary connective tissue dysplasia. Materials of IV Congress of Obstetricians–Gynecologists of Russia. M. 2008. 554-555

[50] Podtetenev AD. Forecasting, Prevention and Treatment of Weakness and Discordination of Labor: Avtoref. Dis. … Dr med. sciences. M; 2004. 237 c

Bicuspid Aortic Valve

Ayşe Inci Yıldırım and Aysu Türkmen Karaağaç

Additional information is available at the end of the chapter

Abstract

Bicuspid aortic valve (BAV) is one of the most common congenital diseases, affecting 1–2% of the general population. Although most of them are sporadic, some familial cases have also been detected. BAV is a complex developmental and progressive pathology, which may present with various clinical findings from newborn to adulthood. It may be suspected during cardiac auscultation or may be diagnosed by echocardiography incidentally. Some BAV cases may remain symptomless for years, with findings like valvular stenosis, insufficiency, or dilatation in the ascending aorta, whereas some others may present with early severe aortic valve dysfunction, premature congestive heart failure, and aortic aneurysms even in the newborn period. Such heterogeneous presentations of BAV phenotypes may be associated with congenital, genetic, and/or connective tissue abnormalities. The natural course of BAV is nonpredictable, it may lead to severe morbidity and mortality.

Keywords: aortopathy, aortic regurgitation, aortic stenosis, aortic dilatation, aortic dissection

1. Introduction

Bicuspid aortic valve (BAV) is one of the most common congenital heart diseases. It is phenotypically variable and genetically heterogeneous. The prevalence of the disease has been determined according to the results of echocardiographic screening and necropsy studies. Some patients with isolated BAV may remain asymptomatic throughout their lives, so they may be diagnosed accidentally in echocardiographic screening. Although it is difficult to define the real incidence of BAV, it is accepted to have a prevalence of 0.5–2% in the general population, with a higher prevalence in males than females: M/F = 3/1 [1, 2]. The clinical presentation of BAV is highly variable. Its major manifestations are aortopathy, valvular

dysfunctions, endocarditis, and dissection. In the patients presenting with valvular dysfunction earlier in life, aortic regurgitation (AR) is more common, whereas aortic stenosis (AS) is more prevalent later in life, after the fourth decade. Valve phenotypes, genetic, and hemodynamic factors have been proposed as underlying mechanisms of aortopathy. Ascending aortic aneurysm is generally due to aortopathy and hemodynamics; however, the aortic root aneurysm is considered to be a consequence of aortopathy rather than hemodynamics, especially in younger patients. The asymptomatic BAV patients with normal valvular function require surgical treatment less frequently than those with valvular dysfunction and aortopathy during their lives.

Moreover, BAV may be associated with several genetic disorders with cardiovascular manifestations such as hypoplastic left-heart syndrome, congenital left-sided obstructive lesions (coarctation of aorta, Shone complex), ventricular septal defect, and syndromic conditions (Turner, Loeys Dietz). This chapter enrolls only the isolated bicuspid aortic valves.

2. Genetic and inheritance

2.1. Associated with genetic syndrome

Although most of the BAV patients are sporadic or familial, some may have the symptoms knowngenetic syndromes as Trisomy 18, Williams syndrome, and Turner syndrome. The highest penetrance of BAV (>30%) occurs in woman with Turner syndrome caused by partial or complete absence of one X chromosome [3]. In the general population, BAV is more prevalent in men than women, suggesting that the loss of genes on the X chromosome may predispose to BAV phenotype [3, 4].

2.2. Familial inheritance and genetic etiologies

The heritability of BAV is now well established; however, the genes linked to the defect remain largely unknown. Autosomal dominant, X-linked, and familial modes of inheritance have been reported. BAV heritage revealed a high incidence of familial clustering. The study performed in the Canadian population revealed that 11 of 30 families (36%) had at least 1 additional member with BAV, and the recurrence rate in first-degree relatives was 9% [5]. Another study reported that 100 out of 448 subjects in a Mediterranean population had BAVs, 348 of which were first-degree relatives. In this study, the BAV recurrence rate in the first-degree relatives was 4.6%. This value was clearly lower than that in the Canadian population. The populations or geographic areas may affect the prevalence of BAVs [6].

Epidemiologic studies have demonstrated that BAV is heritable and follows an autosomal dominant mode of transmission with reduced penetrance and variable expressivity [7, 8]. Through the linkage analysis of BAV pedigrees, investigators have found multiple genetic loci and chromosomes associated with BAV disease [7–16]. The most significantly associated genes and the chromosomes they are located on are shown in **Table 1**. However, some of these gene mutations have been found to be related with aortopathies. Several mouse studies have showed that the NOTCH1 gene mutation plays an important role in the development of

Candidate genes	Chromosomal regions
TGFBR2 (Transforming growth factor, beta receptor II)	3p24.1
NKX2.5 (NK2 Homeobox 5)	5q35.1
NOTCH1 (Translocation-associated notch protein TAN-1)	9q34.3
ACTA2 (Actin, alpha 2)	10q23.31
MYH6 (Myosin heavy chain 6)	14q11.2
MYH7 (Myosin heavy chain 7, cardiac muscle, beta)	14q11.2
FBN1 (Fibrillin 1)	15q21.1
ENG (Endoglin)	9q34.11
AXIN1 (Axin 1)	16p13.3
KCNJ2 (Potassium channel, inwardly rectifying subfamily J, member 2)	17q24.3
GATA5 (GATA binding protein 5)	20q13.33
PDIA2 (Protein disulfide isomerase family A, member 2)	16p13.3
TGFBR 1 (Transforming growth factor, beta receptor I)	9q22.33

Table 1. Genes with association with bicuspid aortic valve.

ascending aorta aneurysm and BAV [8, 9, 16]. Although the FBN1 gene mutation frequently accompanies Marfan syndrome, its association with BAV and ascending aorta dilatation has been shown in a recent study [17]. The pathologic hallmark of aortic aneurysm is medial degeneration. Disruption of the smooth muscle cells' (SMC) contractility due to mutations may lead to aortic aneurysm. Mutations in the MYH11 and ACTA2 genes are associated with the familial thoracic aortic aneurysms [18].

Consequently, BAV and aortopathy are complex multifactorial and multigenetic pathologies. Genetic, epigenetic, and environmental modifiers may be responsible for the variable penetrance and phenotypic expression [4].

3. Aortic root

3.1. Embryology of aortic root

Cardiac and valve morphogenesis occur in early fetal life. Actually the abnormal valvulogenesis of BAV has not been clearly understood. Earlier theories proposed that abnormal blood flow across the developing valves would result in the failure of cusp separation. Current theories suggest that cell migration, signaling pathway, and genetic susceptibility are the main factors in the development of BAV disease.

The embryonic heart and aorta are developed from three precursor cells: proepicardial cells, cardiogenic mesodermal cells (contribute to first and second heart fields [SHfs]), and neural crest cells. Second heart field (SHF) and the cardiac neural crest (CNC) contribute to the

development of aortic root, ascending aorta, and aortic arc. Paraxial mesoderm plays role in the development of descending aorta [19, 20]. First heart field (FHF) forms the early embryonic heart tube that contributes to the left ventricle and a portion of the right ventricle and atria. SHF contributes to the myocardium of the outflow tract to form the truncus arteriosus. Mesenchymal cells originating from the migrating cardiac neural crest cells reach the outflow tract cushions and contribute to the formation of the aortic and pulmonary valves together with the endocardially derived mesenchymal cells. Abnormal migration of neural crest cells has been postulated as a common pathway that results in BAV and aortopathy [21–24].

Several proteins are used to determine the positional and functional relationship of various cellular populations during embryogenesis. Conical Wnt, non-conical Wnt, TGF-β, fibroblast growth factor, bone morphogenetic protein, and Notch are some important proteins in the development of aortic valve and aorta. Errors of this pathway may result in various outflow tract structural abnormalities including BAV disease [11, 16, 19, 23].

3.2. Histopathology of the aorta

The normal aortic valve involves three layers. The first layer is the inner intimal layer, which consists of endothelial cells. The second layer is the thicker medial layer formed of smooth muscle cells (SMCs) and elastin. The elastin is arranged in fenestrated sheets (lamellae) between which collagen fibers, thin layers of proteoglycan-rich extra-cellular matrix (ECM), and SMCs are located. Thin elastic fibers embed lamellae into a three-dimensional network and connect them with SMCs. The third layer is the strong adventitial layer with collagen fibers wrapping the aorta [25, 26]. The relatively high collagen content of the adventitia prevents vascular rupture at extremely high pressures [27]. SMC and ECM play an important role both in the normal tissue development and in the main mechanical function of the aortic media [2, 28, 29]. SMCs are the major cell types of the aortic wall that synthesize and organize the ECM with the elastic fiber network in the arterial wall [25, 26, 30]. SCMs also provide lamellar organization, depending on the diameter and stress applied upon the vessels during embryogenesis. ECM, mainly composed of elastin and collagen, is important for the aortic strength and flexibility to withstand the arterial blood pressure [26]. The number of lamella is greater in larger vessels facing greater wall tension and it seems to remain stable after birth. In the normal aorta, SMCs have a little active role in managing wall tension; microfibrillar structure is the major passive contributor [26, 30]. As the vessel wall matures, SMCs condense down around the endothelial tube to form the circumferential layers, which will finally define the elastic lamellae of the mature vessel [30].

3.3. Pathogenesis of aortopathy

Aortopathy is very complex pathology, in which both cellular and extracellular mechanisms are involved. Possible mechanisms for aortopathy in patients with BAV include medial degeneration (elastic fiber fragmentation and smooth muscle cell apoptosis), fibrilin-1 deficiency, increased metalloproteinase (MMP), and decreased MMP tissue inhibitor expression.

Medial degeneration: Failure of the balance between the synthesis and degradation of ECMs in the aortic wall leads to aortic aneurysm. Especially elastin is the major fibrillar component

in the arterial wall, so its destruction directly leads to the expansion of aorta. Moreover, some intrinsic medial degenerative differences have been identified between TAV and BAV patients. While degeneration in TAVs has been attributed to inflammation and accelerated aging, it has been attributed to the maturation defect in BAVs. Several BAV studies have revealed noninflammatory loss of vascular SMCs, less-differentiated vascular SMC, low laminin A/C, and progerin expression as the other causes of medial degeneration [27, 30, 31]. The total thickness of the aortic media is the same for BAV and TAV aortas, but the distance between the elastic lamellae is greater and the lamellae themselves are thinner and more fragmented in BAV patients [30, 32]. It was suggested that matrix disruption and SMC apoptosis were earlier in BAVs with stenosis than TAVs with respect to the dilatation of aorta [33]. The patients with ascending aorta dilatation with BAV showed lesser cystic medial necrosis (focal loss of vacsular smooth muscle cell (VSMC) nuclei in the media) than those with TAV [30]. Nondilated BAV aortas may have higher rates of vascular SMC apoptosis, particularly at the convexity, where wall stress is expectedly higher. Stress-dependent BAV matrix changes may trigger early apoptosis [33].

Deficiency of fibrilin-1: Maturation defect is maintained in the dilated aortic wall in BAV patients. Fibrillin-1, which stabilizes the vascular wall, is secreted by the SMC. It is low in BAV patients because of the immaturity of SMC [21]. Deficiency of fibrillin-1 results in vascular SMC detachment, matrix disruption, and apoptosis, which ultimately result in a fragile aorta, less suited to deal with stress associated with valvular dysfunction. Decreased levels of fibrillin-1 may also lead to tinning and weakening of the aortic wall. Some studies have showed that aortic tissues in BAVs have significantly less fibrillin-1 than TAV aortas [34, 35].

Increased activity of MMPs: To date, most studies have focused on MMP-2 and MMP-9, which belong to a subclass of MMP. An increase in MMPs, enzymes that process or degrade the extracellular matrix, may lead to the weakening of the aortic wall and may be associated with the development of aortic aneurysms. In particular, MMP-2 and MMP-9, secreted from macrophages, which have infiltrated the inflammatory site, are known as powerful proteinases that degrade elastin fiber. BAV patients have dilated aortas with a higher content of MMP and a lower level of tissue inhibitor of MMP compared to TAV patients, indicating an increased collagen turnover. MMP-9 has been closely associated with the formation of abdominal aortic aneurysms [31, 36]. MMP-2 has been identified as a key molecular modulator and a circulation biomarker of aortic dilation in patients with BAV [36]. Several markers as c-Kit (a marker for differentiated vascular SMCs), pc-Kit (phosphorylated state of c-Kit, triggered by the presence of MMP9), HIF1a (influencing hypoxia-inducible-factor-1alpha), and endothelial nitric oxide synthase might play an important role in the pathogenesis of the aortopathy [31]. Increased collagen turnover and decreased collagen cross-linking may be another factor in the formation of aneurysms in BAV cases [37].

4. Phenotypic presentation of aortic valve and root

4.1. Morphology of bicuspid aortic valve

Normal aortic valve is tricuspid, meaning it possesses three leaflets (or cusps: the left coronary, the right coronary, and non-coronary cusps, named after their relationship to the coronary

arteries). However, BAV is formed of two functional leaflets. There are two types of BAV. The typical one is the most frequent and is formed of two leaflets of unequal size with complete or incomplete fusion of two cusps. Adjacent cusps fuse into a single cusp, that is generally bigger than its counterpart cusp, but these fused cusps are smaller than two normal cusps combined. In such cases, there may be one or two raphe. The term "raphe" refers to the fused area of two underdeveloped cusps turning into malformed commissure between both cusps [28, 29]. The second and less commonly encountered type of BAV is "true BAVs," which have leaflets equal in size with no raphe [28]. Morphology of the aortic valve is defined according to spatial position of cusps, fusion types, and the number of raphe. The valve morphologies, raphe number, and fusion types are shown in **Table 2**. The fusion positions between the right and left coronary cusps (RL BAV), right and non-coronary cusps (RN BAV), and true BAVs are shown in **Figure 1**. The most prevalent aortic valve morphologies are RL BAV phenotypes and second, RN BAV phenotypes, and the least common are LN BAV phenotypes [28, 29, 38, 39].

4.2. Aortic phenotype

The aorta is anatomically composed of ascending aorta, aortic arch, thoracic aorta, and abdominal aorta. The aortic root contains aortic sinuses, aortic valve, and coronary ostia. The tubular portion of the ascending aorta begins at a point distal to the aortic root (sinotubular junction) and ends at the origin of the innominate artery. The aortic arch includes the origins of innominate artery, the left common carotid artery, and the left subclavian artery [40]. **Figure 2** shows the echocardiographic images and the measurements of aortic root, tubular portion of the ascending aorta, and aortic arc. There are computerized tomography images of various aortic phenotypes in **Figure 3**.

Several classifications have been made according to the structure, diameter of aorta, and the extent of aortic dilatation. BAV aortopathies generally present with ascending aorta dilatation or root dilatation or both. The types of aortopathies are summarized in **Table 3**. The most common types of aortic dilatation which are seen are the ascending aorta and varying degrees of aortic root. This type was associated with an older age at diagnosis (>50 years), valvular stenosis, and the RL BAV fusion pattern [29, 40, 41]. Isolated dilatation of the aortic root is a rare type and associated with younger age at diagnosis (<40 years), male sex, aortic

Morphology of aortic valve	Type 1	Type 2	Type 3
Raphe present (Complete or incomplete fusion)	Right–left coronary cusps fusion (RL BAV)	Right-non-coronary cusps fusion (RN BAV)	Left-non-coronary cusps fusion (LN BAV)
Valve opening	Anterior–posterior	Right–left	Right–left
Raphe number*	1 raphe	2 raphe	
Raphe absent Valve opening	Anterior–posterior	Right–left	Right–left
*Type 0: no raphe			

Table 2. The bicuspid aortic valve morphologies, fusion types, and raphe number.
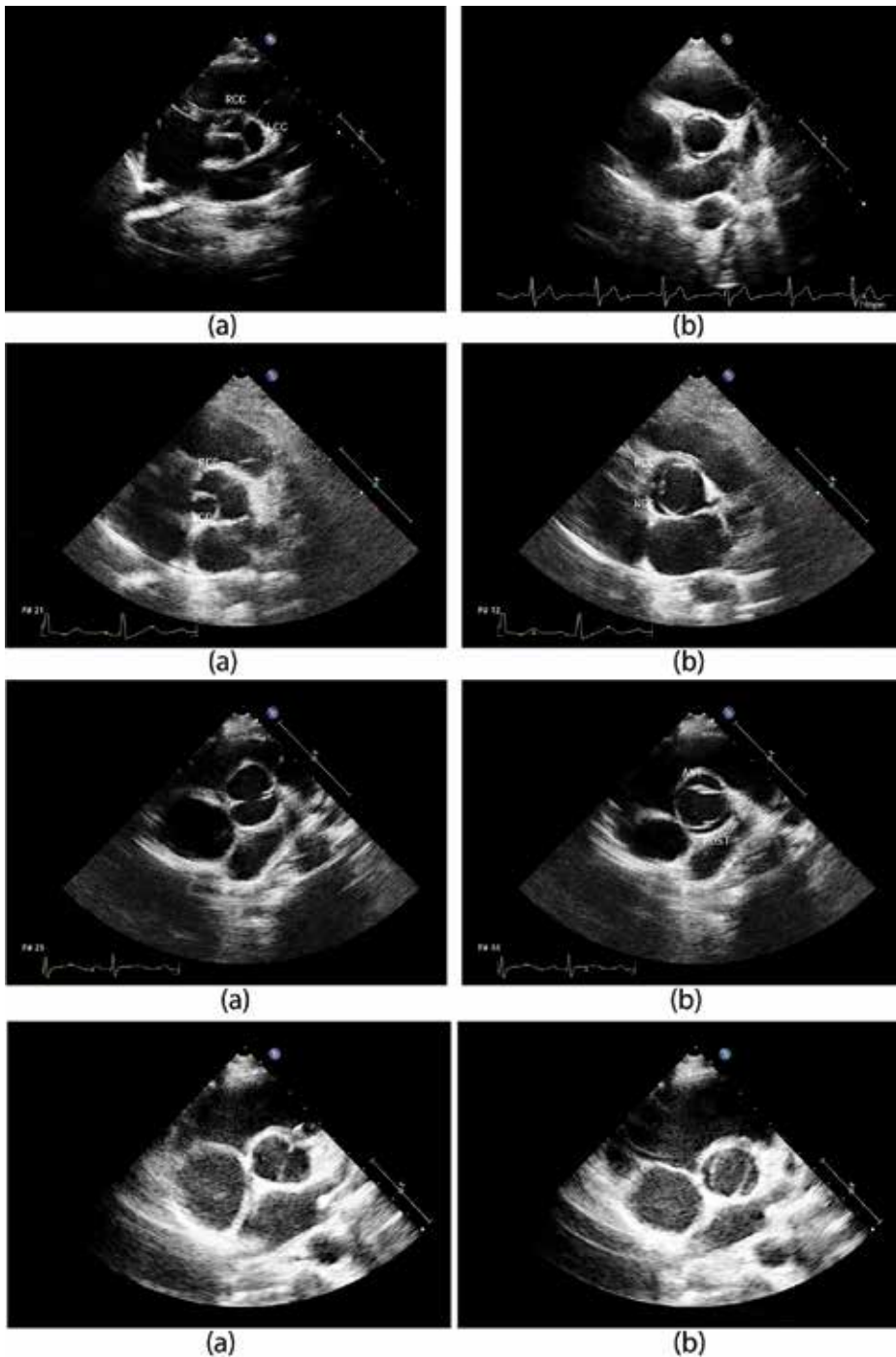
Figure 1. Echocardiographic views of commissural fusion patterns of BAVs and true BAVs. In the first view: Right-left coronary cusp fusion a) closed b) opened position; in the second view: Right non coronary cusp fusion a) closed b) opened position; in the third view: true BAV anterior-posterior valve position a) closed b) opened position; in the fourth view: True BAV right-left position a) closed b) opened position. RCC: right coronary cusp, LCC: left coronary cusp, NCC: non coronary cusp, ANT: anterior, POST: posterior.

Figure 2. Echocardiografic images revealing the measurements of a) aortic root in the long axis view at the annular, sinus valsalva, sinotubular junction and ascendi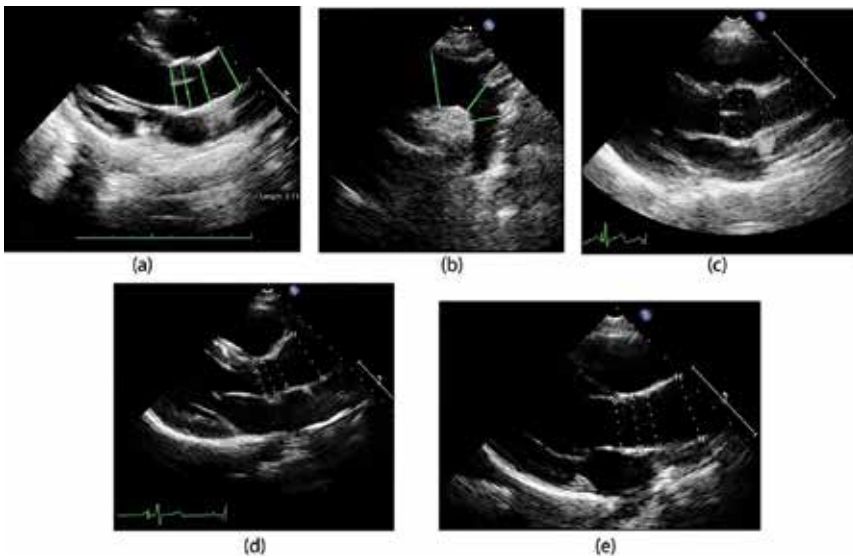ng aorta levels b) aortic arc at the transverse arc, isthmus and descending aorta levels c) sinus valsalva dilatation in long axis view d) ascending aorta dilatation in which aortic root was spared in long axis view e) aortic root and ascending aorta dilatation in long axis view.

regurgitation, and aortopathy. This type was considered most likely to be related with a genetic cause [29, 40–42].

4.3. Aortic dilatation

Aortic dimensions are generally measured at the levels of annulus, sinus Valsalva, sinotubular junction (STJ), ascending aorta, aortic arch, descending aorta, and abdominal aorta, from inner edge to inner edge, at the end of diastole in the echocardiographic evaluation. **Figure 3** shows computerized tomography images of aortic root and ascending aorta. Because the aorta increases in diameter with somatic growth in children, the aortic diameter is typically corrected, mostly for body surface area (BSA), age, and gender. It is important to evaluate children under the age of 18 according to the z scores of these measurements. Aorta is accepted to have dilatation if the aortic z score is >2, aortic/expected aortic diameter is >1.15, or it is 2 SD above the mean expected diameter. Aortic dilation was defined as mild (z score > 2 and ≤ 4), moderate (z score > 4 and ≤ 6), or severe/aneurysm (z score > 6 or > 6 SD above the mean for BSA) [43]. In adults, aortic dilatation is present if the diameter of sinus Valsalva is >35 mm, ascending aorta diameter is >34–38 mm, and an aneurysm is present if the aortic/expected diameter is >1.4 or ascending aorta is >45 mm [44–47].

Aortic dilatation may begin early in life and progress with age. It is three times more common in BAV patients than in TAVs [48]. In total, 40% of patients in referral centers were reported to have BAV-associated aortopathy [49]. BAV patients have significantly larger proximal aorta than those with TAV, even in the absence of significant valvular hemodynamic disturbance. Children with BAV have larger sinus Valsalva and ascending aorta, which increase in size at a higher rate than TAVs [48, 50]. Studies showed that aortic aneurysm also was more common
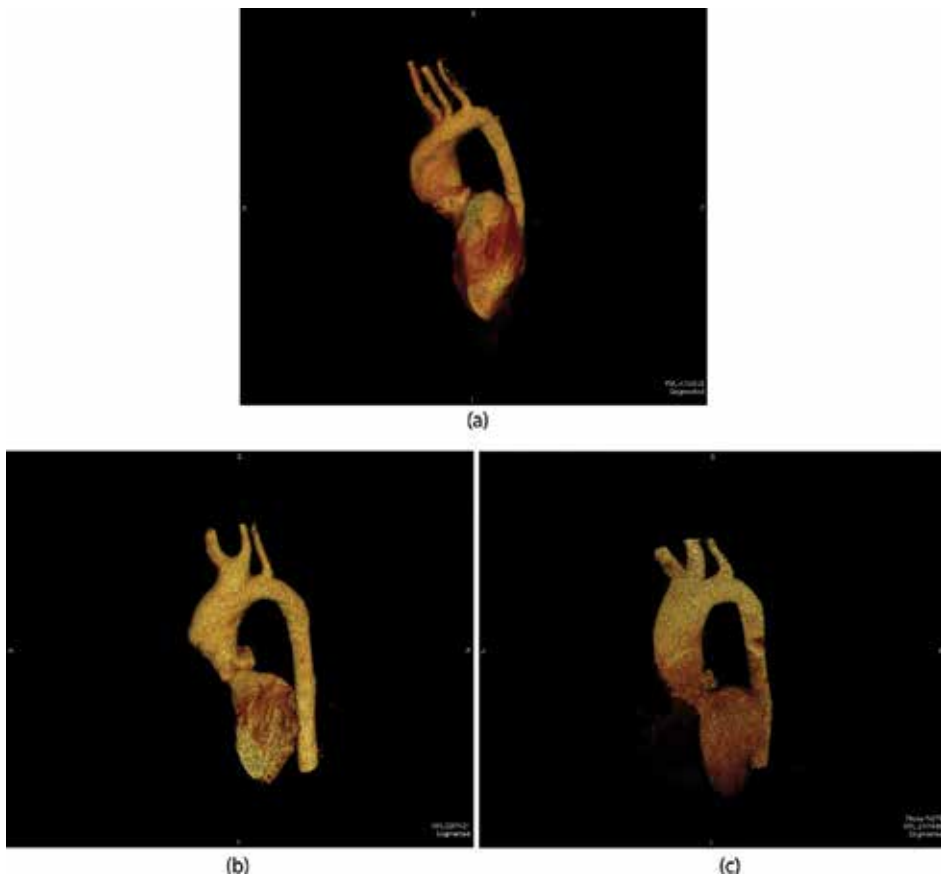
Figure 3. Three dimensional computerized tomography images showing a) ascending aorta dilatation b) sinus valsalva and ascending aorta dilatation extended to arcus aorta c) aortic root and ascending aorta dilatation.

in BAV than in TAV patients. The most common type of dilatation of aorta in BAVs was the ascending aorta dilatation, root dilation was the second, and the least common was the root dilatation together with the ascending aorta [44, 48, 51]. Aortic aneurysms in BAVs commonly involve aortic root, ascending aorta, and aortic arch [42].

The relationship between the aortic valve structure and dilatation has been investigated in several studies. It was reported that RL BAV phenotype was usually associated with aortic root and/or sinus Valsalva and/or proximal aortic dilatation [28, 29, 44, 49, 52–55]. RN BAV phenotype was more commonly associated with ascending aorta dilatation and LN BAV phenotypes with aortic root dilatation [29, 56]. In addition, the RN BAV phenotype was associated with a more rapid growth of the ascending aorta [43]. On the contrary, a relationship between the RL BAV phenotypes and increased risk of rapid aortic dilatation in BAV patients has been reported [57]. Clinical variation of the BAV patients may be related to different etiological entities of cusp phenotypes. Recently preclinical studies have shown that RN and RL cusps' fusion have different pathogenesis [58, 59]. In contrast to these studies, only minor differences in aortic shape can be demonstrated in different BAV phenotypes. Aortic dilatation was primarily caused by intrinsic mechanisms of the aortic wall regardless of valve type [48].

Classification				
Shafer et al. [28]	Type N (normal root)	Type A (ascending dilatation)	Type E (effaced roots)	
	Ascending < sinuses >STJ	Ascending > sinuses >STJ	Sinuses < STJ	
Fazel et al. [43]	Cluster I	Cluster II	Cluster III	Cluster IV
	Aortic root alone	Tubular ascending aorta alone	Tubular portion and transverse arch	Aortic root and tubular portion with tapering across the transverse arc
Verma et al. [41]	Type 1	Type 2	Type 3	
	Dilatation of tubular ascending aorta primarily along convexity of aorta, with mild-to-moderate root dilatation	Arch dilatation with involvement of tubular ascending aorta, with relative sparing of root	Isolated aortic-root involvement with normal tubular ascending aorta and arch dimensions	

STJ: sinotubular junction

Table 3. Aortic dilatation pattern.

4.4. Hemodynamic effect

Flow abnormalities, related to turbulent and helical flow patterns, as a result of the asymmetric movement of valve leaflets, may be a major contributor to aortic dilation in BAV. Even normally functioning BAVs may have abnormal transvalvular flow patterns, resulting in regional increases in wall shear stress [60, 61]. The asymmetric opening of even "clinically normal" BAV has been demonstrated. The orifice of the open BAV has been shown to be irregular and dome shaped due to the restricted motility of conjoined leaflets. This asymmetric and morphologically stenotic orifice leads to a nonaxial, turbulent transvalvular flow jet, which propagates eccentrically toward the wall of ascending aorta [61]. Restricted systolic conjoint cusp motion may cause flow deflection even if the BAV is normofunctional on echocardiographic evaluation. Systolic flow deflection toward the right, affecting the right anterolateral-ascending wall, has been demonstrated by magnetic resonance imaging (MRI) [62]. Abnormal cusp motions of BAV, including folding or wrinkling of the valve tissue and increased cusp doming during the cardiac cycle, may result in altered flow characteristics even when the cusps are not stenotic [63].

MRI studies have shown that RL BAV phenotype is associated with rightward flow deviation (flow jet directed toward the right anterior aortic wall, which is then propagated in a right-handed helical direction) and dilatation of tubular portion of the ascending aorta. Right anteriorly oriented flow jet may also result in larger aortic root dimensions and asymmetric dilatation of midascending tract [53]. However, RN BAV phenotype has been linked to the leftward deviation (flow jet directed toward left posterior aortic wall) and diffuse dilatation of the ascending aorta extending to the arch [64, 65]. The RN BAV phenotypes have shown more severe hemodynamic flow abnormalities than the RL BAV phenotypes [65].

The increase in regional wall shear stress may explain the RL BAV phenotype with dilatation of the aortic root and asymmetric dilatation of the tubular ascending aorta. Conversely, a RN BAV phenotype may result in a flow toward the posterior aorta, with increased wall shear stress at the right posterior aspect of the aorta leading to dilatation of the aortic arch [39].

4.5. Aortic regurgitation and stenosis

BAV disease is strongly associated with different degrees of stenosis, regurgitation, and mixed presentations. Although most of the neonates and infants remain asymptomatic, dysfunction may present in older ages. Valve interventions may be necessary in a minority, mainly early in life, typically for aortic stenosis (AS) [66]. The progression of stenosis is probably similar to that of TAV stenosis but it becomes manifested at least 5–10 years earlier in patients with BAV [67]. AS and aortic regurgitation (AR) are equally found in TAVs and BAVs with normal aortic dimensions. If the aorta is dilated, AS is predominantly associated with BAV, whereas AR is with TAV [48].

Aortic aneurysms associated with AS have been considered to be poststenotic dilatation because of the chronic impact of the high-flow velocity turbulent transvalvular jet on the aortic wall. Aortic stenosis in BAVs may present a significant additional risk for patients with aneurysm [68]. However, not the severity of AS, but the degree of ascending aorta dilation and the presence of moderate or more AR is associated with higher aortic root and ascending aortic diameter z scores [43]. Moderate–severe AR is generally associated with larger sinus Valsalva diameters compared with normally functioning aortic valve and AS. On the other hand, moderate–severe AS is associated with a larger ascending aortic diameter compared with the normally functioning aortic valve without AR [55]. It is very confusing whether the AR causes aortic root dilatation or if the visa versa is true, so careful follow-up of these patients is important to understand which presents earlier. The root aneurysm and AR with BAV has been linked more often to a genetic/aortopathy cause, which occurs earlier in life, independent of hemodynamic factors [44]. In young adults, it has been shown that RN BAV pattern is more commonly associated with moderate or severe AS and moderate or more AR when compared with other BAV phenotypes. In addition, RN BAV phenotype is associated with progressive valve dysfunction and is strongly predictive of valve intervention when compared with RL BAV phenotype [39, 66]. Similarly, AS has been revealed to be more common in RN BAV phenotype, whereas AR is most commonly encountered in the patients with NL BAV and RL BAV phenotypes [45, 56, 69]. Consequently, despite a variety of study results, it can be concluded that RN or RL BAV phenotypes may show progression and AS or AR may accompany with both valve morphologies.

5. Diagnosis

Most patients with BAV are unaware of the diagnosis until elderly because the symptoms and physical findings are usually absent for many years. Unless echocardiography is requested for other indications, the diagnosis is usually made at the time of an adverse cardiovascular outcome.

The systolic ejection murmur of the aortic stenosis, auscultated on the left side of the sternum, and the diastolic murmur of the aortic regurgitation, heard mainly on the apex, are highly valuable in the diagnosis. In the current area, transthoracic echocardiogram usually confirms the diagnosis of BAV disease. For the confirmation, the valve must be visualized in systole and diastole in the short axis view. The valve openings are fish-mouth shaped. Diastolic images can be misleading because the cusp fusion in the larger leaflet of a bicuspid valve may simulate a tri-leaflet valve in the closed position. It may be more difficult to make the diagnosis if there is an incomplete fusion between the cusps. The valve closure is usually eccentric and the leaflets show doming in the long axis views.

It may be difficult to make the diagnosis in the obese patients due to the nonqualified, blurred vision. In such cases, the diagnosis can be established by means of transoesaphagial echocardiography (TEE) or cardiac MRI or computerized tomography (CT) imaging.

6. Clinical course

The clinical course of BAV patients is highly non-predictable. The factors determining the prognosis are older age, RN or RL BAV phenotype, flow dynamics (right-handed flow), male gender, elevated systolic blood pressure, smoking, presence of valvular and ventricular dysfunctions, aortic dilatation, endocarditis, high total cholesterol levels, valve degeneration score, and genetic predisposition [45, 69]. Aneurysm formation, aortic dissection, severe valvular dysfunction, and endocarditis are the most important causes of morbidity and mortality of BAV disease. AR is the most common complication in younger patients, more common in males, whereas AS is more common in elderly and females [45, 55]. In addition, RN BAV phenotype is strongly predictive of valve intervention when compared with RL BAV phenotype. RN BAV phenotype has a fourfold risk of time-related valve intervention compared with RL BAV phenotype during childhood [39, 66].

Some BAV cases may present with severe stenosis or regurgitation especially in infants or children. Children who present with AS in infancy have more severe disease and poor outcomes. Fortunately, balloon valvuloplasty is the successful treatment of choice for severe AS in this age group because of very little calcification [70].

With respect to the BAV manifestations, it is estimated that only 1 in 50 children would have a clinically significant valve disease by adolescence. The majorities of BAV patients have relatively normal valve function and remain undiagnosed until 40 years of age, when stenosis develops because of leaflet calcification. In total, 53% of the BAV patients with isolated AS undergo valve replacement [65, 70, 71]. In the elderly population, AS is the most common presentation which causes 75% of patients to undergo surgery, while AR was the reason for intervention in only 13–16% of BAV patients [45, 72]. Asymptomatic adults without significant valve dysfunction enjoy excellent long-term survival with a 10- and 20-year survival rate of 97 and 90%, respectively, identical to the expected survival of the population matched for age and sex [73]. Mean follow-up of 15 years showed a 6.7% death ratio, 1.4% of which were related with the aortic valve endocarditis, 0.47% with AS, and 0.47% with AR. In total, 18.3% of these patients underwent aortic valve surgery, most of which were due to severe AS [73]. The 10-year survival rate of the asymptomatic young adults with BAV was found to be 96%.

Aortic valve and ascending aorta surgery were performed in 29% of these patients [46]. On the other hand, patients with BAV-AR and root aneurysm have shown a higher risk of aortic dissection and rupture [74].

Aortic dissection occurs 9 times more often and at an average of 1 decade earlier among patients with BAV than those with TAV [63]. The patients with BAV and aortic aneurysm >4.5 cm have been found eight times more likely to undergo an aortic dissection [75]. The patients with BAV-AR have a tenfold higher risk of post-AVR aortic dissection than the patients with BAV-AS [76]. The aortic dissection rate in BAVs has been found to be 0.77% and the frequency of aortic dissection is 0.1% per patient's year of follow-up [45].

The aortic diameter at the baseline is also an important predictor of aortic dilatation. In children under 18 years old, ascending aorta z score has been shown to progress with time and an initial z score > 2 with the presence of AS has been accepted as a clinical marker for higher z scores in early adulthood [48]. The z scores of 4 or above, present in 13% of the patients under 18 years old, have been considered to reveal significant aortic dilation which predicts the subsequent aneurysm development [75] Relevantly, it has been shown that an aortic diameter of 4 cm or more at the baseline evaluation independently predicts the subsequent development of aneurysm. The incidence of aortic dissection in these patients during 16 years of follow-up was 3.1%, significantly higher than the general population [75]. Dissection rates in the patients with the aortic diameters of above 3.5, 4.5, and 5.5 cm are 8.5, 57.1, and 10%, respectively [77]. The aortic size larger than 4.5 cm or aortic cross-sectional area/height > 8–10 should be considered for concurrent aortic valve and ascending aorta surgery [78, 79].

BAV types can predict the progression of aortic valve dysfunction or the development of aortic aneurysms [80]. The presence of a raphe has been associated with a higher prevalence of significant AS and AR, which increase the need for surgery. Despite the higher mortality in patients with BAV and raphe, raphe is not independently associated with increased all-cause mortality.

7. Treatment strategies

7.1. Medical treatment

Beta-adrenergic blockers, angiotensin converting enzyme inhibitors, and angiotensin receptor blockers are the antihypertensive agents of choice. Beta-adrenergic blockers have the theoretical advantage of reducing aortic wall shear stress, whereas angiotensin receptor blockers have been shown to reduce the rate of aortic growth in patients with Marfan's syndrome [24]. The studies about the various treatment modalities are continuing vigorously.

7.2. Intervention

During childhood, insertion of a prosthetic valve is suboptimal because of the continuing growth of the child. Fortunately, at this stage, the aortic valve is usually not calcified and valvuloplasty can successfully disrupt the commissural fusion and relieve obstruction. Valvuloplasty is the interventional strategy of choice in children and in some young adults with BAV and AS [70].

7.3. Surgical treatment

Patients who have an aortic root or ascending aorta with a diameter of 45–50 mm may be considered for surgery only if they have high-risk features such as a family history of aortic dissection, rupture, or sudden death, and an aortic growth rate of more than 5 mm per year and if there is no need for valvular surgery [81]. Currently, aortic root surgery is not usually performed if the root measurement is <45 mm, or ratio of maximum ascending aorta area to body-height ratio is <10 cm^2/m [82]. Guidelines recommend ascending aortic replacement in patients with BAV if the ascending aortic diameter is ≥50 mm. Concomitant aortic surgery is suggested if the diameter exceeds 45 mm [83]. Nonetheless, some authors have recommended ascending aorta surgery at 40 mm along with concomitant aortic valve regurgitataion (AVR), if the operation risk is low and expected survival is 1 decade or longer. Moreover, many surgeons consider reinforcing or replacing the ascending aorta at the time of valve surgery if there is an increased risk of further root dilation [84–86]. Aortic root dilatation may progress after AVR in the patients with pure AR. BAV patients with AR and root dilatation of 40–50 mm (root phenotype) are associated with significant risk (34%) of post-AVR aortic events. Therefore, simultaneous aortic root surgery is suggested in the patients with BAV-AR and aortic root diameter > 40 mm during their initial AVR procedure [86]. Some of the surgeons recommend aortic repair at the time of BAV surgery if either the aortic diameter exceeds approximately 45 mm or the aortic cross-sectional area/height is above 8–9 cm^2/m or z score is above 7 [82].

8. Conclusion

BAV is a very common, congenital, phenotypically variable, and genetically heterogeneous heart disease. It has a complex developmental process and distinct morphological phenotypes. The clinical course is highly non-predictable. Children with BAV are mostly asymptomatic. However, the cases with severe AS may be encountered early in life and need intervention. Aortic dilatation and valvular dysfunction may begin in infancy and make progress with age. The factors determining the prognosis of BAV disease are older age, RN or RL BAV phenotype, flow dynamics (right-handed flow), male gender, elevated systolic blood pressure, smoking, presence of valvular and ventricular dysfunctions, aortic dilatation, endocarditis, high total cholesterol levels, valve degeneration score, and genetic predisposition. Surgery is recommended for the patients with severe valvular dysfunction (AS, AR), aortic dilatation, or aneurysm.

Author details

Ayşe Inci Yıldırım* and Aysu Türkmen Karaağaç

*Address all correspondence to: ayildirimmd@yahoo.com

University of Healthy Sciences Kartal Koşuyolu Heart and Research Hospital, Istanbul, Turkey

References

[1] Basso C, Boschello M, Perrone C, Mecereno A, Cera A, Bicego D, Thiene D, D Dominics E. An echocardiographic survey of primary school children for bicuspid aortic valve. The American Journal of Cardiology. 2004;**93**:661-663

[2] Fedak PW, Verma S, David TE, Leask RL, Weisel RD, Butany J. Clinical and pathophysiological implications of a bicuspid aortic valve. Circulation. 2002;**106**(8):900-904

[3] Klásková E, Zapletalová J, Kaprálová S, Šnajderová M, Lebl J, Tüdös Z, Pavlíček J, Černá J, Mihál V, Stará V, Procházka M. Increased prevalence of bicuspid aortic valve in turner syndrome links with karyotype:The crucial importance of detailed cardiovascular screening. Journal of Pediatric Endocrinology and Metabolism. 2017;**30**(3):319-325

[4] Prakash SK, Bossé Y, Muehlschlegel JD, Michelena HI, Limongelli G, Della Corte A, Pluchinotta FR, Russo MG, Evangelista A, Benson DW, Body SC, Milewicz DM. A roadmap to investigate the genetic basis of bicuspid aortic valve and its complications: Insights from the international BAVCon (bicuspid aortic valve consortium). The Journal of the American College of Cardiology. 2014;**64**(8):832-839

[5] Huntington K, Hunter AG, Chan KL. A prospective study to assess the frequency of familial clustering of congenital bicuspid aortic valve. The Journal of the American College of Cardiology. 1997;**30**(7):1809-1812

[6] Robledo-Carmona J, Rodríguez-Bailón I, Carrasco-Chinchilla F, Fernández B, Jiménez-Navarro M, Porras-Martin C, Montiel-Trujillo A, García-Pinilla JM, Such-Martínez M, De Teresa-Galván E. Hereditary patterns of bicuspid aortic valve in a hundred families. The International Journal of Cardiology. 2013;**168**(4):3443-3449

[7] Cripe L, Andelfinger G, Martin LJ, Shooner K, Benson DW. Bicuspid aortic valve is heritable. The Journal of the American College of Cardiology. 2004;**44**(1):138-143

[8] Laforest B, Nemer M. GATA5 interacts with GATA4 and GATA6 in outflow tract development. Developmental Biology. 2011;**358**:368-378

[9] Martin LJ, Ramachandran V, Cripe LH, Hinton RB, Aldenfinger G, Tabangin M, Shooner K, Keddache M, Benson DW. Evidence in favor of linkage to human chromosomal regions 18q, 5q and 13q for bicuspid aortic valve and associated cardiovascular malformations. Human Genetics. 2007;**121**:275-284

[10] Goh D, Han L, Judge D. Linkage of familial bicuspid aortic valve with aortic aneurysm to chromosome 15q. The American Journal of Human Genetics. 2002;**71**:211

[11] Choudhury N, Bouchot O, Rouleau L, Tremblay D, Cartier R, Butany J, Mongrain R, Leask RL. Local mechanical and structural properties of healthy and diseased human ascending aorta issue. Cardiovascular Pathology. 2009;**18**(2):83-91

[12] Yassine NM, Shahram JT, Body SC. Pathogenic mechanisms of bicuspid aortic valve aortopathy. Frontiers in Physiology. 2017;**8**:687. DOI: 10.3389/fphys.2017.0068

[13] Foffa I, Ait Alì L, Panesi P, Festa P, Botto N, Necoli C, Andreassi MG. Sequencing of NOTCH1, GATA1, TGFBR1 and TGFBR2 genes in familial cases of bicuspid aortic valve. BMC Medical Genetics. 2013;**14**:44

[14] Qu XK, Qiu XB, Yuan F, Wang J, Zhao CM, Liu XY, Zhang XL, Li RG, Xu YJ, Hou XM, Fang WY, Liu W, Yang YQ. A novel NKX2.5 loss-of-function mutation associated with congenital bicuspid aortic valve. The American Journal of Cardiology. 2014;**114**:1891-1895

[15] Girdauskas E, Schulz S, Borger MA, Mierzwa M, Kuntze T. Transforming growth factor-beta receptor type II mutation in a patient with bicuspid aortic valve disease and intraoperative aortic dissection. The Annals of Thoracic Surgery. 2011;**91**:70-71

[16] Koenig SN, LaHaye S, Feller JD, Rowland P, Hor KN, Trask AJ, Janssen PM, Radtke F, Lilly B, Garg V. 2017 Notch1 haploinsufficiency causes ascending aortic aneurysms in mice. JCI Insight. 2017;**2**(21)

[17] Pepe G, Nistri S, Giusti B, Sticchi E, Atlanasio M, Porciani C, et al. Identification of fibrillin 1 gene mutations in patients with bicuspid aortic valve (BAV) without Marfan syndrome. BMC Medical Genetics. 2014:15-23

[18] Milewicz DM, Guo DC, Tran-FaduluV LAL, Papke CL, Inamoto S, et al. Genetic basis of thoracic aortic aneurysms and dissections, focus on smooth muscle cell contractile dysfunction. The Annual Review of Genomics and Human Genetics. 2008;**9**:283-302

[19] Jiang X, Rowitch DH, Soriano P, McMahon AP, Sucov HM. Fate of the mammalian cardiac neural crest. Development. 2000;**127**:1607-1616

[20] Waldo KL, Kumiski DH, Wallis KT, Stadt HA, Hutson MR, Platt DH, et al. Conotruncal myocardium arises from a secondary heart field. Development. 2001;**128**(16):3179-3188

[21] Snarr BS, Kern CB, Wessels A. Origin and fate of cardiac mesenchyme. Developmental Dynamics. 2008;**237**:2804-2819

[22] Plein A, Fantin A, Ruhrberg C. Neural crest cells in cardiovascular development. Current Topics in Developmental Biology. 2015;**111**:183-200

[23] Jiao J, Xiong W, Wang L, Yang J, Qiu P, Hirai H, et al. Differentiation defect in neural crest-derived smooth muscle cells in patients with aortopathy associated with bicuspid aortic valves. eBioMedicine. 2016;**10**:282-290

[24] Groenink M, den Hartog AW, Franken R, Radonic T, de Waard V, Timmermans J, et al. Losartan reduces aortic dilatation rate in adults with Marfan syndrome: A randomized controlled trial. European Heart Journal. 2013;**34**:3491-3500

[25] Humphrey D, Schwartz MA, Tellides G, Milewicz DM. Role of mechanotransduction in vascular biology focus on thoracic aortic aneurysms and dissections. Circulation Research. 2015;**116**(8):1448-1461

[26] Wagenseil JE, Mecham RP. Vascular extracellular matrix and arterial mechanics. Physiological Reviews. 2009;**89**:957-989

[27] Thompson RW, Geraghty PJ, Lee JK. Abdominal aortic aneurysms: Basic mechanisms and clinical implications. Current Problems in Surgery. 2002;**39**:110-230

[28] Sievers HH, Schmidtke C. A classification system for the bicuspid aortiv avlve, from 304 surgical specimen. The Journal of Thoracic and Cardiovascular Surgery. 2007;**133**(5):1226-1233

[29] Schaefer BM, Lewin MB, Stout KK, Gill E, Prueitt A, Byers PH, et al. The bicuspid aortic valve: An integrated phenotypic classification of leaflet morphology and aortic root shape. Heart. 2008;**94**:1634-1638

[30] Grewal N, Gittenberger-de Groot AC, Poelmann RE, Klautz RJ, Lindeman JH, Goumans MJ, Palmen M, Mohamed SA, Sievers HH, Bogers AJ. Ascending aorta dilation in association with bicuspid aortic valve: A maturation defect of the aortic wall. The Journal of Thoracic and Cardiovascular Surgery. 2014;**148**(4):1583-1590

[31] Grewal N, Gittenberger-de Groot AC, Marco C, DeRuiter MC, Klautz RJ, Poelmann MRE, et al. Bicuspid aortic valve: Phosphorylation of c-kit and downstream targets are prognostic for future aortopathy. European Journal of Cardio-Thoracic Surgery. 2014;**45**:831-839

[32] Nataatmadja M, West M, West J, Summers K, Walker P, Nagata M. Abnormal extracellular matrix protein transport associated with increased apoptosis of vascular smooth muscle cells in Marfan syndrome and bicuspid aortic valve thoracic aortic aneurysm. Circulation. 2003;**108**:II329-II334

[33] Della Corte A, Quarto C, Bancone C, Castaldo C, Di Meglio F, Nurzynska D, De Santo LS, De Feo M, Scardone M, Montagnani S, Cotrufo M. Spatiotemporal patterns of smooth muscle cell changes in ascending aortic dilatation with bicuspid and tricuspid aortic valve stenosis: Focus on cell-matrix signaling. Journal of Thoracic and Cardiovascular Surgery. 2008;**135**:8-18

[34] Fedak PW, de Sa MP, Verma S, Nili N, Kazemian P, Butany J, Strauss BH, Weisel RD, David TE. Vascular matrix remodeling in patients with bicuspid aortic valve malformations: Implications for aortic dilatation. Journal of Thoracic and Cardiovascular Surgery. 2003;**126**(3):797-806

[35] Paes Leme M. Molecular evaluation of the great vessels of patients with bicuspid aortic valve disease. Revista Brasileira de Cirurgia Cardiovascular. 2003;**18**:148-156

[36] Ikonomidis JS, Jones JA, Barbour JR, Stroud RE, Clark LL, Kaplan BS, et al. Expression of matrix metalloproteinases and endogenous inhibitors within ascending aortic aneurysms of patients with bicuspid or tricuspid aortic valves. Journal of Thoracic and Cardiovascular Surgery. 2007;**133**:1028-1036

[37] Broberg CS, Therrien J. Understanding and treating aortopathy in bicuspid aortic valve. Trends in Cardiovascular Medicine. 2015;**25**:445-451

[38] Pees C, Behnke IM. Morphology of the bicuspid aortic valve and elasticity of the adjacent aorta in children. The American Journal of Cardiology. 2012;**110**:1354-1360

[39] Fernandes SM, Sanders SP, Khairy P, Jenkins KJ, Gauvreau K, Lang P, Simonds H, Colan SD, et al. Morphology of bicuspid aortic valve in children and adolescents. The Journal of the American College of Cardiology. 2004;**44**:1648-1651

[40] Verma S, Siu SC. Aortic dilatation in patients with bicuspid aortic valve. The New England Journal of Medicine. 2014;**370**(20):1920-1929

[41] Girdauskas E, Borger MA, Secknus MA, Girdauskas G, Kuntze T. Is aortopathy in bicuspid aortic valve disease a congenital defect or a result of abnormal hemodynamics? A critical reappraisal of a one sided argument. The European Journal of Cardio-Thoracic Surgery. 2011;**39**:809-814

[42] Fazel SS, Mallidi HR, Lee RS, Sheehan MP, Liang D, Fleischman D, Herfkens R, Mitchell RS, Miller DC. The aortopathy of bicuspid aortic valve disease has distinctive patterns and usually involves the transverse aortic arch. Journal of Thoracic and Cardiovascular Surgery. 2008;**135**(4):901-907

[43] Fernandes S, Khairy P, Graham DA, Colan SD, Galvin TC, Sanders SP, et al. Heart. 2012;**98**:1014-1019

[44] Della Corte A, Bancone C, Quarto C, Dialetto G, Covino F, E Scardone M, et al. Predictors of ascending aortic dilatation with bicuspid aortic valve, a wide spectrum of disease expression. European Journal of Cardio-Thoracic Surgery. 2007;**31**:397-404

[45] Tzemos N, Therrien J, Yip J, Thanassoulis G, Tremblay S, Jamorski MT, et al. Outcomes in adults with bicuspid aortic valves. JAMA. 2008;**300**(11):1317-1325

[46] Beroukhim RS, Kruzick TL, Taylor AL, Gao D, Yetman AT. Progression of aortic dilation in children with a functionally normal bicuspid aortic valve. The American Journal of Cardiology. 2006;**98**:828-830

[47] Merkx R. Aortic diameter growth in children with a bicuspid aortic valve. American Journal of Cardiology. 2017;**120**:131-136

[48] Jackson V, Petrini J, Caidahl K, Eriksson MJ, Liska J, Eriksson P, Franco-Cereceda A. Bicuspid aortic valve leaflet morphology in relation to aortic root morphology: A study of 300 patients undergoing open-heart surgery. The European Journal of Cardio-Thoracic Surgery. 2011;**40**:118-124

[49] Masri A, Kalahasti V, Alkharabsheh S, Svensson LG, Sabik JF, Roselli EE, et al. Characteristics and long-term outcomes of contemporary patients with bicuspid aortic valves. Journal of Thoracic and Cardiovascular Surgery. 2016;**151**:1650-1651

[50] Gurvitz M, Chang RK, Drant S, Allada V. Frequency of aortic root dilation in children with a bicuspid aortic valve. American Journal of Cardiology. 2004;**94**(10):1337-1340

[51] Holmes KW, Lehmann CU, Dalal D, Nasir K, Dietz HC, Ravekes WJ, Thompson WR, Spevak PJ, et al. Progressive dilation of the ascending aorta in children with isolated bicuspid aortic valve. American Journal of Cardiology. 2007;**99**:978-983

[52] Khoo C, Cheung C, Jue J. Patterns of aortic dilatation in bicuspid aortic valve-associated aortopathy. Journal of the American Society of Echocardiography. 2013;**26**:600-605

[53] Russo CF, Cannata A, Lanfranconi M, Vitali E, Garatti A, Bonacina E. Is aortic wall degeneration related to bicuspid aortic valve anatomy in patients with valvular disease? The Journal of Thoracic and Cardiovas Surgery. 2008;**136**:937-942

[54] Mahadevia R, Barker AJ, Schnell S, Entezari P, Kansal P, Fedak PW, et al. Bicuspid aortic cusp fusion morphology alters aortic three-dimensional outflow patterns, wall shear stress, and expression of aortopathy. Circulation. 2014;**129**:673-682

[55] Roman MJ, Pugh NL, Devereux RB, Eagle KA, Holmes K, LeMaire SA, et al. GenTAC investigators aortic dilatation associated with bicuspid aortic valve: Relation to sex, hemodynamics, and valve morphology (the National Heart Lung and Blood Institute-Sponsored National Registry of Genetically Triggered Thoracic Aortic Aneurysms and Cardiovascular Conditions). American Journal of Cardiology. 2017;**120**(7):1171-1175

[56] Huang FQ, Le Tan J. Pattern of aortic dilatation in different bicuspid aortic valve phenotypes and its association with aortic valvular dysfunction and elasticity. Heart Lung Circulation. 2014;**23**(1):32-38

[57] Thanassoulis G, Yip JW, Filion K, Jamorski M, Webb G, Siu SC, et al. Retrospective study to identify predictors of the presence and rapid progression of aortic dilatation in patients with bicuspid aortic valves. Nature Reviews Cardiology. 2008;**5**(12):821-828

[58] Fernandez B, Duran AC, Fernandez-Gallego T, Fernandez MC, Such M, Arque JM, et al. Bicuspid aortic valves with different spatial orientations of the leaflets are distinct etiological entities. The Journal of the American College of Cardiology. 2009;**54**:2312-2318

[59] Phillips HM, Mahendran P, Singh E, Anderson RH, Chaudhry B, Henderson DJ. Neural crest cells are required for correct positioning of the developing outflow cushions and pattern the arterial valve leaflets. Cardiovascular Research. 2013;**99**:452-460

[60] Braverman AC. The bicuspid aortic valve and associated aortic disease; in valvular heart disease. In: Otto CM, Bonow RO, editors. A companion to Braunwald's Heart Disease, 4th ed. Philadelphia: Saunders/Elsevier; 2013. pp. 179-198

[61] Robicsek F, Thubrikar JM, Cook JW, Fowler B. The congenitally bicuspid aortic valve: How does it function? Why does it fail? Annals of Thoracic Surgery. 2004;**77**:177

[62] Della Corte A, Bancone C, Conti CA, Votta E, Redaelli A, Del Viscovo L, Cotrufo M. Restricted cusp motion in right-left type of bicuspid aortic valves: A new risk marker for aortopathy. The Journal of Thoracic and Cardiovascular Surgery. 2012;**144**(2):360-369

[63] Braverman AC. Aortic involvement in patients with a bicuspid aortic valve. Heart. 2011;**97**:506-513

[64] Burris NS, Hope MD. Bicuspid valve-related aortic disease: Flow assessment with conventional phase contrast MRI. Academic Radiology. 2015;**22**(6):690-696

[65] Bissell MM, Hess AT, Biasiolli L, Glaze SJ, Loudon M, Pitcher A, Davis A. Aortic dilation in bicuspid aortic valve disease flow pattern is a major contributor and differs with valve fusion type. Circulation. Cardiovascular Imaging. 2013;**6**:499-507

[66] Fernandes SM, Khairy P, Sanders SP, Colan SD. Bicuspid aortic valve morphology and interventions in the young. The Journal of the American College of Cardiology. 2007;**49**:2211-2214

[67] Roberts WC, Ko JM, Jm K. Frequency by decades of unicuspid, bicuspid, and tricuspid aortic valves in adults having isolated aortic valve replacement for aortic stenosis, with or without associated aortic regurgitation. Circulation. 2005;**111**:920-925

[68] Davies RR, Kaple RK, Mandapati D, Gallo A, Botta DM, Elefteriades JA, et al. Natural history of ascending aortic aneurysms in the setting of an unreplaced bicuspid aortic valve. The Annals of Thoracic Surgery. 2007;**83**(4):1338-1344

[69] Koenraadt WCM, Grewal N, Gaidoukevitch OY, DeRuiter MC, Gittenberger-de Groot AC, Bartelings MM. The extent of the raphe in bicuspid aortic valves is associated with aortic regurgitation and aortic root dilatation. Netherlands Heart Journal. 2016;**24**(2):127-133

[70] Siu SC, Silversides CK. Bicuspid aortic valve disease. The Journal of the American College of Cardiology. 2010;**55**:2789-2800

[71] Lewin MB. OttoCM. The bicuspid aortic valve adverse outcomes from infancy to old age circulation. 2005;**111**(7):832-834

[72] Collins MJ, Butany J, Borger MA, Strauss BH, David TE. Implications of a congenitally abnormal valve: A study of 1025 consecutively excised aortic valves. Journal of Clinical Pathology. 2008;**61**:530-536

[73] Michelena HI, Desjardins VA, Avierinos JF, Russo A, Nkomo VT, Sundt TM, et al. Natural history of asymptomatic patients with normally functioning or minimally dysfunctional bicuspid aortic valve in the community. Circulation. 2008;**117**:2776-2784

[74] Girdauskas E, Disha K, Raisin HH, Secknus MA, Borger MA, Kuntze T. Risk of late aortic events after an isolated aortic valve replacement for bicuspid aortic valve stenosis with concomitant ascending aortic dilation. The European Journal of Cardio-Thoracic Surgery. 2012;**42**:832-837

[75] Michelena HI, Khanna AD, Mahoney D, Margaryan E, Toplisky Y, Suri RM, et al. Incidence of aortic complications in patients with bicuspid aortic valves. JAMA. 2011;**306**:1104-1112

[76] Girdauskas E, Rouman M, Disha K, Espinoza A, Misfeld M, Borger MA, et al. Aortic dissection after previous aortic valve replacement for bicuspid aortic valve disease. The Journal of the American College of Cardiology. 2015;**66**:1409-1411

[77] Davies RR, Gallo A, Coady MA, Tellides G, Botta DM, Burke B, et al. Novel measurement of relative aortic size predicts rupture of thoracic aortic aneurysms. The Annals of Thoracic Surgery. 2006;**81**:169-177

[78] Svensson LG, Kim KH, Blackstone EH, Rajeswaran J, Gillinov AM, Mihaljevic T, et al. Bicuspid aortic valve surgery with proactive ascending aorta repair. Journal of Thoracic and Cardiovascular Surgery. 2011;**142, 622-629**:e1-e3

[79] Abdulkareem N, Soppa G, Jones S, Valencia O, Smelt J, Jahangiri M. Dilatation of the remaining aorta after aortic valve or aortic root replacement in patients with bicuspid aortic valve: A 5-year follow-up. The Annals of Thoracic Surgery. 2013;**96**:43-49

[80] Kong WK, Delgado V, Poh KK, Regeer MV, Ng AC, McComack L, et al. Prognostic implications of raphe in bicuspid aortic valve anatomy. JAMA Cardiology. 2017;**2**:285-292

[81] Hiratzka LF, Bakris GL, Beckman JA, Bersin RM, Carr VF, Casey DE, et al. ACCF/ AHA/AATS/ACR/ASA/ SCA/SCAI/SIR/STS/SVM guidelines for the diagnosis and management of patients with thoracic aortic disease: A report of the American College of Cardiology Foundation/American Heart Association task force on practice guidelines, American Association for Thoracic Surgery, American College of Radiology, American Stroke Association, Society of Cardiovascular Anesthesiologists, Society for Cardiovascular Angiography and Interventions, Society of Interventional Radiology, Society of Thoracic Surgeons, and Society for Vascular Medicine. Circulation. 2010, 2010;**121**(13):e266-e369

[82] Svensson LG, Adams DH, Bonow RO, Kouchoukos NT, Miller DC, O'Gara PT, et al. Aortic valve and ascending aorta guidelines for man- agement and quality measures: Execu tive summary. The Annals of Thoracic Surgery. 2013;**95**:1491-1505

[83] Vahanian A, Alfieri O, Andreotti F, Antunes MJ, Baron-Esquivias G, Baumgartner H, et al. Guidelines on the management of valvular heart disease (version 2012). The European Journal of Cardio-Thoracic Surgery. 2012;**42**:S1-S44

[84] Wald O, Korach A, Shapira OM. Should aortas in patients with bicuspid aortic valve really be resected at an earlier stage than tricuspid? PRO. Clinical Cardiology. 2010;**28**:289-298

[85] Russo CF, Mazzetti S, Garatti A, Ribera E, Milazzo A, Bruschi G, et al. Aortic complications after bicuspid aortic valve replacement: Long-term results. The Annals of Thoracic Surgery. 2002;**74**:S1773-S1776. discussion S1792-9

[86] Girdauskas E, Disha K, Rouman M, Espinoza A, Borger MA, Kuntze T. Aortic events after isolated aortic valve replacement for bicuspid aortic valve root phenotype, echocardiographic follow-up study. The European Journal of Cardio-Thoracic Surgery. 2015;**48**:e71-e76

Contemporary Surgical Options for the Aortic Root

Ziv Beckerman and Edward P. Chen

Additional information is available at the end of the chapter

Abstract

Aortic root pathology is diverse, and it is the most common cause of aortic valve incompetence in the United States. Aortic root surgery is undergoing continuous development and refinements. From the original description of Bentall on aortic root replacement, many advances have been made in the field of aortic root surgery. The surgical armamentarium available today provides advanced repair options as well as replacement options for the aortic root. The aim of this chapter is to provide an insight into the basics of aortic root surgery as well as to further describes the current up-to-date solutions for aortic valve and aortic root pathologies.

Keywords: aortic root replacement, aortic valve repair, aortic root, aortic operation

1. Introduction

Aortic root pathology is diverse, and it is the most common cause of aortic valve incompetence in the developed countries. The aortic root serves three main purposes: (1) being the outflow tract of the left ventricle, (2) a conduit for coronary perfusion, and (3) path for blood flow to the end-organs.

Current conventional treatment for significant aortic incompetence (AI) caused by a dilated, aneurysmal aortic root is replacement of the ascending aorta using a synthetic graft, replacement of the aortic valve with a prosthesis (the graft and prosthesis are usually combined as a "composite graft"), and reimplantation of the coronary arteries, i.e., the Bentall procedure. The options for both root and valve replacement vary, and each option entails its pros and cons.

This chapter will discuss the different contemporary surgical options for replacement and repair of the aortic root.

2. Historical perspective

The first successful replacement of a fusiform ascending aortic aneurysm was reported by Cooley and De Bakey in 1956 [1]. That first report was made possible thanks to the introduction of cardiopulmonary bypass to aortic aneurysm surgery. Following, several surgeons forged ahead and described similar experiences with similar pathologic entities.

Handling of the aortic root, below the sinotubular junction was first reported in 1964, when Wheat reported his team's efforts to replace the entire ascending aorta [2]. Although the procedure performed may not have involved the entire aorta as the title claimed, its legacy was secured as a description of how to handle pathology extending proximal to the coronary ostia. Their approach to the displaced coronary ostia was to resect the aorta 1.5–2 cm proximal to this level, while leaving a tongue of tissue surrounding the two coronary takeoffs. In this way, they maintained the integrity of the ostia and ensured the sutures were far enough from the coronary arteries.

While others continued to work tirelessly, the group at Oregon, including Drs. Herr and Starr, were diligently at work devising mechanical valves that would eventually be used for Bentall's historic procedure [3, 4]. In 1968, they published their ongoing clinical experience and engineering progress. Their ingenuity to use a composite valve-graft prosthesis was a major step in the progression of aortic root surgery, and the composite valve-graft, whether using a mechanical (as originally done) or tissue valve, is still considered the gold standard today [5].

Following, new concepts evolved for sparing the aortic valve and replacing the aortic root only. The first was developed by Sir Yacoub, and had been used in his practice since 1979 [6, 7]. The procedure, which he designed, later became referred to as the "remodeling technique." The functional focus was to preserve the native valve, while recreating the aortic sinuses. This goal was achieved by fashioning a scalloped Dacron® graft such that three tongues extended to replace the intrinsic sinuses. Interposed between these three extensions, native tissue was left intact at the attachment of the cusps. Once the graft was attached, the coronary arteries would be mobilized and anastomosed to the neoaorta.

In the late 1980s, David and his colleagues at the University of Toronto developed an alternative class of valve-sparing procedures [8]. Their procedure went through numerous iterations and variations, but classically the technique became referred to as the "reimplantation technique." [9, 10] This approach had the benefit of stabilizing the aortic annulus by sewing the native valve directly into a Dacron® graft of a fixed circumference.

3. Surgery of the aortic root

There are several indications to repair the aortic root and the ascending aorta. The most frequent one is the aneurysmal dilation of the aortic root ± ascending aorta that is associated with aortic valve dysfunction (in general regurgitation). In this case, the aortic valve leaflets may be fundamentally normal. This may lead to insufficient coaptation of the leaflets and

therefore cause valve-regurgitation. In other patients, the aortic valve leaflets may be abnormal because of bicuspid morphology and the disease is associated with an enlarged ascending aorta. When the primary indication to operate on the patient is the aortic valve disease or myocardial revascularization, the ascending aorta is usually replaced very liberally (this means if the diameter is larger than 4.5 cm). Another situation that calls for the repair of the aortic root and ascending aorta is the patient that presents with severe aortic valve stenosis (either bicuspid or tricuspid aortic valve) and with post-stenotic dilation of the ascending aorta. In this category of patients, if the sinotubular junction is maintained and the aortic root diameter at the level of sinuses of Valsalva does not exceed 4 cm, it is generally accepted that a separate aortic valve replacement and supracoronary replacement of the ascending aorta with a prosthetic graft can be performed.

During the last decade, the authors have been increasingly aggressive in the replacement of the complete ascending aorta and base of the aortic arch using a short period of antegrade cerebral perfusion, performing the distal anastomosis without aortic cross clamp.

Contemporary surgical options for the aortic root include either a full aortic root replacement (biological or mechanical), or valve sparing aortic root replacement. Different graft options and/or valve options exist and are further discussed below.

3.1. Graft and valve options for aortic root surgery

The aortic root can be replaced with either a synthetic material (usually Dacron) or a biologic prosthesis. Biologic options come in the form of xenografts or homografts. Synthetic graft options includes expanded poly (ethylene terephthalate) (Dacron) or poly(tetrafluoroethylene) (ePTFE), and represent the most widely employed vascular substitutes in cardiovascular surgery. Dacron grafts can come in a straight tubular shape or in a specifically designed form that, on implantation and pressurization, generates pseudosinuses of Valsalva.

3.1.1. Xenografts

Xenografts can come in the form of stented or stentless valve. Some of the stentless valves present as a full root products and can either be implanted as a full root replacement and/or as a valve replacement alone. The stented valves may be used for valve replacement alone, or may be composed to any graft type in order to be served for full root replacement.

Some options for stentless valves include the following:

3.1.1.1. Freestyle™ porcine aortic root bioprosthesis (medtronic)

This third-generation device presents as the complete porcine aortic root with thin polyester covering of the septal myocardium. The tissue is glutaraldehyde fixed using the physiologic root pressure technique: there is zero net pressure applied to the valve cusps to preserve collagen crimp while the aorta is distended to normal configuration. The graft may be implanted as a valve replacement in the subcoronary position, as an inclusion root cylinder, or as a full aortic root replacement.

3.1.1.2. Toronto SPV glutaraldehyde-preserved porcine xenograft (St. Jude Medical)

The aortic tissue is removed from all three sinuses, and the graft is covered with a thin coat of polyester. It can only be implanted as a subcoronary valve replacement. It has no antimineralization treatment. Hemodynamic performance has been excellent and equivalent to the Medtronic Freestyle device.

3.1.1.3. Edwards Prima (Edwards Lifesciences)

The Prima device is a low-pressure glutaraldehyde-fixed porcine aortic root similar to the Freestyle device. It has a thin cloth reinforcement over the muscle bar. The porcine coronaries were excised in the earlier version but preserved in the later version without ligation. The **Prima Plus** is a low-pressure fixed valve with proprietary XenoLogiX treatment for calcium mitigation.

3.1.1.4. CryoLife-O'Brien (CryoLife International)

Stentless porcine aortic valve is a manufactured composite of the noncoronary sinus and cusp from three porcine aortic roots. It is designed to be implanted below the coronary arteries in a supra-annular position in the sinuses of Valsalva by a single suture line.

The tissue is fixed in glutaraldehyde but there is no specific antimineralization treatment of this valve. Experience is limited to a few centers, and the technical aspects of implantation may be more difficult than with other stentless bioprostheses.

3.1.1.5. Pericarbon Freedom (Sorin Group).

The Pericarbon Freedom stentless valve is composed of two sheets of bovine pericardium sewn together to produce a cylindrical shape and fixed with glutaraldehyde.

3.1.1.6. Biocor stentless (Biocor Industria e Pesquisas LTDA)

Biocor stentless (Biocor Industria e Pesquisas LTDA) is a porcine aortic valve treated with the No-React (Shelhigh Inc., Union, NJ) process.

3.1.2. Allografts

3.1.2.1. Cryopreserved aortic allograft

Human donor aortic valve allografts are presented as the complete aortic root, ascending aorta, and some or all of the aortic arch. The anterior leaflet of the mitral valve typically remains attached.

3.1.2.2. Pulmonary autograft

Pulmonary autograft, the patient's own pulmonary trunk, including the pulmonary valve, may be used to replace the aortic valve, usually as a full aortic root replacement. The pulmonary

trunk is then replaced with a cryopreserved pulmonary allograft as described earlier. This operation (Ross procedure) is hemodynamically superior to other procedures for replacing the aortic valve, because the patient's own pulmonary valve is properly sized to accept cardiac output with little or no pressure gradient.

3.1.3. Straight tubular grafts

Straight tubular Dacron grafts of different manufacturers can be used for a full aortic root replacement when combined with either a stented or a stentless biological valve, and/or a mechanical valve. The advantages/disadvantages of straight tubular grafts versus grafts incorporating pseudosinuses of Valsalva are discussed in the following paragraph.

3.1.4. Grafts incorporating pseudosinuses of Valsalva

The native aortic root is not a stiff tube but rather a highly dynamic structure that accommodates to changes in the pressure-volume relationship in a very subtle way. During the early 1990s, Robicsek described the dynamic function of the aortic root and especially the sinuses of Valsalva [11]. The sinuses of Valsalva reduce the shear stress on the cusps of the aortic valve and promote optimal coronary blood flow during diastole [11, 12]. Another important aspect is of the facilitation of vortex formation that seems to help in smooth valve closure with less bending deformation in the longitudinal direction, and reduce the stress on the coronary anastomosis [12–15]. All the above factors can affect the durability and performance and longevity of the aortic bio-prosthetic valves.

Many attempts had been made by both surgeons and commercial companies to create a graft that resembles in shape and function of the native aortic root. The Valsalva graft is a Dacron graft with a specific design that, on implantation and pressurization, it generates three independent pseudosinuses. It is commonly used either in aortic-valve sparing procedures or in aortic root replacements when it is combined with a stented or stentless biological valve.

3.1.5. Composite grafts

Combination of either a tubular or a pseudosinuses-graft, with a biological (stented or non-stented) or mechanical valve, will create a composite graft.

Various such combinations are clinically common. The clinical differences stem mainly from the type of valve used, and in cases a pseudosinuses-graft is used, its potential benefits can be added to that of the valve it is combined with.

3.2. Composite versus valve sparing root replacement

The question of whether to replace the aortic root with a composite graft or to perform a valve-sparing operation is dependent on multiple patient characteristics as well as the surgeon preference. Over the last decade surgeons have debated which technique provides the best peri-operative and long-term results. The etiology of the aortic root disease, as well as individual patient preferences, must be taken into account so the correct procedure is performed for each patient.

Patients with connective tissue disorders, bicuspid valves, or history of valve infection may be best served with Bentall-type replacement rather than valve-sparing reconstruction. Despite the surgical complexity, long-term experience with VSRR among bicuspid and/or patients with connective tissue disorders are associated with excellent outcomes [16].

The current literature still lacks a definite answer to that question. Different authors publish very promising short, intermediate and long-term outcomes with both types of surgery. One recent large series published by Girardi et al. describes the outcomes of 890 patients (289 mechanical composites, 421 biological composites, and 180 VSRR). Operative mortality was 0.2% (0% in the VSRR group); the incidence of major postoperative complications was less than 0.5%. Predictors of adverse in-hospital outcome were age, nonelective operation, renal status, reoperation, New York Heart Association class, ejection fraction, and concomitant procedures. Five-year survival was 89.4%. In the propensity-matched groups, the type of operation performed did not affect in-hospital and late outcome. Aortic reintervention rates at 5 years were 0% for the mechanical composite valved graft group, 2.4% for the biologic composite valved graft group, and 7.3% for the valve-sparing reconstruction series. The authors concluded that in the current era, aortic root replacement can be performed with low perioperative risk in high-volume aortic centers. The type of operation performed does not affect early or late survival. Although the mechanical composite valved graft remains the gold standard for durability, the biologic composite valved graft and valve-sparing reconstruction are excellent options for those who cannot take or want to avoid long-term anticoagulation.

Another recent paper by David et al. was looking into the outcomes of a young (<70 years) patients group (total of 616 patients); and used propensity matching to compare valve-sparing root replacement to mechanical composite root replacement. The mean age at the work was 46 ± 14 years, mean follow up was 9.8 ± 5.3 years. Their outcomes showed reduced cardiac mortality among the valve-sparing group, the authors concluded that valve-sparing surgery should be the operation of choice for young patients with aortic root aneurysm and normal or near-normal aortic cusps [17].

4. Surgical technique

4.1. Aortic root replacement

4.1.1. Aortic root replacement with a composite graft

This operation is frequently referred to as the Bentall procedure, regardless of whether the composite is a mechanical or biological. Construction of the composite graft can be done either before opening the chest, or during the surgery itself, depending on the surgeon's preference. Constructing a biological composite with a graft and a stentless valve (i.e., Valsalva graft and Freestyle valve), might require more time then when using a stented valve and a tubular Dacron graft, and in these cases it is preferable to construct the composite before opening the chest.

CPB is established at 34°C using a single two-stage venous cannula and left atrial vent. The aorta is occluded just proximal to the brachiocephalic artery. Cardioplegia is given. The ascending aorta is opened transversely in its midportion. The patient's aortic root is dissected from the surrounding tissues. Traction stitches are placed above each aortic valve commissure to expose the aortic root. The aortic valve is excised. The coronary arteries are mobilized, retaining a generous button of sinus aorta. A limited dissection of the coronary artery is sufficient to ensure that excision of the coronary artery is complete and that the coronary button will move easily up to the composite prosthesis without kinking or creating undue tension on the artery. The remaining sinus aorta is removed. Diameter of the annulus is calibrated, and an appropriately sized composite prosthesis is chosen. Stitches are placed through the annulus of the aortic valve and brought up through the sewing ring of the prosthesis preferably using single interrupted braided sutures. It is the authors' preference to implant the valve in the vascular graft 2–3 mm above the lower end of the graft, and to place the root stitches through the graft itself and not through the valve ring itself. Doing so, provides the future option of explanting the valve itself if need be for replacement without disrupting the entire root. The composite valve is brought down, and sutures are tied down. Next, a direct anastomosis of the coronary ostia to the graft is made.

The distal end of the graft is then shortened to approximate the distal end of the aorta. The anastomosis is constructed using continuous stitches of 4–0 or 5–0 polypropylene, depending on the thickness and strength of the aorta.

It is the author's preference to use a composite graft constructed from a 27 to 29 mm Freestyle MS valve (Medtronic) sutured into a 28–30 mm Gelweave Valsalva prosthesis (Sulzer Vascutek, Renfrewshire, Scotland) as the choice when implanting a biological tissue valve. This composite requires 30–40 min preparation time, but provides the patient with the potential benefits of: (1) avoiding the need for anticoagulation, (2) excellent hemodynamic performance of stentless valves, (3) incorporation of sinuses of Valsalva into the neoaortic root can improve the function and longevity of stentless valves.

4.1.2. Aortic root replacement with an allograft

This is typically performed in the setting of an aortic root infection. An aortic allograft may be used to replace the patient's aortic root completely. The initial steps of the surgery are similar to those mentioned in Section 4.1.2. Typically, the allograft is used intact and in natural anatomic orientation, with only the excess of septal myocardium and the anterior leaflet of the mitral valve removed. Size match is not nearly as important as it is for freehand subcoronary valve replacement, but if the aortic annulus is more than 3 mm larger in diameter than the largest available aortic allograft, the patient's aortic root should be narrowed to approximate the size of the allograft. This can be done conveniently by placing a pledgeted mattress stitch through the aortic annulus alongside the commissures so that when tied, the intercusp triangle below the commissure is obliterated. The allograft is attached to the LVOT at the aortic annulus and below the commissures by simple interrupted stitches of 3–0 or 4–0 polypropylene.

The allograft is slipped over the sutures into the desired position in the LVOT. The sutures are then tied down. Incorporating a felt strip within the suture loops or using pledged sutures has been advocated by some authors, however, it was not found to be necessary in our experience.

The remainder of the operation proceeds as described for aortic root replacement with a composite graft.

4.1.3. Aortic root replacement with an autograft

The aortic valve may be replaced with the patient's own pulmonary valve (pulmonary autograft) and a pulmonary/aortic allograft used to replace the pulmonary valve. This operation was devised by Ross and carries his name. The detailed surgical technique is described elsewhere. The operation has the advantage of placing autogenous tissue in the high pressure aortic position that theoretically should last indefinitely. The allograft tissue is placed in the low-pressure pulmonary position, where even if it should fail, valve regurgitation is tolerated for a long time.

One main surgical pitfall of this technique entails potential coronary injury, separating the pulmonary trunk from the RVOT above the infundibular septum.

4.2. Valve sparing aortic root replacement

The exact surgical details of the remodeling and reimplantation procedures are beyond the scope of this chapter, but the main differences are discussed below.

The remodeling operation consists of removing the sinus aorta except for a small rim of aortic tissue around the coronary ostia and a rim of about 5 mm of aortic wall above the aortic valve annulus. Commissures are positioned to achieve good coaptation of the aortic valve cusps. An appropriately trimmed Dacron graft is sutured to the aortic root along the valve circumference (**Figure 1**). It is recommended that when aortic root remodeling procedures, such as the Yacoub operation, are performed in patients with Marfan syndrome, or when the aortic annulus is dilated, an aortic annuloplasty should be performed.

Reimplantation Procedure, in this procedure, the aortic valve is reimplanted within a polyester tubular graft. The graft is secured to a level plane in the LVOT just below the valve, except in the one sixth of the circumference occupied by the conduction system. This fixes the diameter of the LVOT, but one may reduce the diameter if necessary. The aortic valve is attached (reimplanted) to the inside of the prosthetic graft. The graft determines the diameter of the sinotubular junction.

The reimplantation procedure has undergone a number of modifications by both David and other surgeons. However, the basic concept has been retained (**Figure 1**).

The graft is usually 30–32 mm in diameter, although 28- or 34-mm grafts are occasionally used.

A classification schema beyond simply calling a procedure reimplantation versus remodeling can be seen in **Table 1**. David's classic reimplantation procedure using a cylindrical tube graft is described as David-I, while Yacoub's classic remodeling procedure is described as a David-II. In this system, David-III referred to a remodeling variation where a synthetic strip is placed over the fibrous portion of the left ventricular outflow tract, achieving a narrowing
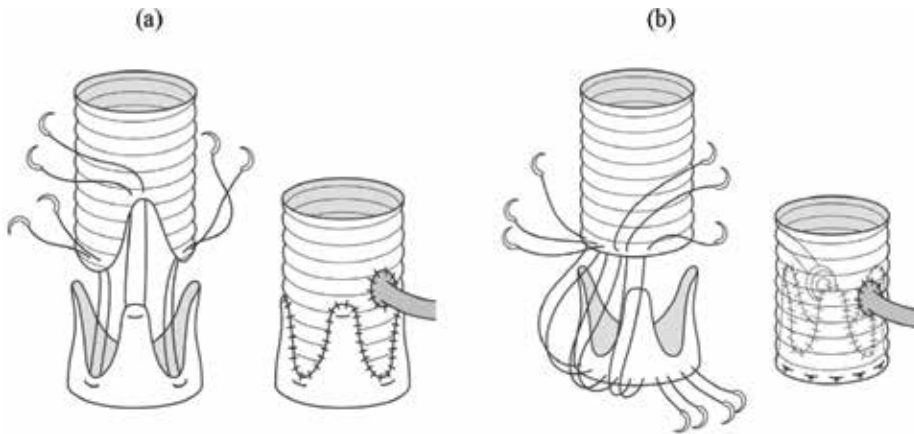
Figure 1. Schema of valve-sparing aortic root repair. (a) Remodeling and (b) reimplantation [18].

Type	#	Modification
Reimplantation	I	Classic
Remodeling	II	Classic
Remodeling	III	Adding an external synthetic strip over the fibrous portion of the LVOT
Reimplantation	IV	Adding a graft plication (diameter + 4 mm) at the sinotubular junction
Reimplantation	V	Adding a graft plication (diameter + 6–8 mm) at both the sinotubular junction and basal ring to create pseudosinuses

Table 1. David classification by Millar for valve-sparing aortic root replacement surgery.

and reinforcing annuloplasty. The final two methods identified are variations on reimplantation. David-IV refers to the technique of using a graft 4 mm larger than the annulus to allow for plication, and David-V employs an even larger graft (6–8 mm larger than the diameter) in order to facilitate the creation of pseudosinuses. Thus, David-I, -IV, and -V are variations on reimplantation, whereas David-II and -III are variations on the remodeling technique originally devised by Yacoub. In the late 1990s through the present day, attention shifted to focus on the finest details in technique, such as cusp reinforcement, graft sizing to allow for billowing, and plication as a means to recreate sinuses.

Dr. Cameron and the group at Johns Hopkins have published some of the largest series on elective repair of patients with connective tissue disorders in need of aortic root surgery [19]. Although a "classic" Bentall (i.e., composite valve-graft replacement) remains the gold standard in their practice, over the years they have introduced valve-sparing procedures when possible.

Their initial valve-sparing approach focused on preservation of sinuses with a remodeling procedure, but it soon became apparent that recurrent aortic insufficiency and annular dilation occurred in a significant number of patients soon after their initial procedure. At their center, as these results began to bear out, they transitioned to the reimplantation technique. This transition coincided with the newly approved De Paulis Valsalva graft and this combination became their exclusive procedure for valve-sparing operations [20].

4.3. Reoperation of the aortic root

Structural failure of the root, pseudoaneurysms, or infection may necessitate redo aortic root replacement. This is an operation that typically carries a higher risk of mortality and morbidity. Some special considerations include: calcified homografts or stentless valves, coronary artery length, and infection.

In patients with a heavily calcified neo-aortic wall it is often extremely difficult to dissect out the wall and redo the root as it becomes very adherent to the adjacent structures and pulmonary artery and coronaries can be injured. Replacing just the aortic valve within the calcified root is an option. With the advent of transaortic valve implantation (TAVI), this may be an option in high risk patients. El-Hamamsy et al. compared the Freestyle graft with homograft aortic root replacement in a prospective, randomized trial, and showed an improved age of survival, lower rate of reoperation, and echocardiographically less signs of valvular deterioration in the Freestyle group [21].

There can be difficulty with mobilizing the coronary buttons and placing them in into the new root or they can be damaged. The Cabrol technique should then be deployed, where a graft is sutured end to end to both the right and left coronary buttons then sutured side to side to the aorta. A second option is to place an interposition vein graft between the coronary buttons and the graft. This is the author's preferred method as we find the grafting to be easier. Lastly bypass-grafting can be done with ligation of the coronary arteries. This is typically a last resort when bleeding and technical difficulties with the anastomosis are encountered.

Infected roots pose a major problem because of the amount of debridement and reconstruction that is required. The same surgical principles apply of removal of all infected and foreign tissue. Results have been promising using homograft replacements as demonstrated in perioperative and with long-term follow-up studies.

5. Conclusion

The anatomic complexity and serious pathology that affect the aortic root challenge the cardiac surgeon. In the 61 years since De Bakey and Cooley first replaced an ascending aneurysm with the aid of cardiopulmonary bypass, a number of surgeons' devised innovative steps to improve patient outcomes. Leaders in the field of cardiac surgery such as Bono, Bentall, Yacoub, and David have contributed greatly to our surgical armamentarium for treatment of aortic root pathology.

The design of the De Paulis Valsalva graft is another great addition to the surgeon's arsenal and reinforces the need to continue analyzing and improving surgical techniques based on the dynamic physiologic environment of the aortic root during aortic valve sparing procedures. While it is common to hear surgeons refer to aortic root replacements as a "Bentall," the procedures currently employed have undergone an evolution, enough so that what is done now does not resemble the aortic inclusion and side-to-side coronary anastomosis technique.

Conflict of interest

None.

Author details

Ziv Beckerman and Edward P. Chen*

*Address all correspondence to: edward.p.chen@emory.edu

Division of Cardiothoracic Surgery, Department of Surgery, Emory University School of
Medicine, Atlanta, GA, USA

References

[1] Cooley DA, De Bakey ME. Resection of entire ascending aorta in fusiform aneurysm
using cardiac bypass. Journal of the American Medical Association. 1956;**162**:1158-1159.
DOI: 10.1001/jama.1956.72970290003013a

[2] Wheat MW Jr, Wilson JR, Bartley TD. Successful replacement of the entire ascending
aorta and aortic valve. Journal of the American Medical Association. 1964;**188**:717-719.
DOI: 10.1001/jama.1964.03060340015004

[3] Starr A, Edwards ML, McCord CW, Griswold HE. Aortic replacement: Clinical experi-
ence with a semirigid ball-valve prosthesis. Circulation. 1963;**27**:779-783. DOI: 10.1161/01.
CIR.27.4.779

[4] Herr RH, Starr A, Pierie WR, Wood JA, Bigelow JC. Aortic valve replacement: A review
of six years' experience with the ball-valve prosthesis. Annals of Thoracic Surgery.
1968;**6**:199-218. DOI: 10.1016/S0003-4975(10)66015-8

[5] Bentall H, De Bono A. A technique for complete replacement of the ascending aorta.
Thorax. 1968;**23**:338-339. DOI: 10.1136/thx.23.4. 338

[6] Yacoub M. Valve-conserving operation for aortic root aneurysm or dissection. Operative
Techniques in Thoracic and Cardiovascular Surgery. 1996;**1**:57-67. DOI: 10. 1016/S1085-
5637(07)70081-5

[7] Yacoub MH, Gehle P, Chandrasekaran V, Birks EJ, Child A, Radley-Smith R. Late results
of a valve-preserving operation in patients with aneurysms of the ascending aorta and
root. Journal of Thoracic and Cardiovascular Surgery. 1998;**115**:1080-1090. DOI: 10.1016/
S0022-5223(98)70408-8

[8] David TE. Remodeling the aortic root and preservation of the native aortic valve.
Operative Techniques in Thoracic and Cardiovascular Surgery. 1996;**1**:44-56. DOI: 10.
1016/S1085-5637(07)70080-3

[9]   David TE, Armstrong S, Ivanov J, Feindel CM, Omran A, Webb G. Results of aortic valves-sparing operations. Journal of Thoracic and Cardiovascular Surgery. 2001;**122**:39-46. DOI: 10.1067/mtc.2001. 112935

[10]   Fazel SS, David TE. Aortic valve-sparing operations for aortic root and ascending aortic aneurysms. Current Opinion in Cardiology. 2007;**22**:497-503. DOI: 10.1097/HCO. 0b013e3282efa0f4

[11]   Robicsek F. Leonardo da Vinci and the sinuses of Valsalva. Annals of Thoracic Surgery. 1991;**52**:328-335

[12]   De Paulis R, Tomai F, Bertoldo F, et al. Coronary flow characteristics after a Bentall procedure with or without sinuses of Valsalva. European Journal of Cardio-Thoracic Surgery. 2004;**26**:66-72

[13]   Kvitting JP, Ebbers T, Wigstroem L, Engvall J, Olin C, Bolger F. Flow patterns in the aortic root and the aorta studied with time-resolved, 3-dimensional, phase-contrast magnetic resonance imaging: Implications for aortic valve-sparing surgery. Journal of Thoracic and Cardiovascular Surgery. 2004;**127**:1602-1607

[14]   Beck A, Thubrikar MJ, Robicsek F. Stress analysis of the aortic valve with and without the sinuses of valsalva. Journal of Heart Valve Disease. 2001;**10**:1-11

[15]   Katayama S, Umetani N, Sugiura S, Hisada T. The sinus of Valsalva relieves abnormal stress on aortic valve leaflets by facilitating smooth closure. Journal of Thoracic and Cardiovascular Surgery. 2008;**136**:1528-1535

[16]   Klotz S, Stock S, Sievers HH, Diwoky M, Petersen M, Stierle U, et al. Survival and reoperation pattern after 20 years of experience with aortic valve sparing root replacement in patients with tricuspid and bicuspid valves. The Journal of Thoracic and Cardiovascular Surgery. 2018;**155**(4):1403-1411

[17]   Ouzounian M, Rao V, Manlhiot C, Abraham N, David C, Feindel CM, et al. Valve-sparing root replacement compared with composite valve graft procedures in patients with aortic root dilation. Journal of the American College of Cardiology. 2016;**68**:1838-1847

[18]   Shimizu H, Yozu R. Valve-sparing aortic root replacement. The Annals of Thoracic Surgery. 2011;**17**(4):330-336

[19]   Cameron DE, Alejo DE, Patel ND, Nwakanma LU, Weiss ES, Vricella LA, et al. Aortic root replacement in 372 Marfan patients: Evolution of operative repair over 30 years. Annals of Thoracic Surgery. 2009;**87**:1344-1349. DOI: 10.1016/j.athoracsur.2009.01.073

[20]   Patel ND, Williams JA, Barreiro CJ, Bethea BT, Fitton TP, Dietz HC, et al. Valve-sparing aortic root replacement: Early experience with the De Paulis Valsalva graft in 51 patients. Annals of Thoracic Surgery. 2006;**82**:548-553. DOI: 10.1016/ j.athoracsur.2006.03.073

[21]   El-Hamamsy I, Clark L, Stevens LM, Sarang Z, Melina G, Takkenberg JJM, Yacoub MH. Late outcomes following freestyle versus homograft aortic root replacement: Results from a prospective randomized trial. Journal of the American College of Cardiology. 2010 Jan 26;**55**(4):368-376. DOI: 10.1016/j.jacc.2009.09.030

Ebstein's Anomaly

Sinem Altunyuva Usta, Ayşe Inci Yıldırım,
Aysu Türkmen Karaağaç and Kaan Kırali

Additional information is available at the end of the chapter

Abstract

Ebstein's anomaly (EA), a rare congenital heart disease, results from the failure of delamination of tricuspid valve (TV) leaflets from the endocardium of the right ventricle (RV) and apical displacement, particularly of the septal and posterior leaflets of TV. The most commonly accompanying cardiac malformation is atrial septal defect. Most EA cases are sporadic; familial ones are rare. EA patients may present at any age. Symptoms result from TV regurgitation, RV dysfunction, inadequate left ventricular filling owing to ventricular septal bowing, inadequate pulmonary flow, and arrhythmias. Atrial tachyarrhythmias are the most common late complications. There have been more techniques of tricuspid repair reported in the literature than any other congenital or acquired cardiac lesion. Neonatal operation has a higher risk of mortality than the operations performed beyond infancy. Late survival rate and the quality of life for hospital survivors are excellent.

Keywords: congenital heart anomaly, heart failure, tricuspid regurgitation

1. Introduction

EA is a congenital malformation involving the tricuspid valve (TV) and right ventricle (RV). This myopathy is associated with the failure of TV delamination and highly variable tricuspid valve morphology that usually results in severe regurgitation and atrialized right ventricular dilatation. This anomaly has an extremely variable natural history depending on the degree of abnormality of the right ventricle and the tricuspid valvar apparatus. If the deformity of the TV is severe, it may result in profound congestive heart failure in the neonatal period or even in intrauterine death. At the other end of the spectrum, patients with mild degrees of displacement and dysfunction may remain asymptomatic until late adult life or may remain

symptomless throughout life. There is a genetic heterogeneity; most of the cases are sporadic, familial ones are rare. Asymptomatic patients with EA can be conservatively treated and kept under close follow-up, whereas surgical operation is indicated for those with the evidence of right heart dilation and progressively impaired ventricular systolic function. A biventricular repair is suitable for most of the patients. While 1.5-ventricular repair (bidirectional Glenn shunt) is indicated for the patients with poor right ventricular function, heart transplantation is suggested for the patients with severe left ventricular dysfunction.

2. History

This anomaly was first described by Wilhelm Ebstein, a German physician, in a report titled "Concerning a very rare case of insufficiency of the tricuspid valve caused by a congenital malformation" [1, 2]. Ebstein's own description of the malformation in 1866, with illustrations by Dr. Weiss, was based upon the anatomical findings related to the heart of Joseph Prescher, a 19-year-old cyanotic laborer with dyspnea, palpitations, jugular venous distension, and cardiomegaly [1, 2]. Ebstein described an enlarged and fenestrated anterior leaflet of the tricuspid valve in the findings of the autopsy. The posterior and septal leaflets were hypoplastic, thickened, and adherent to the right ventricle. There was also a thinned and dilated atrialized portion of the right ventricle, an enlarged right atrium, and a patent foramen ovale [3, 4]. The first case described in the English literature was not published until 1900 years [5–7]. In the 1950s, successful surgical palliation was achieved.

3. Prevalence

EA occurs in about 1/200.000 live births. It accounts for no more than 0.3–0.5% of congenital heart disease [8, 9]. The male–female incidence is equal [9].

4. Anatomy of tricuspid valve

Normally, the TV has three valvar leaflets referred to as the anterosuperior, the septal and the mural leaflets. However, in EA, the anterosuperior is the largest, redundant anterior leaflet, which contains fenestrations. It stretches from the infundibulum anteriorly to the inferolateral wall posteriorly, whereas the septal leaflet, the smallest, arises medially from the annulus above the interventricular septum. Mural or posterior leaflet attaches along the posterior margin of the tricuspid annulus from the septum to the inferolateral wall [10]. The leaflets of TV develop equally from the endocardial cushion tissues and the myocardium [10]. EA is a myopathy of the RV with abnormalities in both myocardial structure and function, besides the characteristic valvar deformities [9, 11]. Embryonic failure of delamination of the septal, inferior and anterior leaflets of the TV results in the apical displacement of the tricuspid leaflets to the underlying RV myocardium. Such failure in delamination creates the characteristic downward (apical) displacement of the functional orifice and dilation of the atrialized right ventricle (aRV), with

various degrees of hypertrophy and thinning of the wall. This malformation is characterized by the displacement of the points of attachment, or the hinges, of the septal and mural leaflets into the right ventricle, away from the atrioventricular junction. As the anterosuperior leaflet has a different developmental origin, its junctional hinge usually retains a normal position [8, 13, 14].

The failure in delamination also results in various degrees of displacement of TV leaflets, and the movement of the tricuspid hinge points both anteriorly and toward the right ventricular apex. The adherent portions of the valvar leaflets usually have little or no motion. This generally leads to tricuspid regurgitation or rarely to stenosis. [10–13]. Chordae tendinea of anterior leaflets are generally short, tethered, poorly formed and severely deformed. Therefore, the only mobile leaflet tissue is displaced into the right ventricular outflow tract (RVOT), where it may cause obstruction or forms a large sail-like intracavitary curtain. The septal and mural leaflets are usually rudimentary, dysplastic or may be absent due to failure of delamination. These leaflets may be freely mobile or adhered (tethered) to the endocardium [9, 13].

The maximal displacement is at the commissure level between the mural and septal leaflets of the TV [14]. Apical displacement of the septal leaflet by at least 8 mm/m^2 of body surface area is considered as a diagnostic feature of EA in the echocardiographic evaluation [12]. The spectrum of the malformation in EA may range from a minimal displacement of the septal and mural leaflets to an imperforate membrane or muscular shelf between the inlet and trabecular zones of the right ventricle. There is often a marked dilatation of the true TV annulus, and the aRV separating this true annulus from the functional right ventricle (fRV) [6, 12].

4.1. Atrium and atrioventricular sulcus

The right atrium is usually very dilated, and the right atrioventricular junction, or true annulus of the TV, is enlarged circumferentially. The valve of the inferior vena cava (eustachian valve) is often very prominent.

4.2. Coronary arteries

In the usual form of Ebstein's anomaly, the coronary arteries are normal except the right coronary artery (RCA). It may be displaced superiorly and posteriorly because of an aneurysmatic dilatation of aRV. Therefore, the surgeon should carefully follow the course of the RCA during the operation. It demarcates the level of the true annulus and may become kinked during plication annuloplasty procedures or TV replacement [12].

4.3. Right ventricle

Because of the displaced TV, the RV is divided into two regions in Ebstein's anomaly: the inlet portion [atrialized right ventricle (aRV)] and the trabecular or outlet portion [functional ventricle (fRV)]. The inlet portion, directly involved with the malformation, is functionally integrated with the right atrium, whereas the outlet portion constitutes the functional RV. The aRV usually has a thinner wall than the fRV and may account for more than half of the RV volume in extreme cases, instead of its usual location in one-third of the RV [8, 9]. There is often a marked dilatation of the true TV annulus and a large chamber separating this annulus from the functional RV. Two-thirds of EA cases possess dilated RV, which commonly involve

the functional RV apex and outflow tract. In some cases, RV dilatation is so significant that the ventricular septum bulges leftward, compressing the left ventricular (LV) chamber, and may cause episodic left ventricular outflow tract (LVOT) obstruction [8]. In such cases, the short-axis view demonstrates a circular right ventricle and a crescentic left ventricle.

4.4. Conduction tissue

EA cases have specialized conduction tissues [9, 14]. The sinoatrial node appears to be normally positioned, but various abnormalities of the right bundle branch have been reported. It may be located superficially in the subendocardium of the atrialized ventricle and encased in fibroelastic tissue. Arrhythmias such as accessory conduction pathways (Wolff-Parkinson-White (WPW) syndrome), atrial fibrillation or flutter are common. They occur with increasing frequency with advancing age [15]. Patients who have accessory conduction pathways are diagnosed and treated by catheter ablation technique with high succession rates.

4.5. Left ventricle

Histology of the left LV in patients with EA has shown variable degrees of fibrosis, hypertrophy, and nonspecific dysplasia [14]. LV dysfunction leads to abnormal leftward bowing of the ventricular septum and mitral valve prolapse. Regional dysfunction of LV may also develop secondary to RV dilatation.

4.6. Associated cardiac defects

The most commonly associated cardiac defects are atrial septal defect and patent foramen ovale, present in 80–94% of EA patients [16]. Other associated anomalies include bicuspid or atretic aortic valves, pulmonary atresia or hypoplastic pulmonary artery, subaortic stenosis, coarctation, mitral valve prolapse, accessory mitral valve tissue or muscle bands of the left ventricle, ventricular septal defects (VSD), and pulmonary stenosis [17]. Abnormalities of LV morphology and function, as well as other left-sided heart lesions, may also occur in EA [9, 10, 16–23]. Most patients with congenitally corrected transposition of the great arteries have an abnormal systemic TV, which fulfills the criteria for EA in 15–50% of cases. It is unclear whether the fundamental nature of the anomaly is identical in concordant and discordant atrioventricular connections [24–26]. The morphological RV is rarely dilated in congenitally corrected transposition.

5. Classifications

There are two approaches in the description of the anatomic severity of EA. The first approach is based on the echocardiographic appearance. The abnormality is described anatomically as mild, moderate, or severe. The amount of displacement and tethering of the leaflets and the degree of RV dilatation are assessed. This classification is imprecise but simple. The second approach is to describe the exact anatomy of each of the involved cardiac structures as visualized at operation. This nomenclature system emphasizes the characteristics that surgeons find

GOSE score	Ratio	Mortality rate (%)
Grade 1	<0.5	5–8
Grade 2	0.5–0.99	8–10
Grade 3	1–1.49	45 (acyanotic)
		100 (cyanotic)
Grade 4	>1.5	100

Table 1. The Great Ormond Street Echocardiography (GOSE) score and mortality rate are seen.

important when considering repair versus replacement of the TV [10]. In 1988, according to the classification of Carpentier, EA was divided into four types. Type A: The volume of the true RV is adequate. Type B: Large atrialized component of the RV exists, but the anterior leaflet of the TV moves freely. Type C: The anterior leaflet is severely restricted in its movement and may cause significant obstructions of the RVOT. Type D: Almost complete atrialization of the ventricle except for a small infundibular component [27].

The Celermajer classification [28] of EA was according to echocardiographic measurements calculating the ratio of the combined area of the right atrium and aRV to that of the fRV and the left heart in a four-chamber view at the end diastole (GOSE = RA + aRV/fRV + LV + LA). There is an echocardiographic grading score for neonates with Ebstein's anomaly, The Great Ormond Street Echocardiography (GOSE) score, with grades 1 to 4. Increasing severity, that is, a higher grade, was associated with a high mortality rate. This classification is particularly helpful with neonatal Ebstein's anomaly [28]. The Great Ormond Street Echocardiography (GOSE) score and mortality rate are demonstrated in the **Table 1**.

6. Causation and genetics

No specific cause has been consistently associated with EA. Based on retrospective case reporting, treatment with lithium during the first trimester of pregnancy was thought to be strongly associated, a 400-fold relative risk, with the occurrence of EA in the fetus. However, recent cohort and case–control epidemiologic studies have not confirmed these initial findings.

There are heterogeneous genetic factors in EA. Most cases are sporadic; familial ones are rare. Duplication of 15q affects the early morphogenesis of cardiac structures, including the normal formation of TV. Therefore, the gene located on the long arm (q) of chromosome 15 is likely to be involved in the development of EA [29, 30]. Distinct rearrangements of the chromosomal region 11q arm and deletion of 10p13–p14 and 1p34.3–p36.11 have also been described in association with EA. Genetic bases of this anomalies may be associated with the mutations in the genes MYH7 and NKX2.5 and among others [31–38]. Moreover, heterozygous mutations of NKX2.5 have been identified in the EA cases accompanied by atrioventricular (AV) block, atrial septal defect (ASD), ventricular septal defect (VSD), tetralogy of Fallot or double-outlet RV, and other TV abnormalities [39].

7. Pathophysiology

The broad spectrum of anatomic severity in EA is due to the wide spectrum of clinical and hemodynamic manifestations. The pathophysiologic changes are related to the RV functional impairment and the degree of TV regurgitation or, rarely, stenosis; the size of the interatrial communication; LV dysfunction and other associated congenital cardiovascular malformations. The aRV acts as a passive reservoir during contraction of the atrium due to the decreasing volume of ejected blood. The overall effect on the right atrium is dilatation and an increase in size of the interatrial communication. Tricuspid regurgitation increases with perogressive annular dilatation. To a lesser degree, the pathologic substrates predisposing to tachyarrhythmias produce an additional dimension contributing to the pathophysiology.

Dysfunction of the RV myocardium, and the abnormalities of the TV contribute to the impaired flow into the right heart and the pulmonary circulation. The dilated right atrium and RVa decrease the right heart flow. There is no valvar tissue separating this area from the true atrial chamber and the great veins. This results in increased venous pressure, which leads to an elevation in resistance to forward flow. A larger volume of RA due to RA distension results in right to left shunting at the atrial level in the presence of an ASD. When the aRV relaxes, it will expand, and can even balloon outwards during true atrial contraction. This creates a reservoir for venous blood and decreases the amount of effective forward flow that crosses the abnormal TV. This to-and-fro flow pattern between the right atrium and the aRV not only decreases effective output from the right heart but also provides an ongoing stimulus for atrial dilatation and atrial arrhythmias. The degree of functional impairment has been directly related to these anatomic and physiologic abnormalities. A small fRV and large aRV, extreme displacement or absence of the septal leaflet, the degree of displacement or tethering of the anterosuperior leaflet, and the aneurysmal dilation of the RVOT were all associated with a reduced functional state of the New York Heart Association [40]. A small fRV and large aRV, and extreme displacement of the septal leaflet is shown in https://mts.intechopen.com/download/index/process/176/authkey/53ae2bbd4b7866a29632305139289c32.

Although the primary focus in patients with EA has been on right-sided structures, there have been an increasing number of reports of left-sided abnormalities, especially in LV size, shape, and function [35–37]. Radionuclide scans and cineangiograms have shown disturbed LV function at rest in nonoperated patients. During formal exercise testing, these patients show an appropriate increase in LV ejection fraction due to a reduced end-systolic volume and unchanged end diastolic volume [37]. EA is related to the abnormal echocardiographic appearance of the LV myocardium: myocardial noncompaction and hypertrabeculated segments. Most patients have satisfactory LV function; a small percentage show severe systolic and diastolic dysfunction even if patients have LV myocardial abnormalities [41]. These left-sided myocardial abnormalities, although seen in only a few patients, support the concept that EA is actually a global myocardial disorder that primarily manifests itself within the RV and TV. Pulmonary vascular resistance is always high immediately after birth and usually decreases rapidly in the first days of life. It is highly difficult for the infant with severe EA to deal with neonatal circulation due to the high pulmonary vascular resistance. The combination

of RV myopathy, tricuspid regurgitation, and elevated pulmonary resistance can lead to poor pulmonary perfusion when the arterial duct constricts or closes. Venous pressures rise, leading to right-heart failure and cyanosis due to right-to-left shunting across the foramen ovale. Until the pulmonary resistance decreases, and the pulmonary flow increases, these infants present a diagnostic and therapeutic dilemma. Patency of the pulmonary outflow tract and valve must be confirmed [42]. This can be achieved by demonstrating the opening of the pulmonary valvar leaflets by cross sectional echocardiographic scans, or by documenting either forward or more commonly regurgitant flow across the valve using Doppler techniques.

8. Clinical presentation

The manifestations of EA are cyanosis, right-sided heart failure, arrhythmias, and sudden cardiac death. The hemodynamic variations and clinical presentation depend on the age at presentation, anatomic severity, hemodynamics, and the degree of right-to-left interatrial shunting [38, 41].

Patients with EA may present at any age and the majority is diagnosed in infancy or childhood, but a small percentage with less severe malformations present in adulthood. The most severe cases present prenatally or as newborns. Prenatal diagnosis is dependent upon ultrasonic screening examinations. The mortality rate is higher in the patients with severe EA. In the severe forms of EA, cardiomegaly, hydrops, and tachyarrhythmias may be seen in the fetal echocardiography. Marked cardiac enlargement may lead to pulmonary parenchymal hypoplasia in the most severe cases. Prenatal arrhythmia is not common. Neonates usually present with cyanosis and heart failure and secondary TV regurgitation resulting from decreased pulmonary blood flow, depressed RV function, and low cardiac output [42]. Murmurs and arrhythmias are frequently encountered presenting complaints in children, adolescents and adults. Adults also present with progressive cyanosis, decreasing exercise tolerance, fatigue, or right-sided heart failure. Palpitations in a cyanotic child should raise the possibility of EA [38, 41, 42]. In the presence of an interatrial communication, the risk of paradoxical embolization, brain abscess, and sudden death increases. Exercise tolerance is dependent on the cardiac function and oxygen saturation [43, 44].

9. Physical findings

Growth and development are generally normal. Physical signs vary depending on the severity of pathology and magnitude of the right-to-left atrial shunt, which may lead to cyanosis and digital clubbing in patients with interatrial communication. Cyanosis is typically pronounced in the neonate and infants, whereas it is milder (sometimes only exertional) in older children. Many have an unusual facial coloration, described as violaceous hue, red-cheeked, or malar rush. Usually these patients have an associated mild polycythemia. Asymmetry of the chest is a frequent finding secondary to the right heart dilatation. Arterial and venous pulsations are

usually normal, even in the presence of tricuspid insuficiency. The jugular venous pulsations may not have a large V wave because of poor transmission of the venous pulse wave in the presence of a dilated and compliant right atrium [41, 42]. Jugular venous and hepatic distention may be present in advanced cases. The praecordium is usually not overactive. After the neonatal period, it is auscultation that often alerts the physician to the diagnosis of EA. The systolic murmur of tricuspid regurgitation is variable and its intensity depends on the degree to which contractility of the fRV is preserved. Multiple first heart sounds are heard because the highly mobile anterosuperior valvar leaflets and anterior leaflet mimic ejection clicks. Occasionally, the heart sounds are soft, but usually they are of normal intensity. The first heart sound is widely split because of the increased excursion of the anterosuperior leaflet and the subsequent delayed closure of the abnormal TV. The second heart sound is often split owing to the late closure of the pulmonary valve as a result of the conduction delay associated with severe RV enlargement. A holosystolic murmur is found along the left sternal border in those with an organized jet of tricuspid regurgitation. Diastolic murmurs are rare, unless there is coexisting pulmonary regurgitation. Low-intensity diastolic murmurs can be auscultated in the same location as a result of antero-grade flow across the TV [42]. Importantly, murmurs may be very soft or absent if the coaptation gap is very large; the velocity of to-and-fro flow is low, and rapid equalization of pressure across the functional TV does not result in blood flow turbulence.

10. Diagnosis

10.1. Electrocardiography

The electrocardiogram (ECG) is usually abnormal and helps to confirm the clinical diagnosis. Sinus rhythm is usually present at the time of initial diagnosis. ECG may show tall and broad P waves as a result of right atrial enlargement, as well as complete or incomplete right bundle-branch block. Complete AV block is rare and first degree AV block is present in approximately half the patients. The QRS axis in the frontal plane occasionally shows right-axis deviation. Most patients have right bundle branch block and many have low-voltage QRS complexes in the right precordial leads. Right ventricular hypertrophy criterion are extremely uncommon [41, 45].

The downward displacement of the septal leaflet of the TV is associated with discontinuity of the central fibrous body and septal atrioventricular ring with direct muscular connections, thus creating a potential substrate for accessory atrioventricular connections and preexcitation. Occasionally, the pattern is transient or intermittent. Paroxysmal tachyarrhythmias in EA are based on fast conducting atrioventricular accessory pathways with both antegrade and retrograde conduction properties in most patients. In addition, wide QRS tachycardia over a septal accessory atrioventricular pathway, ventricular tachycardia, or flutter, as well as ectopic atrial tachycardia, atrial flutter, and atrial fibrillation can occur. Concealed accessory pathways, without manifest delta waves, are also common. Absence of anterograde preexcitation, therefore, neither indicates that the accessory connection is no longer present nor that the patient is no longer susceptible to tachycardia. The patient may still have retrograde conduction, which allows for atrioventricular reciprocating tachycardia. The presence of left axis

Figure 1. ECG of a patient with Ebstein's anomaly and the wolf Parkinson white syndrome showing the typical changes, with reduced PR interval, and preexcitation (delta wave) configuration of the QRS complex.

deviation in a patient with EA suggests the presence of the Mahaim variant of preexcitation, produced by atriofascicular tracts.The patients with arrhythmias or symptoms compatible with arrhythmia are significantly older than those without symptoms or arrhythmias [46–48]. Accessory conduction pathways [Wolff-Parkinson-White (WPW) syndrome] arrhythmias are seen approximately 15–20%. Atrial fibrillation or flutter can occur with increasing frequency with older age. ECG shows EA patients with WPW syndrome in **Figure 1**.

Even prior to the widespread application of complex surgical antiarrhythmic procedures, surgical intervention appeared to decrease the frequency of arrhythmias, at least in early, short-term follow-up. Despite the overall reduction in arrhythmias, when arrhythmias were observed early during postoperative recovery, these patients had an increased risk of late sudden death [15, 49].

10.2. Chest radiography

The cardiac silhouette may vary from nearly normal to extreme cardiomegaly. When the heart is severely dilated, it takes a globular shape similar to that observed with large pericardial effusions or severe dilated cardiomyopathy. The dilated right atrium is responsible for most of the enlarged cardiac silhouette. In the frontal view, the right atrium produces a significant convexity of the right heart border, and in the lateral view, the right atrium may fill the entire retrosternal space. The convex left border is primarily due to dilation of the right ventricular outflow tract. The convexities of both left and right heart borders produce the characteristic

globular cardiac silhouette. In cyanotic patients with a right-to-left shunt, the pulmonary vascularity is decreased. A cardiothoracic ratio of 0.65 carries a poor prognosis [14].

10.3. Echocardiography

Two-dimensional echocardiography is the diagnostic test used also in the long-term assessment of patients with EA. More recently 3D echocardiography has been utilized as an adjunct for the assessment of additional details about TV anatomy-leaflets and subvalvar apparatus, the size and function of the cardiac chambers, and other associated cardiac defects. The single most sensitive and specific diagnostic feature is the displacement of the annular hinge of the septal leaflet. The distance between the valvar hinge points can easily be measured. Apical displacement of the septal leaflet of the TV from the insertion of the mitral anterior leaflet hinge point should be at least 8 mm/m^2 when evaluated in the apical four-chamber view [14]. An echocardiogram (four-chamber view) of a patient with severe Ebstein's anomaly showing a displaced septal leaflet, atrialized RV and small functional RV is shown in **Figure 2**.

Other echocardiographic features that help in diagnosis include: (1) elongation of the anterosuperior leaflet, (2) tethering of the leaflets to the underlying myocardium, (3) shortened cordal support, (4) attachment of the leading edge of the anterosuperior leaflet to the right ventricular myocardium, (5) displacement of the annular attachment of the anterosuperior leaflet, (6) absence of the septal or mural leaflets, (7) congenital fenestration of the leaflets, and (8) enlargement of the valvar annulus [24].

Echocardiography is also used to evaluate the suitability for valvar repair, associated cardiovascular abnormalities, and myocardial function. The most important determinant of a durable monoleaflet repair is a freely mobile anterosuperior leaflet, especially its leading edge. The mobile leaflet tissue should be visualized within the right ventricular inflow tract, and this assessment must be made in the apical four-chamber view. Extensive adherence of more than half of the anterosuperior leaflet to the ventricular myocardium makes a successful repair unlikely. A single central jet of regurgitation is more easily eliminated than multiple regurgitant orifices. Even when there is a significant amount of leaflet tissue, direct muscular insertions from the ventricular free wall into the body of the anterosuperior leaflet can make repair impossible. The functional impact of the malformation of the RV and TV should be determined. Anatomic and functional severities are usually similar, but they are not always the same. For example, a patient can have a severe anatomic displacement with EA but only mild functional impairment. This generally occurs if the interatrial communication is small, the displaced valve is relatively competent, and the myocardium is only mildly dysfunctional. Both aspects of severity play an important role in determining the functional state, prognosis, and reparability of the TV. The degree of RA and RV enlargement and functional state of the RV myocardium should also be defined. Other important features include the degree of dilation of RVOT, the presence and size of any ASD, and the degree of transvalvar regurgitation. The left ventricular myocardium has also been described as being abnormal in a significant number of patients with EA. Therefore, quantitative evaluation of LV performance should also be a routine component of the echocardiographic evaluation in EA patients. VSD and pulmonary stenosis may also be associated with EA. Doppler and color flow echocardiographic
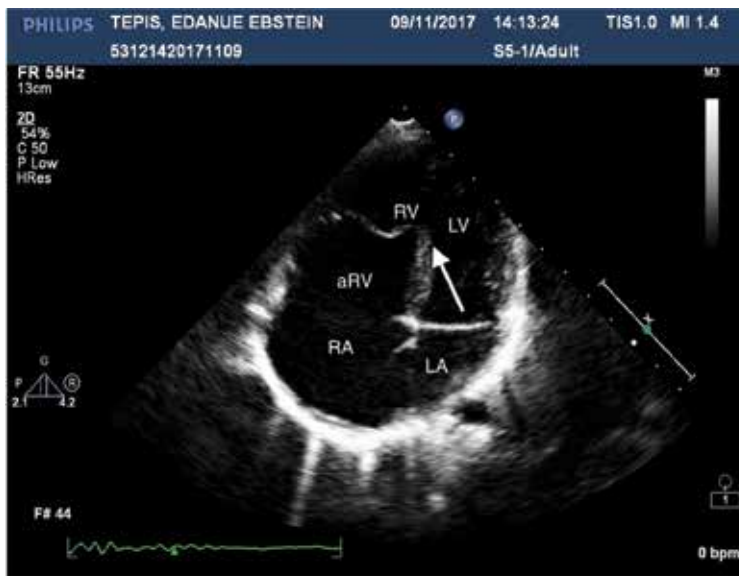
Figure 2. (a) Echocardiographic view (four-chamber view, apex up) of a patient with Ebstein's anomaly showing a displaced septal leaflet (arrow). (b)The anterior leaflet is severely tethered and nearly immobile. The functional right ventricle (RV) is small. aRV indicates atrialized right ventricle; LA, left atrium; LV, left ventricle; and RA, right atrium.

assessment can help determine hemodynamic alterations such as valvar regurgitation and intracardiac shunting [13, 17, 24, 40]. An echocardiogram shows the displacement septal leaflet of TV and the anterosuperior leaflet which is the largest, redundant and contains fenestrations that led to tricupid regurgitations **Figure 3**.

Figure 3. An echocardiogram (four-chamber view, apex up)showing the displacement of septal leaflet(in the right hand panel), anterior leaflet fenestrations, and tricuspid regurgitations (in the left hand panel). The hinge point of the normal septal tricuspid leaflet is positioned slightly toward the cardiac apex relative to the septal hinge point of the anterior mitral leaflet. This displacement is exaggerated in hearts with Ebstein's malformation, as shown in the image (outlined by the arrow, in the right hand panel) This can be quantitated by the displacement index, dividing the distance between the valvar insertions divided by the body surface area. A value of greater than 8 mm/m^2 is diagnostic of Ebstein's malformation. It should be noted that the valvar leaflets are also abnormal in Ebstein's malformation. LA, left atrium; LV, left ventricle; RA, right atrium; RV, right ventricle.

Echocardiography also plays an important role in the intraoperative and postoperative assessment of adequacy of TV repair or replacement. The most important use of intraoperative echocardiography is the immediate evaluation of the repaired valve functions. The postoperative examination is used to assess prosthetic valvar function, the changes in right and left ventricular functions and to exclude significant residual atrial level shunting. Postoperative echocardiography is also important to evelute the adequacy of the surgical repair, presence of pericardial or pleural effusion, mediastinal hematoma, intracardiac thrombus, and the degree of residual tricuspid regurgitation or tricuspid stenosis. The flow can rarely be compromised in the RCA because of its proximity to the plicated portion of the aRV [13, 41].

10.3.1. Prenatal detection of Ebstein's malformation

Echocardiography can accurately define the EA features in the fetus. Characteristics related with the early neonatal mortality include marked enlargement of the right heart, severe tethering of the anterosuperior leaflet, left ventricular compression, and associated lesions as pulmonary atresia [42]. Pulmonary hypoplasia develops as a result of severe cardiomegaly and hydrops with pleural and pericardial effusions. Detection of rhythm disturbances, such as supraventricular tachycardia, should be attempted at the time of fetal echocardiography due

to its contribution to the development of hydrops. If the ratio of the combined right atrial and atrialized ventricular area compared to the combined area of the functional right ventricle and left heart is greater than one, fetal or neonatal outcome is very poor. Other fetal or neonatal findings associated with increased risk of mortality were a larger ASD, functional or anatomic pulmonary atresia, or reduced LV function [40–42].

10.4. Cardiac catheterization and hemodynamics

Diagnostic cardiac catheterization is rarely necessary in EA patients, except for preoperative coronary angiography or diagnosis of the associated cardiac anomalies. RV and pulmonary artery pressures are usually normal, even if the RV end-diastolic pressure is increased. RA pressure may be normal, despite severe TV regurgitation, especially if the right atrium is markedly dilated. Oximetry may show systemic arterial desaturation in the presence of an interatrial communication and right-to-left shunting [13, 14].

10.5. Cardiac magnetic resonance imaging

Cardiac magnetic resonance imaging (CMRI) is used for the quantitative measurement of right atrial and ventricular size and systolic function in Ebstein's patient. Axial imaging is a more reliable analysis for defining the disease severity [41]. Cardiac magnetic resonance imaging of a patient with severe Ebstein's anomaly showing displacement of septal leaflet, atrialized right ventricle (ARV) and small functional right ventricle is shown in **Figure 4**, septal bowing in **Figure 5**.
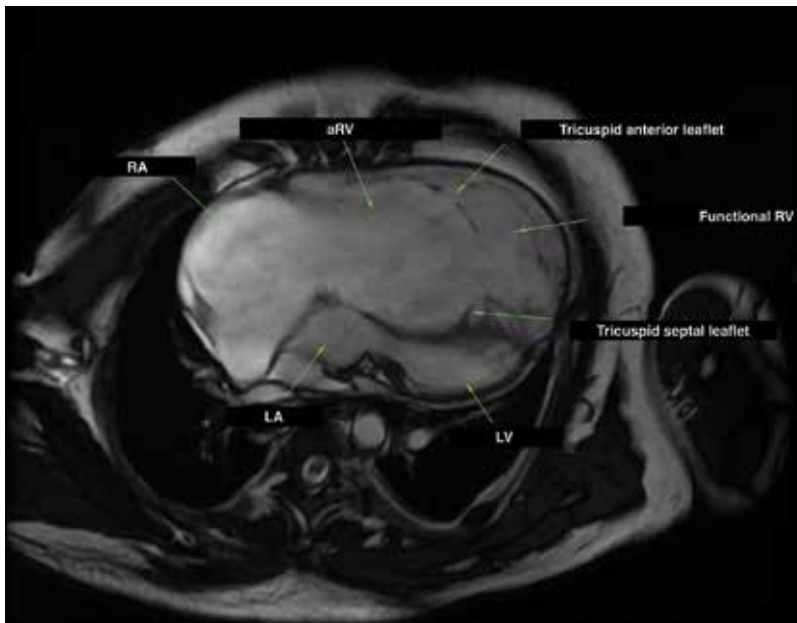

Figure 4. Cardiac MRI of a patient with Ebstein's anomaly showing displacement of septal leaflet, atrialized right ventricle (ARV) and small functional right ventricle (fRV); LA, left atrium; LV, left ventricle; and RA, right atrium.
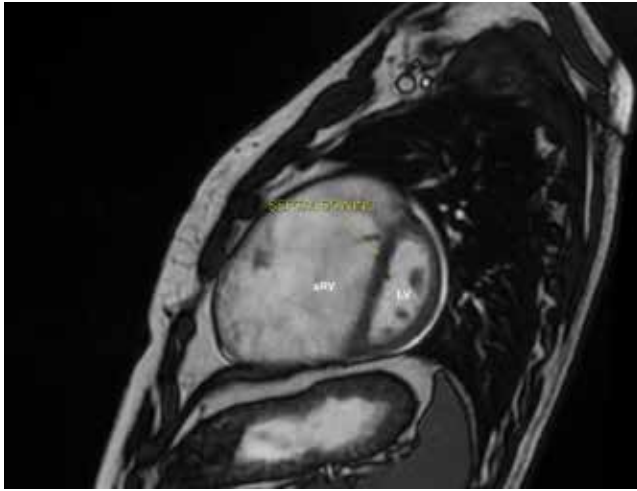
Figure 5. An example of a cardiac MRI showing septal bowing in short axis views. (Used with permission of the Sonomed Imaging Center).

11. Management

11.1. Medical treatment

Any patient with EA needs to be evaluated regularly by a cardiologist who has expertise in congenital heart disease. Prophylaxis for endocarditis is recommended despite its low risk. In neonates, congestive heart failure or profound cyanosis may be substantial. Medical therapy is the initial and preferred line of treatment. However, failure in weaning from the ventilator or persistent metabolic abnormalities often result in the need for operation. Patients with EA and cardiac failure who are not candidates for surgery are treated with standard cardiac failure therapy, including diuretics and digoxin. The efficacy of angiotensin-converting enzyme inhibitors in the patients with right-sided heart failure is unproved. Medical management of arrhythmias should be individualized and combined with operative or catheter-based intervention.

11.2. Catheter ablation

Electrophysiological evaluation and radiofrequency ablation of symptomatic accessory pathways should be performed when feasible in EA patients with tachyarrhythmias. Catheter ablation has a lower success rate in patients with an accompanying anomaly than in those with structurally normal hearts, and the risk of recurrence is increased [45, 46]. Supraventricular tachyarrhythmia associated with EA can also be ablated at the time of operative repair [45].

Tachycardia mediated via an accessory pathway is very common. Ten percent of the patients have other mechanisms for their tachyarrhythmias. The pathways are right-sided or septal in the majority of patients with reentrant arrhythmias, with only 4% being left-sided. Thirty percent of the patients may have multiple pathways. Radio-frequency ablation is able to eliminate

the tachycardia in almost 90% of cases, depending on its mechanism; however, recurrence is common. Long-term success is achieved in only one-third of the cases [15, 46–48].

11.3. Surgical treatment

11.3.1. Indications for operation

Children who have survived infancy generally remain asymptomatic for several years. The surgery can be postponed until symptoms appear, cyanosis becomes evident, or paradoxical emboli occur. Deliberations about an operation should begin if evidence of deterioration exists, such as progressive increase in right heart size, reduction in systolic function, or appearance of ventricular or atrial tachyarrhythmias. Indications for operation in the symptomatic neonates include severe cyanosis, GOSE of three or four with mild cyanosis, cardiothoracic ratio > 80% and severe TR. However, in older ages, operation is clearly indicated if the symptoms progress to New York Heart Association functional class III or IV and medical management has little to offer. A biventricular reconstruction is feasible if the LV is functionally normal, enough RV cavity is present and TV morphology is suitable. A 1.5 ventricle repair can be applied to the patients with the RV failure. Heart transplantation is reserved for the patients with severe biventricular dysfunction.

Some patients with cyanosis on exercise, who have a shunt at the atrial level but only mild or moderate regurgitation of the TV, may benefit from device closure to alleviate cyanosis and to prevent paradoxical emboli. Some centers commonly perform such procedures either as a staged approach or for long-term palliation [50]. The degree of TV regurgitation must be assessed carefully because closure of an ASD alone may worsen RV dysfunction.

11.3.2. Surgical options

A variety of surgical methods were introduced in the treatment of Ebstein's anomaly. Those treatments included a TV repair or replacement for the principle element in the treatment of Ebstein's anomaly and additional concomitant procedures for the correction of comorbid anomalies such as ablation of accessory conduction pathways, resection or plication of the atrialized right ventricle, application of 1.5-ventricular repair (bidirectional cavo-pulmonary shunt), and single-ventricle repair for advanced right ventricular dysfunction. Heart transplantation is suggested for the patients with severe left ventricular dysfunction. Neonatal operation has high operative mortality, whereas operation performed beyond infancy and into adulthood has low operative mortality. Late survival and quality of life for hospital survivors are excellent for the majority of patients in all age brackets [51–54].

12. Conclusion

Ebstein's anomaly is a complex congenital anomaly with a wide anatomic and clinical spectrum. Management is complex and must be individual because of the different anatomic and hemodynamic variables, and associated malformations, in Ebstein's anomaly. These patients

are evaluated by a cardiologist who has expertise in congenital heart disease. Developing better management strategies and survival of patients with this anomaly will continue to improve.

Author details

Sinem Altunyuva Usta[1], Ayşe Inci Yıldırım[1]*, Aysu Türkmen Karaağaç[2] and Kaan Kırali[3]

*Address all correspondence to: ayildirimmd@yahoo.com

1 Pediatric Cardiology, University of Health Sciences, Kartal Koşuyolu Research and Training Hospital, Istanbul, Turkey

2 Pediatry, University of Health Sciences, Kartal Koşuyolu Research and Training Hospital, Istanbul, Turkey

3 Cardiovascular Surgery, University of Health Sciences, Kartal Koşuyolu Research and Training Hospital, Istanbul, Turkey

References

[1] Mann RJ, Lie JT. The life story of Wilhelm Ebstein (1836-1912) and his almost overlooked description of a congenital heart disease. Mayo Clinic Proceedings. 1979;**54**:197-204

[2] van Son JA, Konstantinov IE, Zimmermann V. Wilhelm Ebstein and Ebstein's malformation. European Journal of Cardio-Thoracic Surgery. 2001;**20**:1082-1085

[3] Ebstein W. Ueber einen sehr seltenen Fall von Insufficienz der Valvula tricuspidalis, bedingt durch eine angeborene hochgradige Missbildung derselben. Archives of Anatomy and Physiology. 1866:238-255

[4] Engle MA, Payne TP, Bruins C, Taussig HB. Ebstein's anomaly of the tricuspid valve: Report of three cases and analysis of clinical syndrome. Circulation. 1950;**1**:1246-1260

[5] Soloff LA, Stauffer HM, Zatuchni J. Ebstein's disease: Report of the first case diagnosed during life. The American Journal of the Medical Sciences. 1951;**222**:554-561

[6] Watson H. Natural history of Ebstein's anomaly of tricuspid valve in childhood and adolescence: An international co-operative study of 505 cases. British Heart Journal. 1974;**36**:417-427

[7] Attenhofer JC, Connolly H, O'Leary P. Occurence of left ventricular myocardial dysplasia/noncompaction in patients with ebstein's anomaly. Mayo Clinic Proceedings. 2005;**80**:361-368

[8] Dearani JA, Danielson GK. Ebstein's anomaly of the tricuspid valve. In: Mavroudis C, Backer CL, editors. Paediatric Cardiac Surgery. 3rd ed. Philadelphia, PA: Mosby; 2003. pp. 524-536

[9] Lev M, Liebertson RR, Joseph RH, et al. The pathologic anatomy of Ebstein's disease. Archives of Pathology. 1970;**90**:334-343

[10] Dearani JA, Danielson GK. Congenital heart surgery nomenclature and database project: Ebstein's anomaly and tricuspid valve disease. The Annals of Thoracic Surgery. 2000;**69**(suppl):S106-S117

[11] Lamers WH, Viragh S, Wessels A, Moorman AF, Anderson RH. Formation of the tricuspid valve in the human heart. Circulation. 1995;**91**:111-121

[12] Edwards WD. Embryology and pathologic features of Ebstein's anomaly. Progress in Pediatric Cardiology. 1993;**2**:5-15

[13] Rigby ML, Penny D, Wernovsk AR. Ebstein Anomaly. In: Anderson RH, Baker EJ, editors. 3rd ed. Churchill Livingstone/Elsevier; 2010:713-730

[14] Anderson KR, Zuberbuhler JR, Anderson RH, Becker AE, Lie JT. Morphologic spectrum of Ebstein's anomaly of the heart: A review. Mayo Clinic Proceedings. 1979;**54**:174-180

[15] Khositseth A, Danielson GK, Dearani JA, Munger TM, Porter CJ. Supraventricular tachyarrhythmias in Ebstein anomaly: Management and outcome. The Journal of Thoracic and Cardiovascular Surgery. 2004;**128**:826-833

[16] Danielsen GK, Driscoll DJ, Mair DD, Warnes CA, Oliver WC Jr. Operative treatment of Ebstein's anomaly. The Journal of Thoracic and Cardiovascular Surgery. 1992;**104**: 1195-1202

[17] Jost CH A, Connolly HM, Edwards WD, Hayes D, Warnes CA, Danielson GK. Ebstein's anomaly: Review of a multifaceted congenital cardiac condition. Swiss Medical Weekly. 2005;**135**:269-281

[18] Brickner ME, Hillis LD, Lange RA. Congenital heart disease in adults: Second of two parts. The New England Journal of Medicine. 2000;**342**:334-342

[19] Daliento L, Angelini A, Ho SY, Frescura C, Turrini P, Baratella MC, Thiene G, Anderson RH. Angiographic and morphologic features of the left ventricle in Ebstein's malformation. The American Journal of Cardiology. 1997;**80**:1051-1059

[20] Benson LN, Child JS, Schwaiger M, Perloff JK, Schelbert HR. Left ventricular geometry and function in adults with Ebstein's anomaly of the tricuspid valve. Circulation. 1987;**75**:353-359

[21] Saxena A, Fong LV, Tristam M, Ackery DM, Keeton BR. Late noninvasive evaluation of cardiac performance in mildly symptomatic older patients with Ebstein's anomaly of tricuspid valve: Role of radionuclide imaging. Journal of the American College of Cardiology. 1991;**17**:182-186

[22] Castaneda-Zuniga W, Nath HP, Moller JH, Edwards JE. Left-sided anomalies in Ebstein's malformation of the tricuspid valve. Pediatric Cardiology. 1982;**3**:181-185

[23] Attenhofer Jost CH, Connolly HM, Warnes CA, O'Leary P, Tajik AJ, Pellikka PA, Seward JB. Noncompacted myocardium in Ebstein' s anomaly: Initial description in three patients. Journal of the American Society of Echocardiography. 2004;**17**:677-680

[24] Attenhofer Jost CH, Connolly HM, O'Leary PW, Warnes CA, Tajik AJ, Seward JB. Left heart lesions in patients with Ebstein anomaly. Mayo Clinic Proceedings. 2005;**80**:361-368

[25] Celermajer DS, Cullen S, Deanfield JE, Sullivan ID. Congenitally corrected transposition and Ebstein's anomaly of the systemic atrioventricular valve: Association with aortic arch obstruction. Journal of the American College of Cardiology. 1991;**18**:1056-1058

[26] Dekker A, Mehrizi A, Vengsarkar AS. Corrected transposition of the great vessels with Ebstein malformation of the left atrioventricular valve: An embryologic analysis and two case reports. Circulation. 1965;**31**:119-126

[27] Carpentier A, Chauvaud S, Mace L, Relland J, Mihaileanu S, Marino JP, Abry B, Guibourt P. A new reconstructive operation for Ebstein's anomaly of the tricuspid valve. The Journal of Thoracic and Cardiovascular Surgery. 1988;**96**:92-101

[28] Celermajer DS, Bull C, Till JA, Cullen S, Vassillikos VP, Sullivan ID, Allan L, Nihoyannopoulos P, Somerville J, Deanfield JE. Ebstein's anomaly: Presentation and outcome from fetus to adult. Journal of the American College of Cardiology. 1994;**23**:170-176

[29] Miller MS, Rao PN, Dudovitz RN, Falk RE. Ebstein anomaly and duplication of the distal arm of chromosome 15: Report of two patients. American Journal of Medical Genetics. Part A. 2005;**139A**:141e5

[30] Correa-Villasenor A, Ferencz C, Neill CA, et al. Fort he Baltimore-Washington infant study group. Ebstein's malformation of the tricuspid valve: Genetic and enviromentalfactors. Teratology. 1994;**50**:137-147

[31] Walsh R, Rutland C, Thomas R, Loughna S. Cardiomyopathy: A systematic review of disease-causing mutations in myosin heavy chain 7 and their phenotypic manifestations. Cardiology. 2010;**115**:49e60

[32] Ching YH, Ghosh TK, Cross SJ, Packham EA, Honeyman L, Loughna S, et al. Mutation in myosin heavy chain 6 causes atrial septal defect. Nature Genetics. 2005;**37**:423-428

[33] Matsson H, Eason J, Bookwalter CS, Klar J, Gustavsson P, Sunneg̊ardh J, et al. A-cardiac actin mutations produce atrial septal defects. Human Molecular Genetics. 2008;**17**:256e65

[34] Wright KN. Researchers Aim to Isolate Gene for Tricuspid Valve Dysplasia. Available from: http://www.thelabradorclub.com/ uploads/file/valvedysplasia.pdf. [Accessed: March 3, 2016]

[35] Andelfinger G, Wright KN, Lee HS, Siemens LM, Benson DW. Canine tricuspid valve malformation, a model of human Ebstein anomaly, maps to dog chromosome 9. Journal of Medical Genetics. 2003;**40**:320e4

[36] de Lonlay-Debeney P, de Blois MC, Bonnet D, Amiel J, Abadie V, Picq M, et al. Ebstein anomaly associated with rearrangements of chromosomal region 11q. American Journal of Medical Genetics 1998;**80**:157e9

[37] Postma AV, van Engelen K, van de Meerakker J, Rahman T, Probst S, Baars MJ, et al. Mutations in the sarcomere gene MYH7 in Ebstein anomaly. Circulation. Cardiovascular Genetics. 2011;**4**:43e50

[38] Yuan S-M. Ebstein's anomaly: Genetics, clinical manifestations, and management. Pediatrics and Neonatology. 2017;**58**:211e215

[39] Benson DW, Silberbach GM, Kavanaugh-McHugh A, Cottrill C, Zhang Y, Riggs S, Smalls O, Johnson MC, Watson MS, Seidman JG, Seidman CE, Plowden J, Kugler JD. Mutations in the cardiac transcription factor NKX2.5 affect diverse cardiac developmental pathways. The Journal of Clinical Investigation. 1999;**104**:1567-1573

[40] Shiina A, Seward JB, Edwards WD, Hagler DJ, Tajik AJ. Two-dimensional echocardiographic spectrum of Ebstein's anomaly: Detailed anatomic assessment. Journal of the American College of Cardiology. 1984;**3**:356-370

[41] Attenhofer Jost CH, Connolly HM, Dearani JA, Edwards WD, Danielson GK. Ebstein's anomaly. Circulation. 2007;**115**:277-285

[42] Shinkawa T, Polimenakos AC, Gomez-Fifer CA, Charpie JR, Hirsch JC, Devaney EJ, Bove EL, Ohye RG. Management and long-term outcome of neonatal Ebstein anomaly. The Journal of Thoracic and Cardiovascular Surgery. 2010;(2):354-358

[43] MacLellan-Tobert SG, Driscoll DJ, Mottram CD, Mahoney DW, Wollan PC, Danielson GK. Exercise tolerance in patients with Ebstein's anomaly. Journal of the American College of Cardiology. 1997;**29**:1615-1622

[44] Driscoll DJ, Mottram CD, Danielson GK. Spectrum of exercise intol- erance in 45 patients with Ebstein's anomaly and observations on exercise tolerance in 11 patients after surgical repair. Journal of the American College of Cardiology. 1988;**11**:831-836

[45] Ituralde P, Nava S, Salica G, Medeiros A, Colin L, Gozales M. Electrocardiographic characteristics of patients with Ebstein's anomaly before and after ablation of an accessory Atrioventricular pathway. Journal of Cardiovascular Electrophysiology. 2006;**17**: 1332-1336

[46] Hebe J. Ebstein's anomaly in adults: Arrhythmias: Diagnosis and therapeutic approach. The Thoracic and Cardiovascular Surgeon. 2000;**48**:214-219

[47] Cappato R, Schluter M, Weiss C, Antz M, Koschyk DH, Hofmann T, Kuck KH. Radiofrequency current catheter ablation of accessory atrioventricular pathways in Ebstein's anomaly. Circulation. 1996;**94**:376-383

[48] Chetaille P, Walsh EP, Triedman JK. Outcomes of radiofrequency catheter ablation of atrioventricular reciprocating tachycardia in patients with congenital heart disease. Heart Rhythm. 2004;**1**:168-173

[49] Greason KL, Dearani JA, Theodoro DA, Porter CB, Warnes CA, Danielson GK. Surgical management of atrial tachyarrhythmias associated with congenital cardiac anomalies: Mayo Clinic experience. Seminars in Thoracic and Cardiovascular Surgery. Pediatric Cardiac Surgery Annual. 2003;**6**:59-71

[50] Atiq M, Lai L, Lee KJ, Benson LN. Transcatheter closure of atrial septal defects in children with a hypoplastic right ventricle. Catheterization and Cardiovascular Interventions. 2005;**64**:112-116

[51] Dearani JA, Danielson GK. Tricuspid valve repair for Ebstein's anomaly. Operative Techniques in Thoracic and Cardiovascular Surgery. 2003;**8**:188-192

[52] Dearani JA, Danielson GK. Ebstein's anomaly. In: Sellke FW, del Nido PJ, Swanson SJ, editors. Sabiston and Spencer Surgery of the Chest. 7th ed. Vol. 2. Philadelphia, PA: Elsevier Saunders; 2005;2223-2235

[53] Chauvaud S, Berrebi A, d'Attellis N, Mousseaux E, Hernigou A, Carpentier A. Ebstein's anomaly: Repair based on functional analysis. The European Journal of Cardio-Thoracic Surgery. 2003;**23**:525-531

[54] Ullmann MV, Born S, Sebening C, Gorenflo M, Ulmer HE, Hagl S. Ventricularization of the atrialized chamber: A concept of Ebstein' s anomaly repair. The Annals of Thoracic Surgery. 2004;**78**:918-924

Edited by Kaan Kirali

Heart valves are the basic functional structure of the heart to obtain, sustain, and maintain blood circulations in the body without energy loss, allowing blood regurgitation or obstructing blood flow. There are two basic designs of heart valves: actively protected via subvalvular apparatus (atrioventricular valves) and passively strengthened (ventriculoarterial valves). The embryologic and morphologic development of heart valves is the key stage to continue normofunctional structure and physiological behavior. Fetal anomalies, embryologic defects, or non-development pathologies may damage the structure of heart valves and cause functional deterioration at different grades. In this book, we have focused on specific pathologies, which require special knowledge and treatment modalities.

IntechOpen